THE SKELETAL PROTEOME AND PRODUCTION OF CALCIFYING PROTEINS IN THE STONY CORAL *STYLOPHORA PISTILLATA*

by

JEANA LOUISE DRAKE

A dissertation submitted to the

Graduate School – New Brunswick

Rutgers, The State University of New Jersey

in partial fulfillment of the requirements

For the degree of

Doctor of Philosophy

Graduate Program in Oceanography

Written under the direction of

Paul G. Falkowski

and approved by

_____

_____

_____

_____

_____

New Brunswick, New Jersey

OCTOBER, 2015

Abstract of the Dissertation

The skeletal proteome and production of calcifying proteins in the stony coral *Stylophora pistillata*

by JEANA LOUISE DRAKE

Dissertation Director:

Paul G. Falkowski

Coral biomineralization is important at the organismal, ecosystem, and global scales, yet the biological component has not been well understood. In particular, identities, roles, and environmental susceptibility of the proteins retained in coral skeleton were previously unknown. To address this, my thesis sequenced the first coral skeletal proteome, generated the first application of coral cell cultures to understanding the effects of ocean acidification on coral calcification at the cellular and molecular levels, and made the first use of NanoSIMS to test the co-localization of aspartic acid and newly formed aragonite in corals.

To determine the proteins directly involved in the coral biomineralization process, I used LC-MS/MS sequencing and a novel genome to sequence the skeletal proteome of the stony coral, *Stylophora pistillata*. It contains an assemblage of adhesion and structural proteins as well as two highly acidic proteins that constitute a novel coral SOM protein sub-family. I next used cluster analysis to compare mineralizing genes known from coral skeleton, mollusk shell, and sea urchin spines and tests. The analysis suggests that there are few sequence similarities across all three phyla, supporting the independent

evolution of biomineralization. However, there are core sets of conserved motifs in all three phyla examined, including acidic proteins that appear to be responsible for the nucleation reaction as well as inhibition; structural and adhesion proteins that determine spatial patterning; and signaling proteins that modify enzymatic activities.

With the guidance of the sequenced coral skeletal proteome and the cluster analysis, I chose four proteins to focus on for their expression response to increased CO_2, and their potential control on calcification, in cell cultures. The results suggest that compensatory molecular adjustments to deal with ocean acidification are successful only up to a point, beyond which these mechanisms cannot compete with local chemical conditions unfavorable to biomineralization. Finally, I used NanoSIMS and *S. pistillata* cell cultures to develop a method to co-localize highly acidic proteins and newly formed calcium carbonate. Initial results point to both intra- and extracellular roles for these proteins in transporting Ca to the calcification site and adhering cells to each other, substrate, and new mineral.

Prior Publications

Several sections of this dissertation have been published, or are under review for publication, elsewhere. Chapter 2 was published prior to the data re-analysis and has the following citation: *Proteomic analysis of skeletal organic matrix from the stony coral* Stylophora pistillata. *Proceedings of the National Academy of Sciences, **110**, 3788-3793 (2013).* Chapter 3 was published in its entirety and has the following citation: *The evolution and future of carbonate precipitation in marine invertebrates: Witnessing extinction or documenting resilience in the Anthropocene*? *Elementa: Science of the Anthropocene, **2**, 000026 (2014).* Chapter 4 has been formatted for submission to Global Change Biology and was in preparation with co-authors at the time of dissertation submission.

Acknowledgements

First and foremost, I am grateful to my committee for their guidance throughout this dissertation. My advisor, Paul Falkowski, pushed me to search deeper and think harder than I thought I could, and in exchange opened doors for me where doors didn't previously exist. I am most grateful that he took me on as his student. Debashish Bhattacharya and his lab group provided rigor to my attempts at bioinformatics; Debashish also showed me a true joy for research. Yair Rosenthal was a patient teacher of geochemical methods and, along with his lab, taught me a whole new definition of 'clean'. Both Yair and Rob Sherrell – who was not on my committee – were central to developing the Sr-based calcification rate method used in Chapter 4. Oscar Schofield encouraged me to think about the ecology of the biomineralization process. Throughout my dissertation, Steve Weiner has pushed me to consider how understanding coral biomineralization helps not just the coral crowd, but also the broader biomineralization community. In the end, I have probably received more from that community than I gave to them, and I am grateful to those biologists, geochemists, physical chemists, and modelers for their insights and discussions.

Work for this dissertation was conducted as part of many fruitful collaborations. Co-authors of Chapter 2 are Tali Mass, Liti Haramaty, Ehud Zelzion, Debashish Bhattacharya, and Paul Falkowski. This chapter benefited from the services and support of the Rutgers CABM Biological Mass Spectrometry Facility, Joseph Yaiullo of the Long Island Aquarium, and Frank Natale of IMCS. N. Kröger for helpful comments on an early draft of the published manuscript. Tali Mass and Udi Zelzion performed the

genetic analysis of *Stylophora pistillata* versus *Seriatopora* sp. from the IMCS aquaria for the data re-analysis.

Co-authors of Chapter 3 are Tali Mass and Paul Falkowski. Athena Fu and Mary Battle contributed to sequence data collection and drawings, respectively, for Chapter 3. Morgan Schaller and Ehud Zelzion contributed constructive discussions to the development of the manuscript for this chapter.

Co-authors of the manuscript drawing heavily on Chapter 4 are Morgan Schaller, Tali Mass, Athena Fu, Rob Sherrell, Yair Rosenthal, and Paul Falkowski. Ryan Bu and Max Gorbunov kindly contributed technical advice, while Athena Fu, Liti Haramaty, Thor Jensen, Christine Lee, and Frank Natale assisted in the laboratory and coral aquarium.

Chapter 5 was a collaborative effort with Jess Adkins of the California Institute of Technology. Yunbin Guan, at the CalTech Microanalysis Center, was a patient and knowledgeable teacher as I produced samples appropriate for NanoSIMS analysis. Athena Fu, Valentin Starovoytov, Nicolas Van Oostende, and Bess Ward provided technical assistance. I am also grateful to Beatrice Birrer and Charlene Glascock for sorting out the instrument User Agreement (and just generally for everything).

On a personal level, I am grateful to IMCS faculty and staff for indulging my apparent attempt to use every instrument in this building. The students of the Graduate Program in Oceanography and IMCS post-docs provided a supportive community for 'nerding out' as well as having fun. Specifically, Orly Levitan, Tali Mass, Mansha Seth-Pasricha, Kim Thamatrakoln have been a crucial part of my 'how do I be both a scientist and a real human being' pursuits.

The most supportive people, I am lucky to say, have been my family. My Mom and Dad have encouraged all of my scientific endeavors, no matter how far from Iowa they take me. My grandmother is an inspiration in finding what I love to do and then figuring out how to get paid for it. And to my husband and daughter, there is too much to say so I simply say thank you.

Finally, adequate financial support during graduate work is rare, so I feel incredibly lucky for and am indebted to IMCS and my advisor, committee members, and colleagues for providing an environment where I (1) didn't have to worry about paying my rent and (2) had access to fabulous research instrumentation and opportunities. IMCS provided me with a living wage and health insurance for the majority of my dissertation. Research funding for this work came from National Science Foundation grant EF1041143 to Paul Falkowski, Oscar Schofield, Rob Sherrell, and Yair Rosenthal, grant EF-1416785 to Debashish Bhattacharya, Paul Falkowski, and Tali Mass, and a Sigma Xi Grant-in-Aid-of-Research to me. Conference and workshop travel support was provided on multiple occasions by the Rutgers Graduate School – New Brunswick.

Dedication

For Luke and Clara Drake.

And for my parents, Sue and Don Gerrald, and Jim Goddard and Jackie Thompson, and my grandmother, Mary Lou Hinrichsen.

Table of Contents

List of Tables

List of Figures

Chapter 1: Thesis Introduction

Biomineralization is the process by which a living organism directly or indirectly causes a mineral to be produced (Lowenstam et al. 1989). This ranges from the sulfide minerals precipitated when H_2S released by sulfate reducing bacteria reacts with high concentration metals in the surrounding medium (e.g.;Baas Becking et al. 1961, Fortin et al. 1996, Labrenz et al. 2000) to the highly controlled production and dissolution of hydroxyl-apatite into bones and teeth by our bodies (e.g.;Kawasaki et al. 2009). The roles for biologically controlled biominerals include adhesion to a substrate, protection, cation storage, light modulation, buoyancy, and magnetic perception among others (Lowenstam et al. 1989, Mann 2001).

Biomineralization occurs across the tree of life and is prominent within eukaryotes (Figure 1.1); however, the mechanism(s) remain enigmatic. The questions that address these mechanisms for each organism cross traditional disciplinary boundaries: What biomolecules are involved? And at what time? If an organism possesses multiple cell types, which biomolecules come from which cell? What is the role of each of these biomolecules in forming the mineral, from making a concentration of relevant anions and cations through to terminating any crystallization? How do the functions of these biomolecules result in the 'vital effects' that we observe as a difference in element and isotope ratios between the source medium and the formed mineral? Answering these questions requires insights from molecular biology, bioinformatics, biochemistry, physical chemistry, and geology.

Marine calcification has been of interest over the past decade or so, as the formation and persistence of these carbonates is susceptible to ocean acidification (Feely et al. 2004, Orr et al. 2005). The geochemical perspective proposes less marine calcification due to the lowering $CaCO_3$ saturation state of seawater (Zeebe et al. 2001). Dissolved CO_2 reacts with seawater and dissociates to form bicarbonate and carbonate, releasing a proton (and lowering the pH) with each dissociation per the reaction:

$$CO_2 + H_2O \leftrightarrow H_2CO_3 \leftrightarrow HCO_3^- + H^+ \leftrightarrow CO_3^{2-} + H^+$$

The concentration of each carbonate species in seawater is a function of the pH, with the amount of bicarbonate nearly an order of magnitude higher than that of carbonate at current ocean pH (Figure 1.2). Calcium carbonate saturation state describes the observed concentrations of calcium and carbonate relative to those values at saturation, a relationship driven more by the carbonate component than by calcium:

$$\mathrm{M} = \frac{(Ca^{2+})_{obs} * (CO_3^{2-})_{obs}}{K_{sp}^*}$$

where

$$K_{sp}^* = (Ca^{2+})_{sat} + (CO_3^{2-})_{sat}$$

Hence, increased atmospheric CO_2 leads to decreased ocean pH and carbonate anion, and in turn a lower carbonate saturation state, making it harder for inorganic calcium carbonate to be formed or maintained.

In contrast, the biological view of marine mineralization suggests that, like other biominerals, marine bio-carbonates are very different from inorganic carbonates. Not only are biomolecules located on and within individual crystals (e.g.;Suzuki et al. 2009, Mass et al. 2014), but interim stabilized amorphous phases exist (Gotliv et al. 2003, Politi et al. 2008) and a nano-structure to the crystals is apparent (Cuif et al. 2008, Falini et al.

2013). Additionally, physiological and ecological experiments highlight metabolic costs that are predominantly pH-based (Hofmann et al. 2010) and suggest that the biomineralization process allows for adaptation and plasticity (Kelly et al. 2013, Munday et al. 2013). Hence, it is becoming increasingly clear that marine biomineralization is much more complex than simple inorganic mineral formation and that mineralizing organisms do not all respond in the same way to ocean acidification (Ries et al. 2009, Kroeker et al. 2010), suggesting that the 'bio' component of marine biomineralization requires better understanding.

A biological component of marine biominerals has been known for over a century (Silliman 1846, Wainwright 1963). Specifically in corals, biomolecules make up 0.1-5% of the carbonate mineral (Wainwright 1963, Cuif et al. 2004, Falini et al. 2013). The biomolecules are comprised of polysaccharides, lipids, proteins, with the protein component biased towards the two acidic amino acids aspartic and glutamic acid (Young et al. 1971, Mass et al. 2012). Although the coral skeletal organic matrix (SOM) protein complex has been immunolocalized to the calicoblastic epithelium (Puverel et al. 2005), until recently, the makeup of this complex was unknown. Using gene models (Mass et al. 2013) for the stony coral, *Seriatopora* sp., a member of a clade within *Stylophora pistillata* (Keshavmurthy et al. 2013), I sequenced the *S. pistillata* skeletal proteome (Chapter 2) by liquid chromatography coupled to tandem mass spectrometry (LC-MS/MS). Both the original work as well as a re-analysis of the LC-MS/MS data against two additional *Stylophora pistillata* and *Seriatopora hystrix* transcriptomes and a revised *Seriatopora* sp. genome reveal that coral SOM is composed largely of structural and

adhesion proteins such as cadherin, collagen, and vitellogenin, while also incorporating enzymes such as carbonic anhydrase and the low pI coral acid rich protein 4 (CARP4).

During the oral portion of my qualifying exams, my advisor, Dr. Paul Falkowski, asked me to draw a phylogenetic tree of biomineralization proteins. I told him I didn't think an analysis had been done by others to support my reproduction of such a tree on the white board. Additionally, phylogenetic trees require gene similarity between organisms. Although some vertebrates have sufficiently similar biomineralization genes – such as between *Tyrannosaurus rex* and chickens, frogs, and mice (Asara et al. 2007) – the similarities, and hence shared evolutionary histories, of marine invertebrate biomineralizers was unexamined. To address this, I performed a cluster analysis of over 1500 coral, mollusk, and sea urchin mineral-associated proteins (Chapter 3). For each phylum, the complexes of these proteins could be considered a 'toolkit', a suite of functional proteins from which organisms can draw to build their skeletons, shells, and spines. Several structural, signaling, and protein reworking proteins are conserved across phyla. In contrast, the highly acidic proteins are novel to each phylum suggesting that they evolved through convergent evolution. Additionally, other structural, adhesion, and enzymatic proteins are conserved in function but not sequence across the phyla suggesting that, for the most part, the biomineralization 'toolkits' for each group of invertebrates evolved independently but converged toward the optimal re-assignment of preexisting proteins.

Stony corals are ecologically and economically important members of coastal habitat and are thought to be highly susceptible to current anthropogenic processes including climate change and ocean acidification (White et al. 2000, Cesar et al. 2003,

Hoegh-Guldberg et al. 2007). Therefore, in addition to detailing and understanding the function of coral SOM proteins, it is important to determine how increased CO_{2atm} affects production of both SOM proteins and mineral. Gene expression by corals treated with increased CO_{2atm} has been examined (Moya et al. 2012), but without the benefit of a list of confirmed SOM proteins (Drake et al. 2013, Ramos-Silva et al. 2013). Hence, it was clear that that the effects of ocean acidification at the cellular and molecular levels required further examination.

The study of biomineralization has benefited for the past 30 years from the development of model organisms such as sea urchin larvae and mice (Benson et al. 1986, Rosati et al. 1994). A comparable system exists for corals in the form of cell cultures (Domart-Coulon et al. 2001, Helman et al. 2008, Mass et al. 2012). Although they have not been maintained for longer than one month, coral cell cultures form proto-polyps similar in structure to intact tissue, produce an extracellular matrix, and precipitate aragonite like their mother colony (Mass et al. 2012). These cell cultures can be used to study processes at the cellular and molecular levels on timescales from hours to days. Therefore, I subjected cell cultures of *S. pistillata* to four CO_2 concentrations, from 400 to 2000 ppm, and measured photosynthetic capability, SOM protein gene expression and protein production, and calcification rate from four hours to 1.5 weeks (Chapter 4). *S. pistillata* cells responded dramatically to CO_2 treatments. Protopolyps formed at low and moderate, but not at high and very high, CO_2. SOM genes were up-regulated in low to high CO_2, but most were down-regulated at very high CO_2. And calcification was not detectable at 1000 ppm CO_2 and beyond. These results highlight the molecular

machinery corals possess to maintain calcification under increased CO_2, but this machinery fails above a threshold.

A group of SOM proteins clearly important to the biomineralization process is the CARPs. Found in SOM complexes across coral families (Puverel et al. 2005, Drake et al. 2013, Ramos-Silva et al. 2013, Mass et al. 2014), the CARPs contain a high (>20%) proportion of aspartic and glutamic acids, giving them a net-negative charge and low isoelectric points (pIs). The low pIs allow them to precipitate $CaCO_3$ in vitro from seawater at both pH 8.2 and 7.6 (Mass et al. 2013). They have been immunolocalized not only to precise locations, including early mineralization zones in (e.g.) *S. pistillata* skeleton, but also within individual crystals (Mass et al. 2014). Therefore, the CARPs could act as nucleation sites (Mass et al. 2013) or inhibitors (Shiraga et al. 1992, Treccani et al. 2006), to extend existing crystals, to terminate crystal growth (Gerbaud et al. 2000), or as stabilizers of a pre-nucleation amorphous phase (Ma et al. 2007, Politi et al. 2007), nano-particle accretion (Gal et al. 2015), or liquid precursor (Olszta et al. 2003). To address the role of highly acidic proteins in the biomineralization process, I used nano-scale secondary ion mass spectrometry (NanoSIMS), with a resolution of ~60 nm, to co-localize newly formed calcium carbonate and ^{15}N-labeled aspartic acid incorporated by *S. pistillata* cell cultures (Chapter 5). Preliminary analyses reveal roles for these proteins as intracellular Ca concentrators and extracellular adhesives for cell-cell connections and secure newly formed calcium carbonate to cells and to substrate. This expands the potential role for these proteins in biomineralization.

Figure 1.1 Phylogeny of eukaryotic biomineralization focusing on calcium carbonates (C), calcium phosphates (P), and silicates (S). Reprinted from Reviews in Mineralogy and Geochemistry, Volume 54, Andrew Knoll, Biomineralization and Evolutionary History, p329-356, Figure 2, copyright 2003, with permission of Mineralogical Society of America.

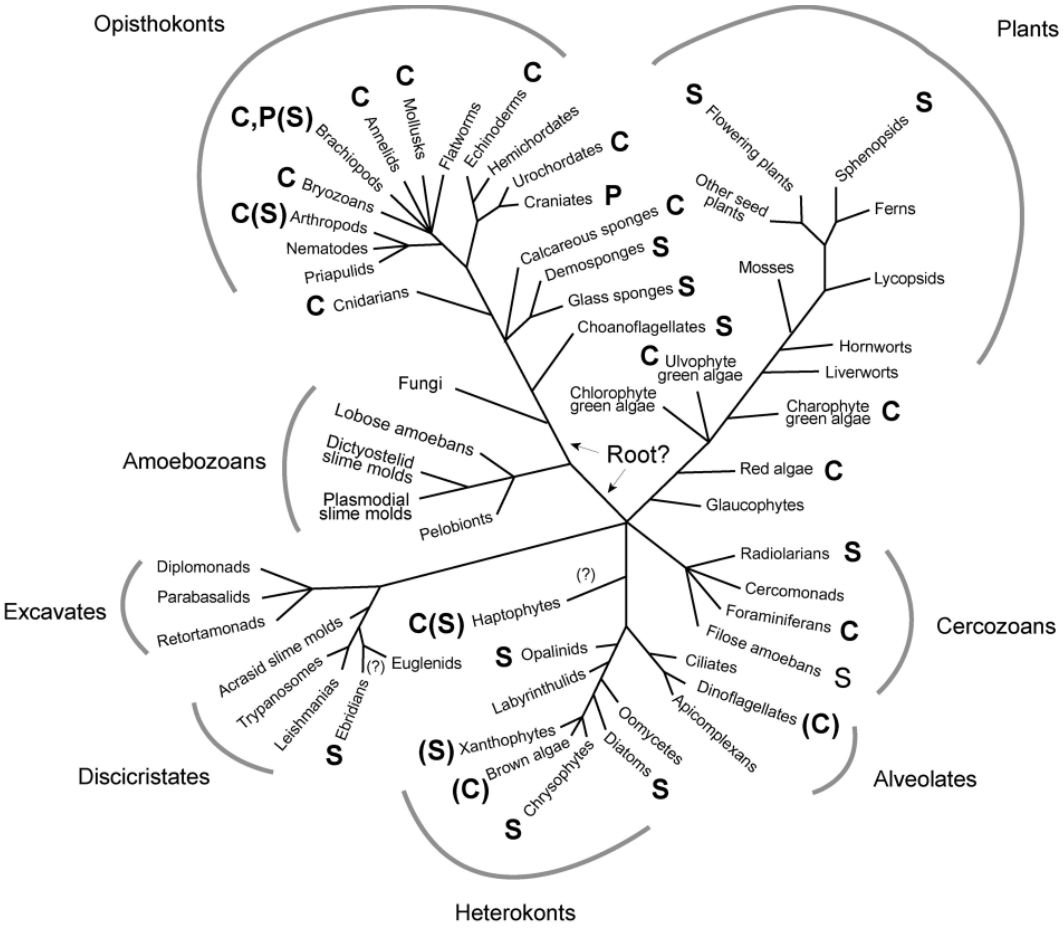

Figure 1.2. Seawater carbonate parameters. Concentrations of CO_2, HCO_3-, and CO_3^{2-} as a function of pH, including the effects of temperature and salinity. Reprinted from CO_2 in Seawater: Equilibrium, Kinetics, Isotopes, Richard E. Zeebe and Dieter Wolf-Gladrow, Chapter 1 Equilibrium, p10, Figure 1.1.4, Copyright 2001, with permission from Elsevier.

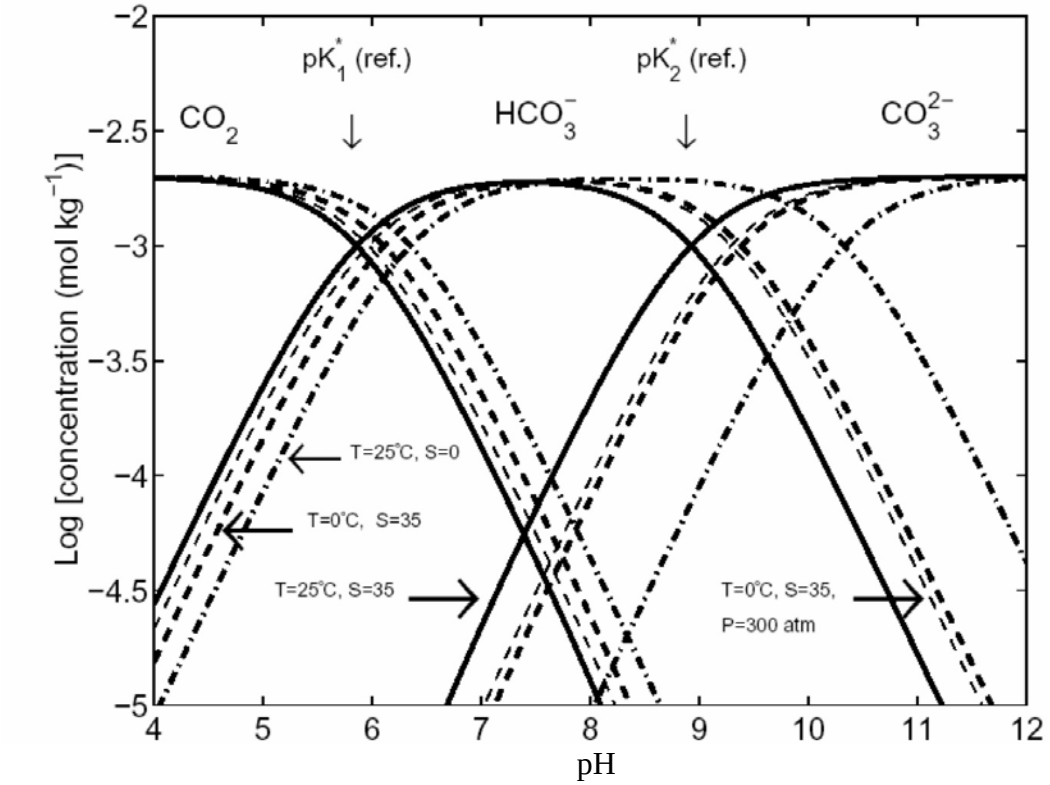

Chapter 2: Proteomic analysis of the skeletal organic matrix from the stony coral *Stylophora pistillata*

Abstract

It has long been recognized that a suite of proteins exists in coral skeletons that is critical for the oriented precipitation of calcium carbonate crystals, yet these proteins remain poorly characterized. Using liquid chromatography-tandem mass spectrometry analysis of proteins extracted from the cell free skeleton of the hermatypic coral, *Stylophora pistillata*, combined with a draft genome assembly from the cnidarian host cells of the same species, we identified 36 coral skeletal organic matrix (SOM) proteins. The proteome of the coral skeleton contains an assemblage of adhesion and structural proteins as well as two highly acidic proteins that may constitute a novel coral SOM protein sub-family. We compared the 36 SOM protein sequences to genome and transcriptome data from three other corals, three additional invertebrates, one vertebrate, and three single-celled organisms. This work represents the first extensive proteomic analysis of biomineralization-related proteins in corals from which we identify a biomineralization "toolkit" - an organic scaffold upon which aragonite crystals can be deposited in specific orientations to form a phenotypically identifiable structure.

Keywords: biomineralization, coral acid-rich proteins, collagen

2.1 Introduction

Biomineralizing organisms are found in all biological kingdoms and incorporate a variety of metals, from sodium to lead, as major components of minerals whose nucleation and growth are under a range of biological control (Lowenstam et al. 1989, Dove et al. 2003, Dobbs et al. 2004, Boorungsiman et al. 2012, Drescher et al. 2012). The skeletal organic

matrix (SOM), occluded in the mineral, has been implicated as a source of the increased strength of biominerals over comparable geominerals and has long been hypothesized to aid in the stabilization, nucleation, growth, and spatial orientation of biominerals (Wainwright 1963, Weiner et al. 1975, Addadi et al. 2006, Beniash 2011, Asenath-Smith et al. 2012). However, the mechanism(s) for the role of the SOM in coral biomineral formation remain to be elucidated, primarily because the organic molecules have yet to be characterized.

At present, the best-characterized SOM is that contained in mammalian bones and teeth and is divided into structural and highly acidic protein categories. Collagen, a well-characterized fibrillar (i.e., framework) protein, plays a structural role in mammal SOM (review in (Beniash 2011)), and has been investigated in the structural components of several coelenterates (Marks et al. 1949, Goldberg 1974), of which Order Scleractinia (i.e., stony corals) is a member. However, the greatest emphasis for nucleation proteins rests on the highly acidic proteins such as bone sialoproteins and dentin matrix proteins in teeth in vertebrates (Hunter et al. 1993, He et al. 2003). Highly acidic proteins also have been identified or hypothesized in mineralizing invertebrates, and several have recently been described, including the Asprich family in the pen shell, *Atrina rigida* (Gotliv et al. 2005), Pif and Aspein in the pearl oyster, *Pinctada fucata* (Takeuchi et al. 2008, Suzuki et al. 2009), the Adi-SAPs (highly acidic proteins proposed to be soluble and/or secreted) in the stony coral *Acropora digitifera* (Shinzato et al. 2011), and the CARPs in *Stylophora pistillata* (Mass et al. 2013). Sequence-based homologs of each have been found in a variety of other invertebrates, yet these proteins, and their consequent biomineralization reactions, appear to have originated several times independently (Knoll

2003, Murdock et al. 2011), and their sequence similarity is most likely explained by convergent evolution. Proteins containing acidic amino acids (Asp and Glu) or phosphorylation sites (on Ser residues) are thought to be used at various stages of aragonite and calcite mineralization to temporarily stabilize amorphous calcium carbonate or nucleate the mineral under appropriate conditions (review in (Marin 2007)).

Stony corals (Class Anthozoa) are early-branching metazoans composed of four cell layers (Veron 1986). Whereas the oral endodermal cells host endosymbiotic photosynthetic algae of the genus *Symbiodinium*, the aboral ectodermal cells, or calicoblastic cells, are the sites of biomineralization. Calicoblastic cells are thought to secrete SOM that adheres the cells to recently formed extracellular skeleton, and are also considered to be intimately involved in nucleation and growth of aragonite crystals (Clode et al. 2002, Goffredo et al. 2011). SOM is retained in the coral skeleton and the amino acid composition of the protein fraction indicates that the SOM is distinct from cellular or mucus protein (Young 1971, Ducklow et al. 1979). To date, only one coral SOM protein, galaxin, has been fully sequenced and its role in the biomineralization process is not well understood because it does not bind calcium (Watanabe et al. 2003). Other proteins hypothesized to play a role in the mineralizing space between the calicoblastic cells and the skeleton include carbonic anhydrases (Moya et al. 2012), collagen (Goldberg 1974), ion transporters (Kaniewska et al. 2012), cysteine-rich proteins (Sunagawa et al. 2009), von Willebrand factor type A domain-containing proteins and zona pellucidas (Hayward et al. 2011), and secreted acidic proteins (SAPs) (Sarashina et al. 2006, Shinzato et al. 2011). Together, these proteins may represent a 'biomineralization toolkit' of calcifying proteins in corals, but most remain to be

independently confirmed in coral skeleton, described as complete genes, or characterized with respect to function.

Here we use a proteomics approach to describe the SOM proteins in the widely distributed, Pocilloporid coral, *Stylophora pistillata*. Using liquid chromatography-tandem mass spectrometry (LC-MS/MS) protein sequencing and a draft genome from *S. pistillata* (Mass et al. 2013), we identify partial and complete sequences of proteins in the *S. pistillata* aragonite skeleton. Comparison of our results with genome and transcriptome data from other mineralizers suggests that a coral skeleton contains a complex group of proteins that guide the biomineralization process to form specific, genetically determined structures. This, the first proteome from a coral skeleton, identifies a 'biomineralization toolkit' in these key, ecologically critical organisms.

2.2 Results and Discussion

Thirty-six proteins from the genes predicted from the draft *S. pistillata* genome assembly were detected by three LC-MS/MS analyses of SOM proteins (Table 2.1). This is similar in number, but not sequence identity, to the 33 shell matrix proteins recently identified by LC-MS/MS from mollusk nacre (aragonite) (Marie et al. 2012). Twenty-five of the coral SOM protein candidates were only observed after deglycosylation (SI T1). 31 could be observed with tryptic digestion while the remaining five were observed only after proteinase K digestion (SI T1).

A major problem in isolating and identifying specific proteins from corals is their post-translational modification, primarily by glycosylation (Sarashina et al. 2006). Although we consistently observed five distinct protein bands in size-fractionated SOM proteins, there was always a strong background smear on silver stained polyacrylamide

gels (SI F1). Periodic acid-Schiff staining confirmed the abundance of glycans in these samples (SI F1). Hence, the results presented here are almost certainly a conservative estimate of the total number of proteins in the skeletal matrix.

Nearly all proteins detected by LC-MS/MS show similarities to proteins known to play roles in the structure and adhesion of cells (Table 2.1). We detected multiple proteins with hits (e-value $\leq 10^{-5}$) to precursor cadherins (P1, P9, P10, and P23) and von Willebrand factor (P3, P5, P13, P14, P18, P32) domains. Blast hits for other proteins include two collagens (P14, P18), three actins (P6, P7, and P11), and a carbonic anhydrase (P35), among others. Five candidate proteins exhibit poor (e-value $> 10^{-5}$) or no blast hits in NCBI (P2, P12, P15, P16, and P22). Although amino acid analyses of SOM from a variety of corals suggest that highly acidic proteins are compositionally important (Young 1971, Mass et al. 2012), we only identified two such predicted proteins by LC-MS/MS.

2.2.1 Structural Proteins

The highest scoring predicted protein, P1, is an incomplete protocadherin fat 1-like protein that contains a von Willebrand factor type A domain. We identified three separate PCR amplicons that map to this gene in *S. pistillata* cDNA, validating its expression. These transcripts encompass 11 of the 15 MS-sequenced peptides for this candidate protein (SI F2). Comparison with a very similar predicted protein from *A. digitifera* and *Favia* sp. (Table 2.1) suggests that the *S. pistillata* protein is incomplete and can be extended ~750 residues towards the N-terminus, likely containing a secretory signal, and over 1000 residues toward the C-terminus (SI T1; (Shinzato et al. 2011, Mehr

et al. 2013)). Two additional proteins among the top 10 detected also show cadherin precursor-like qualities (P9, P10; Table 2.1).

Cadherins are calcium-dependent cell-cell adhesion molecules with specificity for certain cell types such as neurons or osteoblasts (Derycke et al. 2006). Apoptotic osteoblasts and intact retinal cells can cleave the extracellular portion of their respective N-cadherins to produce a 90 kDa soluble protein that may have roles in cell survival and protein expression. In addition, they have been implicated in the aggregation of cells into which they have been cloned (Nose et al. 1988), and could help explain the proto-polyps recently observed in *S. pistillata* cell cultures (Mass et al. 2012).

Of the six detected proteins that contain von Willebrand factor type A (vWFa, an adhesion glycoprotein), four (P3, P5, P14, and P18) show strong sequence similarity between the predicted sequences from *S. pistillata* and those from *A. digitifera, Favia* sp., and *P. damicornis* (Table 2.1; SIT1; (Shinzato et al. 2011, Traylor-Knowles et al. 2011, Mehr et al. 2013)). We compared these four predicted proteins from *S. pistillata* with pre- and post-settlement genes in *A. millepora* larvae as described by Hayward et al. (Hayward et al. 2011). *A. millepora* genes A9, A90, and A102 are ≥40% similar to the P5 protein found in this study, with blastp e-values ranging from 10^{-15} - 10^{-23}. All three proteins in the *A. millepora* expression study were up-regulated in pre-settlement planulae relative to the post-settlement stage and two, A9 and A90 were localized to the aboral region post-settlement (Hayward et al. 2011). This suggests that A9, A90, and A102 – and therefore, possibly P5 – are involved in adhesion of calicoblastic cells to the skeleton. The highly acidic mollusk nacre protein, Pif, also contains a von Willebrand

factor type A, although there is no sequence similarity between Pif and the coral proteins described here (Suzuki et al. 2009).

Collagen and chitin share similar roles in biomineralizing organisms (Ehrlich 2010), although chitin would not be detectable by the procedures we used here. Two alpha collagen-like proteins were detected both before and after deglycosylation (P14 and P18, SI T1). We have confirmed the transcription of a portion of P14 by PCR amplification of *S. pistillata* cDNA, (SI F2). P14 shows strong similarities to two predicted sequences from *A. digitifera* (e-value 10^{-16}) and *Favia* sp. (e-value 10^{-41}) (Table 2.1; (Shinzato et al. 2011, Mehr et al. 2013)). Collagen, a fibrillar protein common in extracellular matrix, is generally considered as a place for non-collagenous proteins to bind and nucleate the mineral (review in (Beniash 2011)), but may also form sites of nucleation in 'holes' of packed collagen molecules (Silver et al. 2011). Although collagen has been confirmed in sea pen axial stalks (Marks et al. 1949) and gorgonian skeletons (Goldberg 1974), little work has been conducted on its presence in scleractinian skeletons. The extracellular matrix portion of coral cell cultures has been shown to positively stain for collagen (Helman et al. 2008), and so it seems highly likely that collagen-like molecules are a component of *S. pistillata* SOM.

Strong similarities were observed for a carbonic anhydrase (P35), which was found only in deglycosylated samples, and gene sequences from *P. damicornis, Favia* sp., *A. digitifera, P. maxima,* and *E. huxleyii* (Table 2.1; SI T1; (Jackson et al. 2010, Shinzato et al. 2011, Traylor-Knowles et al. 2011, Mehr et al. 2013)). The complete sequence of P35 has previously been determined, and was named *S. pistillata* carbonic anhydrase 2 (STPCA2; accession number ACE95141.1) by (Bertucci et al. 2011); it has

been immunolocalized to the cytosol of endo- and ectodermal cells of *S. pistillata* tissue slides and has a very high enzyme efficiency for interconverting HCO_3^- and metabolic CO_2 (Bertucci et al. 2011). Although SPTCA1 and STPCA2 show 35% sequence identity, peptides we detected by LC-MS/MS were unique to STPCA2. Whereas only STPCA1 has previously been localized in *S. pistillata* skeleton (Moya et al. 2008), our results strongly suggest that STPCA2 is also present in the calicoblastic space and is retained in the skeleton after mineralization. Presence of both STPCA1 and 2 in the calcifying space likely appears to be an enzymatic "bet-hedging", a strategy that permits integral pH and bicarbonate control for both coral skeleton (Venn et al. 2012) and mollusk shell (Miyamoto et al. 1996) formation.

The final structural protein of interest is a 184-amino acid, 21 kDa protein with a theoretical pI of 5.06 (P12, Table 2.1). This gene contains a secretory signal at the N-terminus, ends with a stop codon, shows significant sequence identity to a predicted protein from *Favia* sp. (Mehr et al. 2013), contains no known domains, and is predicted to have an N-linked glycosylation site at Asn-79 (Fig 2.1). Lastly, it does not contain disproportionate amounts of acidic, basic, or sulfur-bearing residues. We used PCR amplification of *S. pistillata* cDNA to confirm the correct transcription of an internal portion of P12 that contains one of the LC-MS/MS sequences (Fig. S2).

Consensus structure predictions of P12 in I-TASSER and Phyre^2 (Fig 2.1), suggest that it may be related to the secreted protein noggin that binds to and inhibits the function of some bone morphogenic proteins (BMPs), of which one, a BMP2/4 ortholog, is known to be present in coral calicoblastic cells (Zoccola et al. 2009). The predicted structure (I-TASSER : Tm-score of 0.74, root mean square deviation (RMSD) of 3.5 Å,

and query sequence coverage of 94.6%,) exhibits a -sheet portion and cystine-knot cytokine fold found in the noggin protein family (98.9% confidence by Phyre[2]). In the complete structure, disulfide bonds could occur between Cys107 and Cys144, and Cys 137 and Cys181 (Fig 2.1). The P12 sequence contains CXGC and CXC and the last Cys in the knot is immediately followed by a stop codon, which is standard for this type of fold (Vitt et al. 2001). These structure predictions suggest that P12 may have a role in inhibiting skeleton formation by blocking the coral BMP2/4 ortholog's receptor binding regions.

2.2.2 CARP Sub-Family

We have recently described a family of coral acid-rich proteins (CARPs) that were identified in the *S. pistillata* gene models (Mass et al. 2013). Two of these, CARP4 and CARP5 were sequenced by LC-MS/MS and we propose that they belong to a highly acidic sub-family of proteins that is well conserved across Order Scleractinia but appears to be absent from other known biomineralizers. Six internal peptides of CARP4 (P2) and 4 internal peptides of CARP5 (P15) were sequenced by LC-MS/MS with best sequencing following proteinase K digestion (SI F2). CARP4 and CARP5 have predicted pIs of 4.02 and 4.04, respectively. Two sites of glycosylation, Asn-98 and Asn-126, are predicted for CARP4, whereas only one, Asn-133, is predicted for CARP5 (Fig S3). Detection of CARP5 and the C-terminal end of CARP4 only in deglycosylated samples supports this prediction. Glycosylation of CARP4 is also suggested by the difference between its predicted size and that of a 55 kDa protein that was partially analyzed by Puverel et al. (Puverel et al. 2005) and which contains two internal peptides matching CARP4 (Fig S3). Additionally, anomalous migration of highly charged proteins in SDS-PAGE systems has

previously been observed for Aspein, a highly acidic molluscan protein (Takeuchi et al. 2008).

CARPs 4 and 5 exhibit significant sequence identity (31 to 85%) with predicted genes from three other stony corals (Fig S3). However, similar sequences are absent outside of Order Scleractinia (Table 2.1). Multiple sequence alignment of CARP4- and CARP5-like proteins from *P. damicornis, A. digitifera,* and *Favia* sp. reveals several highly conserved regions of this novel coral protein sub-family (Shinzato et al. 2011, Traylor-Knowles et al. 2011, Mehr et al. 2013). The general pattern appears to be a variable N-terminus followed by one highly acidic region plus a highly conserved non-acidic region; this combination of acidic-plus-non-acidic regions is then repeated before ending in a variable C-terminus (Fig 3). The duplication and then variation of the general gene pattern within each species examined could allow for redundancy in supporting the activity of the protein sub-family. A similar pattern of redundancy, but not sequence similarity, in a highly acidic protein sub-family is observed in the Asprich proteins of the mollusk, *Atrina rigida,* (Gotliv et al. 2005).

Like the Asprich protein family described by Gotliv et al (Gotliv et al. 2005) in *Atrina rigida,* we propose that the two acidic regions of the CARP sub-family in corals are templates on which calcium carbonate nucleation or growth could occur (Weiner et al. 1975). Unlike the Asprich sub-family, these CARPs contain two non-acidic, yet highly conserved regions that we propose to represent potential protein-protein interaction sites based on their degree of conservation (Fig 2.2). Binding to structural proteins described above would allow these highly acidic proteins to be arrayed in an

ordered fashion in the calcifying space for a tighter control by corals over biomineralization.

Additional, highly acidic proteins will almost certainly be found in coral skeleton by other methods. The lack of peptide sequence variability in these proteins makes them poor candidates for identification by LC-MS/MS. Hence, CARPs 4 and 5 should be considered the first, but likely not the only, acidic proteins involved in coral biomineralization.

In summary, the proteomics approach used here identified 36 proteins in *S. pistillata* SOM. Our results suggest that the *in vivo* coral SOM protein complex is laid out as follows: cadherins, integrins, contactin, and similar adhesion proteins play a dual role to: (a) constitute an extracellular matrix that adheres to newly formed skeleton and, (b) attach calicoblastic cells to this skeleton-blanketing matrix. Actins and tubulins allow for flexibility of the calicoblastic space's size and shape during aragonite crystal growth. Collagens provide a structural support within the calicoblastic space to which CARP sub-family and analogous proteins can bind as sites of mineral nucleation and growth, while at least two carbonic anhydrases mediate the subsequent carbonate chemistry effects. Mineral re-working proteins, although not found in this study, are also likely present and P12 may modulate their activity. We suggest that together, these 36 proteins constitute part of the 'biomineralization toolkit' of Order Scleractinia; some proteins may be part of the general toolkit of all calcium carbonate mineralizers (e.g., recent proteomic analyses by (Mann et al. 2010) and (Marie et al. 2012)), while others, particularly the CARP sub-family described here, are clearly limited to the aragonite precipitating corals. Whereas almost certainly more proteins will be discovered in the SOM, this initial set provides a

basis for understanding the spatial relationships between the major components within the skeleton and how their relative expression influences rates of calcification. Future expression studies of the effects of disturbance on coral biomineralization will be guided by pinpointing the spatial and temporal arrangement and function of these 36 SOM proteins in the calicoblastic space.

2.3 Methods

2.3.1 Model organism

Stylophora pistillata, a common hermatypic coral found throughout the Pacific and Indian oceans (Veron 2000), has been well studied both in situ and in laboratory settings. We grew coral nubbins at 28° C in an 800-L flow through system, as previously described (Mass et al. 2012).

SOM extraction

S. pistillata skeletons were soaked for four hours in 3% sodium hypochlorite, copiously rinsed in deionized water, and dried overnight at 60^{o}C. Dried skeletons were ground to a fine powder with an agate mortar and pestle and again bleached, rinsed, and dried. The skeletal powder was decalcified in 1 N HCl at room temperature while shaking. HCl was added gradually so that the solution reached neutral pH within 30 minutes of acid addition; more HCl was only added if skeleton powder remained after 30 minutes. pH of the decalcification solution was brought to neutral with 1 M NaOH. Water-soluble and -insoluble organic fractions were separated by centrifugation and analyzed separately. Trichloroacetic acid (TCA)-acetone precipitations were used to clean and precipitate proteins from the decalcification solution (Jiang et al. 2004). Briefly, one volume of 60% TCA was added to five volumes soluble SOM samples while

1 ml 60% TCA was added to insoluble SOM pellets. Both fractions were incubated at 4° C overnight, centrifuged at 10,000 g at 4° C for 30 min, washed twice with ice-cold 90% acetone at 4° C for 15 min, and centrifuged at 10,000 g at 4° C for 30 min. Additionally, SOM proteins were enzymatically deglycosylated with O-glycosidase, N-glycosidase F, sialidase, B1-4 galactosidase, and B-N-acetylglucosaminidase in a deglycosylation mix per manufacturer instructions (New England BioLabs Inc.).

2.3.2 Protein separation and characterization

SOM proteins were separated by SDS-PAGE and bands were visualized by silver staining (Pierce silver stain for mass spectrometry) and Periodic acid-Schiff staining (Pierce glycoprotein staining kit). Smearing of proteins in gels precluded extraction of individual bands for sequencing.

2.3.3 Proteomics

SOM complexes were digested either by trypsin or proteinase K, and masses and charges of the digested peptides were analyzed on a Thermo LTQ-Orbitrap-Velos ETD mass spectrometer with Dionex U-3000 Rapid Separation nano LC system. The LC-MS/MS data were searched using predicted gene models from *S. pistillata* (Mass et al. 2013) by X! Tandem using an in-house version of the Global Proteome Machine (GPM USB, Beavis Informatics Ltd, Winnipeg, Canada) with carbamidomethyl on cysteine as a fixed modification and oxidation of methionine and tryptophan as a variable modification (Craig et al. 2004). Spectra were also analyzed against a suite of potential microbial genomes to exclude possible microbial contamination of the dry skeleton. Data for LC-MS/MS sequenced proteins have been deposited in GenBank (Table 2.1).

2.3.4 Gene Confirmation

Internal sequences of predicted genes were confirmed in DNA and cDNA by PCR using gene-specific primers (SI T2). Holobiont DNA and cDNA were prepared as previously described from *S. pistillata* colonies maintained in in-house aquaria (Mass et al. 2012). All PCR tubes contained 0.25 μg template, 0.2 mM dNTPs, 1X High Fidelity reaction buffer, 0.5 μl of Phusion® polymerase (New England BioLabs) in a 25 μL reaction volume. Amplifications were performed in a Veriti Thermal Cycler (Applied Biosystems) at 35 cycles of 98 ºC for 10 s, primer-specific annealing temperature for 30 s, and 72 ºC for 30-180 s. PCR products were sequenced by GENEWIZ, Inc. (New Jersey, USA).

2.3.5 Bioinformatics

LC-MS/MS results were filtered to remove hits from standard contamination (common Repository of Adventitious Proteins, or cRAP, database). A non-redundant list of all proteins detected with e-values $\leq 10^{-10}$ was used for blast analysis against NCBI and to query a database we created that contains translated sequences from *Homo sapiens* (Levy et al. 2007), *Thalassiosira pseudonana* (diatom (Armbrust et al. 2004)), *Nematostella vectensis* (anemone (Sullivan et al.)), *Strongylocentrotus purpuratus* (urchin (Sea Urchin Genome Sequencing Consortium et al. 2006)), *Emiliania huxleyi* CCMP1516 (coccolithophore; draft genome), and *Acropora digitifera* (hard coral (Shinzato et al. 2011)) genomes; a transcriptome from *Pocillopora damicornis* (hard coral (Traylor-Knowles et al. 2011)); and expressed sequence tag (EST) libraries from *Favia* sp. (hard coral, (Mehr et al. 2013)), *Reticulomyxa filosa* (foraminiferan (Burki et al. 2006)), and *Pinctada maxima* (oyster, (Jackson et al. 2010)). *N. vectensis* and *R. filosa* do not

biomineralize; all other comparison species produce calcium- or silica-based minerals. Predicted proteins from the comparison species with similarities greater than 35% and e-values $\leq 10^{-10}$ were retained for further analysis.

For CARP sub-family homologs, predicted proteins in comparison species were combined if they closely mimicked matched *S. pistillata* CARPs. These combinations are noted in protein names when they are presented in the multiple sequence alignment. Residues whose conservation suggests a functional role were predicted in ConSurf (Ashkenazy et al. 2010) using CARP4 as the query sequence.

Structures of selected proteins were predicted using both I-TASSER (Roy et al. 2010) and Phyre^2 (Kelley et al. 2009). We used these two programs to obtain a consensus in structure matching, particularly in the case of one *S. pistillata* protein that showed no similarity to proteins in NCBI and contained no known domains. Images of predicted structures were generated in MacPyMOL v1.3r1 (Schrödinger LLC).

Table 2.1. *S. pistillata* SOM proteins. Thirty-six predicted proteins in *S. pistillata* SOM samples detected by LC-MS/MS and their bioinformatics analysis. Returned sequences with e-values $\leq 10^{-10}$ are presented in order of decreasing e-value. "Protein name" is the best BLAST hit in NCBI. "Gene" is the code number in our *S. pistillata* gene prediction model. The "+" and "-" represent presence and absence, respectively, of similar sequences in comparison species; [1] indicates sequence similarity is greater than 70%; [2] indicates most similar sequence by bit score; [3] indicates export signal.

Protein	Gene	Accession No.	Name	*P. damicornis*	*A. digitifera*	*Favia* sp.	*N. vectensis*	*P. maxima*	*S. purpuratus*	*E. huxleyii*	*R. filosa*	*H. sapiens*	*T. pseudonana*
P1	g11108	KC509947	Protocadherin fat-like	-	+	+[1,2,3]	+	+	-	-	-	-	-
P2	g11187	KC493647	CARP4	+	+[3]	+[2,3]	-	-	-	-	-	-	-
P3	g12510	KC342189	Thrombospondin	-	+	+[2]	+	-	-	-	-	-	-
P4	g9861	KC342190	Viral inclusion protein	+[1]	+	+[1,2]	+	-	-	-	-	-	-
P5	g11674	KC150884	Hemicentin	+	+[2]	+[3]	+[3]	+	+	-	-	+[3]	-
P6	g11666	KC149520	Actin	+[1,2]	+[1]	+[1]	+[1]	+[1]	+[1]	+[1]	+[1]	+[1]	+[1]
P7	g4601	KC342191	Actin	+[1]	+[1,3]	+[1]	+[1,2]	+[1]	+[1]	+[1]	+[1]	+[1]	+[1]
P8	g9654	KC342192	Major yolk protein	+[3]	+	+[2,3]	-	+	-	-	-	-	-
P9	g10811	KC000002	Protocadherin fat-like	-	+[3]	+[2,3]	+[3]	-	-	-	-	-	-
P10	g11107	KC509948	Cadherin	+[1]	+	+[2,3]	+	-	-	-	-	-	-
P11	g13727	KC342193	Actin	+[1]	+[1,2]	+[1]	+[1]	+[1]	+[1]	+[1]	+[1]	+[1]	+[1]
P12[3]	g2385	JX891654	-	-	-	+[2,3]	-	-	-	-	-	-	-
P13	g6918	KC342194	Sushi domain-containing	+	+[2]	+	-	-	-	-	-	-	-
P14	g9951	KC342195	Collagen - alpha	-	+	+[2]	-	-	-	-	-	-	-
P15	g1532	KC493648	CARP5	-	+[3]	+[2,3]	-	-	-	-	-	-	-
P16	g11702	KC342196	-	-	+[2]	+[1]	+	-	-	-	-	-	-
P17	g12472	KC149521	Glyceraldehyde 3-phosphatase dehydrogenase	+[1]	+[1,2]	+[1]	+[1]	+	+	+	+	+[1]	+
P18	g810	KC342197	Collagen - alpha	-	+	+[2]	+	-	-	-	-	-	-
P19	g20041	KC342198	Contactin-associated protein	-	+	+[2,3]	+	-	-	-	-	-	-
P20	g6066	KC342199	MAM domain anchor protein	+	+[2,3]	+[1]	+	-	-	+	-	+[3]	-
P21	g18277	KC479163	Zona pellucida	+[1,2,3]	+	+[1,3]	+	-	-	-	-	-	-
P22	g19762	KC493649	-	-	-	-	-	-	-	-	-	-	-
P23	g1057	KC000004	Protocadherin	+	+	+[1]	+[2]	+	+	-	-	-	-
P24	g15888	KC479164	Vitellogenin	-	+	+[1,2,3]	-	-	-	-	-	-	-
P25	g11220	KC479165	Ubiquitin	+[1]	+[1,3]	+[1]	+[1,2]	+[1]	+[1]	+[1]	+[1]	+[1]	+[1]

P26	g1441	KC479166	Vitellogenin	+	-	+[2,3]	-	-	-	-	-	-	-
P27	g18472	KC479167	Integrin - alpha	+[1]	+	+[2,3]	-	-	-	-	-	-	-
P28	g11651	KC149519	Late embryogenesis protein	+[2]	-	-	-	-	-	-	-	-	-
P29	g13377	KC479168	Tubulin - beta	+[1]	+[1]	+[1,2]	+[1]	+[1]	+[1]	+[1]	+[1]	+[1]	+
P30	g11056	KC000003	Myosin regulatory light chain	+[1]	+	+[2,3]	-	+	-	-	-	-	-
P31	g20420	KC479169	Neurexin	-	+	+[2,3]	-	-	-	-	-	-	-
P32	g5540	KC479170	Kielin/chordin llke	+[1,2]	+[3]	+[3]	-	-	-	-	-	+[3]	-
P33	g8985	KC479171	Flagellar associated protein	+[1,2]	+[1]	+[1]	+	-	-	-	-	-	-
P34	g1714	KC479172	MAM/LDL receptor domain containing protein	+	+[3]	+[1,2]	+	-	+	+	-	+	-
P35	g7349	EU532164.1	Carbonic anhydrase (STPCA2)	+[1,2]	+[3]	+	-	+	-	-	-	+	-
P36	g13890	KC479173	Zonadhesion-like precursor	+	+[1,2,3]	+	+[1]	-	+	-	-	-	-

Figure 2.1. Predicted structure of P12, a potential BMP inhibitor. The amino acid sequence (above) and predicted secondary structure (below) of a novel SOM protein after cleavage of the export signal peptide. For the sequence, peptides sequenced by LC-MS/MS are colored orange; translated sequence confirmed from PCR amplification of *S. pistillata* cDNA is underlined; STOP codon is marked with *; the predicted glycosylation site, Asn79 is indicated by a '+'. In the structure, the N-terminal region corresponding to a potential binding site with a bone morphogenic protein is shown in blue, Cys potentially involved in a cystine knot fold disulfide bonds between Cys107 and Cys144, and Cys 137 and Cys181 are colored red.

a.

DETENKCSQTTITEAKDHLRLNGGGPLGTYNENYMAFTLDEVRTNFKNLLTLQPGNFSALAAW

APLSFPATLESGACVKDSGNCEGCPVVKDLGANYYPRFLNEVNCKSSGQICGQGLGECRTSVKS

QRFFRDPSTDLSTCNKDLEEYYYDMEMCCQCMLL*

b.

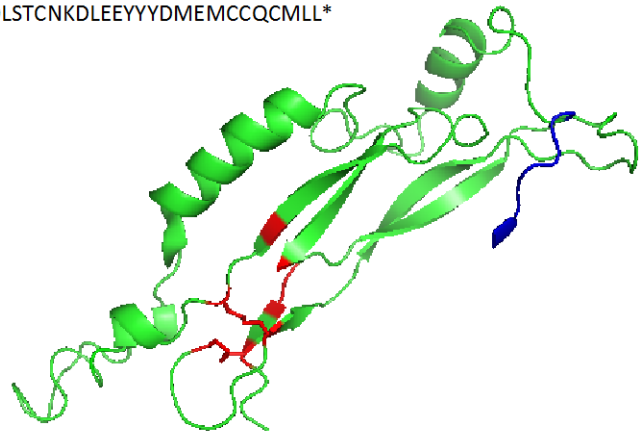

Figure 2.2. CARP4 sub-family general pattern. (a) Conservation of residues in the CARP sub-family as predicted by ConSurf, with CARP4 as the query. Warmer (more red) and cooler (more blue) colors represent conserved and variable amino acid positions, respectively. Residues are predicted to be exposed (e), buried (b), functional (i.e., highly conserved and exposed; f), or structural (i.e., highly conserved and buried, s). Numbers indicate residue number of CARP4. (b) Schematic of the CARP sub-family of SOM proteins. An N-terminal variable region is followed by a repeat of a highly acidic region plus a highly conserved non-acidic region; the C-terminus is variable.

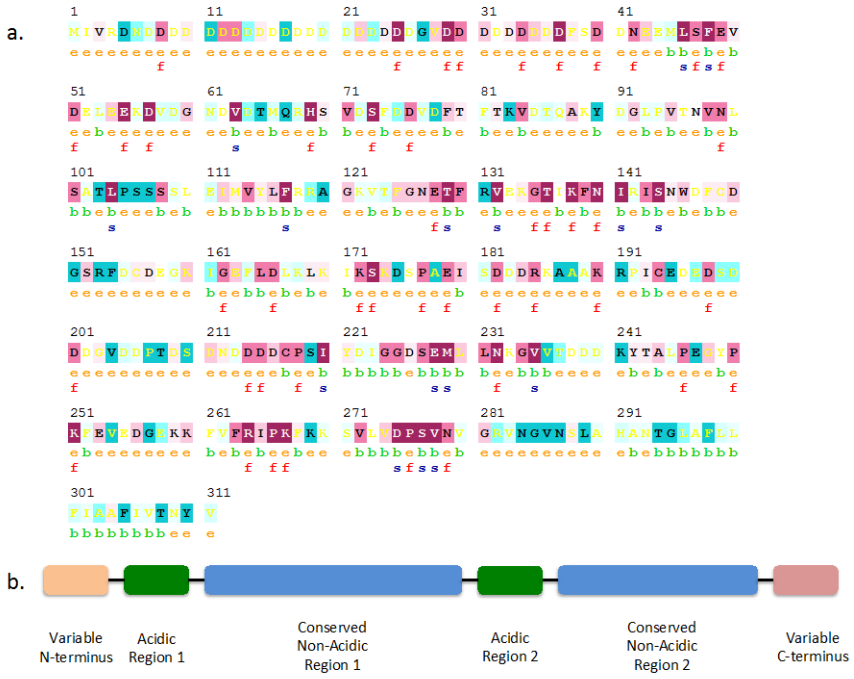

2.4 Supplementary Information

Supplementary information can be obtained from the publisher at http://www.pnas.org/content/suppl/2013/02/19/1301419110.DCSupplemental.

Supplementary Figure 1. SOM proteins separated by SDS-PAGE. (a) Silver staining and (b) Periodic acid-Schiff (PAS) staining of SOM proteins from decalcified *S. pistillata* skeleton. Silver staining (a) was performed on glycosylated soluble SOM (lane 2). PAS staining (b) was performed on glycosylated soluble (lane 2) and insoluble (lane 3) SOM, and deglycosylated soluble (lane 4) and insoluble (lane 5) SOM. Lane 1 of each gel contains molecular weight standards; numbers indicate kDa. Arrows indicate protein bands.

Supplementary Figure 2. Predicted amino acid sequences of 36 *S. pistillata* proteins. Peptides detected by LC-MS/MS after tryptic digestion are in bold and after Proteinase K digestion are *underlined*. Translations of internal sequences confirmed by PCR amplification of *S. pistillata* cDNA using gene-specific primers are highlighted. Discrepancies between the predicted sequence and that determined by translation of PCR product are in red. The secretion signal peptide of P12, STPnv1, is ~~crossed out~~ over the portion that is predicted to be cleaved prior to secretion.

Supplementary Figure 3. Multiple sequence alignment. Aligned sequences of CARP4 and CARP5, two highly acidic predicted proteins detected by LC-MS/MS analysis of deglycosylated *S. pistillata* SOM, and similar proteins from an *A, digitifera* genome, a *Favia* sp. EST library, and a *P. damicornis* transcriptome. Identical amino acids are highlighted in gray. Dashes represent gaps. Yellow highlight residues were previously determined by N-terminal sequencing by (Puverel et al. 2005). Blue stars denote predicted glycosylation sites of CARP4.

Supplementary Table 1. Putative homologous proteins from other mineralizers or related organisms. The most similar predicted protein sequence from each comparison organism is given. Lack of a similar protein sequence for a given species is noted as "-".

Supplementary Table 2. SOM protein primer sets. Gene specific primers used to confirm the DNA and cDNA sequences of selected SOM proteins.

2.5 Data Re-analysis with additional gene models

Introduction

New gene model information for our organism of interest, *Stylophora pistillata*, allows for a reanalysis of the *S. pistillata* skeletal proteome. This reanalysis was undertaken for several reasons. First, the gene models used in the original skeletal organic matrix (SOM) proteome analysis were sequenced from *Seriatopora* sp., rather than *Stylophora pistillata.* Determination of coral species is typically done morphologically, and the candidate nubbin for the original genome sequencing clearly appears to be *S. pistillata* rather than *Seriatopora* sp. (Figure 2.3). However, Cytochrome Oxidase I and Internal Transcribed Spacer PCR amplification and sequencing places our genome source within *Seriatopora* sp. but the coral skeleton, likely sourced from an Australian parent colony, within *S. pistillata* Clade 1 (Figure 2.4). The gene models are still appropriate for the original analysis of *S. pistillata* proteomes, however, as it has been shown that the genus Seriatopora is actually a clade within *Stylophora pistillata* (Keshavmurthy et al. 2013).

Second, the transcriptome used to sequence the *S. pistillata* SOM proteins was incomplete. For instance, the highly abundant SOM protein, protocadherin, was predicted in the original *Seriatopora* sp. transcriptome as at least two separate genes (g11107 and g11108) that exhibited strong sequence similarity to the same gene in other corals (Drake et al. 2013 SI Table1). Third, all but one of the predicted genes from the original *Seriatopora* sp. genome lacked N-termini and stop codons. Fourth, a clear homologue for galaxin, the first SOM protein sequenced from a stony coral (Fukuda et al. 2003), and one of the SOM proteins sequenced from *Acropora millepora* skeleton (Ramos-Silva et al. 2013), was lacking from not just the *S. pistillata* skeletal proteome

but from the entire *Seriatopora* sp. genome. Hence, when two similar *Stylophora/Seriatopora* transcriptomes became available, all LC-MS/MS data were re-analyzed against these three novel gene models.

Methods

All eight LC-MS/MS output datasets were re-analyzed against the original *Seriatopora* sp. genome (Mass et al. 2013), and against *Stylophora pistillata* (Liew et al. 2014), and *Seriatopora hystrix* ((http://people.oregonstate.edu/~meyere/data.html) transcriptome-based gene models by X!Tandem on an in-house version of the Global Proteome Machine (GPM USB; Beavis Informatics) with the same parameters as the original in silico analyses (Drake et al. 2013). Gene models were refined from their source datasets to remove sequences <300 bp, protein duplicates, and likely *Symbiodinium* spp. contaminants (Bhattacharya et al. in review), with the output obtainable from http://comparative.reefgenomics.org/datasets.html. X!Tandem parameters included carbamidomethyl on cysteine as a fixed modification and oxidation of methionine and tryptophan as a variable modification. This returned a list of 84 proteins. Redundant potential SOM proteins from across the three transcriptomes were removed after a blast all-versus-all analysis, leaving 60 proteins.

The list of non-redundant proteins was then screened for potential human contaminants. Proteins were blasted against the NCBI *Homo sapiens* nr database (taxid: 9606); any sequence with both >50% coverage and >50% sequence identity between the proposed coral protein and the *H. sapiens* BLAST hit were removed. These proteins included ATP synthase, actin, and ubiquitin among others (Table 2.2). 49 proteins remained as potential SOM genes.

Finally, a conservative screening was applied to remove proteins that may have resulted from cellular contamination (see discussion below). All potential human contaminants resulted from three of the eight samples submitted for LC-MS/MS sequencing. Because several of these proteins are clearly intracellular, for example cytochrome c and ATP synthase, they could also represent cellular contamination. It was then assumed that other proteins in the three analyses that generated the contaminant list may also be cellular contaminants, but that proteins sequenced from the other five analyses are not cellular contaminants. Therefore, any protein that was only sequenced from one or more of the three potentially cellular protein-contaminated analyses may also be cellular proteins and were removed from the final list of SOM proteins (Table 2.3), leaving 32 likely SOM candidates. This screening probably also removes valid SOM proteins.

Results

The extended transcriptome search and refined processing to remove contaminants returned 32 likely SOM proteins (Table 2.4). Of the original list of *S. pistillata* SOM proteins (Drake et al. 2013), 25 SOM proteins appear robust after this reanalysis. Additionally, 14 of these proteins have homologues also sequenced from *A. millepora* skeleton (Ramos-Silva et al. 2013). However, this analysis removed three actins and a ubiquitin as potential *H. sapiens* contamination, and multiple adhesion proteins as potential cellular contamination.

Discussion

Reanalysis of the *S. pistillata* skeletal proteome LC-MS/MS data against three novel *S. pistillata* and genus-*Seriatopora* gene models supports the majority of the original SOM

proteins while clarifying proteins that were originally predicted as separate partial sequences. Protocadherin Fat 4-like protein was found in both HCl-soluble and –insoluble fractions with and without deglycosylation treatment; hence, this very large predicated protein is likely glycosylated and may be present in multiple cleavage states (Paradies et al. 1993) that affect its solubility. Post-translational cleavage modification may also explain why this protein is found in skeletal crystals of differing solubilities produced at different times over the day (Mass et al. 2014).

A structural-adhesive complex remains an integral component of the SOM under this conservative approach. Transmembrane proteins such as integrins and cadherins likely interact with collagens, hemicentin, and LDL receptor among others to form and modulate the calcifying region (Mass et al. 2014). Additionally, functional proteins such as CARP4 and carbonic anhydrase are clearly important at various stages of the biomineralization process.

The main differences between the original analysis of *S. pistillata* SOM proteins and the current reanalysis are two-fold. First, 12 SOM protein candidates were added. These include a cubulin-like protein, neural cell adhesion molecule, ependymin-like precursor, and a neuroglian-like protein. These represent additional extracellular and membrane-associated proteins known to have roles in cell adhesion.

Secondly, controversial proteins such as actin and ubiquitin (Ramos-Silva et al. 2013) were removed from the final SOM protein list as potential contaminants from human contact with the samples. Their removal stems from the high sequence conservation for these proteins with those from *H. sapiens*. This does not mean, however, that these proteins have no reason to be included as SOM protein candidates.

Reduced SOM incorporation into coral skeleton has been noted when cytoskeletal (i.e., actin) polymerization is inhibited (Allemand et al. 1998), and biomineralization in other organisms does appear to utilize actin (Hildebrand et al. 2008.) In fact, recent analysis of the brachiopod *Magellania venosa* shell proteome detected very high amounts of actin by mass spectrometry sequencing, convincing the authors that the actin is indeed derived from the mollusk rather than from human contamination (Jackson et al. 2015). Additionally, ubiquitylation of biomineralization proteins is known in mollusks (Fang et al. 2012) and diatoms (Hazelaar et al. 2003) as a mechanism to remove proteinaceous structural supports.

Other proteins that could be considered cellular contamination were also removed as potential human contaminants based on strong sequence homology between corals and *H. sapiens*. These include the mitochondrial proteins cytochrome c, succinyl-coA synthetase, and ATP synthase. Non-conserved proteins such as nuclear histones and demethylases are absent from this re-analysis, supporting the supposition that these contaminating proteins are human-derived rather than coral cell-derived.

Multiple viable SOM protein candidates were removed after they were only detected in LC-MS/MS analyses that also returned likely *H. sapiens* contaminants (Table 2.3). The only potential cellular contaminant in this list is a deoxyribunclease. However, extracellular deoxyribonucleases are known from fungi (Cazin et al. 1969, Desai et al. 2000). In fact, fungal extracellular nuclease activity has been correlated with urease activity (Cazin et al. 1969) and urease activity is known in corals (Barnes et al. 1976). Therefore, there is no clear indication of coral cellular contamination from these analyses.

Conclusions

After an in silico re-analysis of the *S. pistillata* skeletal proteome against three *Stylophora*/*Seriatopora* gene models, the majority of the original list of SOM proteins remains robust. Many of the predicted protein sequences have been extended by inclusion of the additional transcriptome data. It is clear from both the original analysis as well as this re-examination that structural and adhesion proteins dominate the SOM protein complex, while enzymes such as CARP4 and STPCA2 remain important players in the biomineralization process.

Table 2.2. Potential contaminant SOM proteins removed from LC-MS/MS protein sequencing results based on high sequence conservation with similar genes in *H. sapiens*.

Name	Reference Species	Reference Gene ID
peptidyl-prolyl cis-trans isomerase	*Stylophora pistillata*	20350
cytochrome c	*Seriatopora* sp.	3633
succinyl-coA synthetase	*Seriatopora* sp.	32134
ATP synthase	*Seriatopora* sp.	28608
ATP synthase	*Seriatopora* sp.	28606
ATP synthase	*Seriatopora* sp.	24911
acetylglucosanyl asparaginase	*Seriatopora hystrix*	29635
actin	*Seriatopora hystrix*	4601
ubiquitin	*Seriatopora hystrix*	7482

Table 2.3. Additional potential SOM proteins removed from LC-MS/MS protein sequencing results because they were only sequenced from samples also containing likely *H. sapiens* contamination.

Name	Reference Species	Reference Gene ID	Previous *Seriatopora* sp. Gene ID	*A. millepora* Gene ID
deoxyribonuclease I	*Stylophora pistillata*	2778	-	-
protocadherin 16-like	*Stylophora pistillata*	13174	g1057	JT011093
plexin domain-containing protein	*Stylophora pistillata*	192	-	-
polycystic kidney disease protein	*Stylophora pistillata*	2480	-	JR991141
protein sidekick	*Stylophora pistillata*	14133	-	-
disintigrin/metalloproteinase domain-containing protein	*Stylophora pistillata*	21790	-	-
nidogen-2/collagen alpha	*Stylophora pistillata*	8994	-	-
MAM and LDL-receptor protein	*Seriatopora* sp.	3633	g11651	JT011118/ JR994474
late embryogenesis protein	*Seriatopora* sp.	29675	g11651	-
molecular chaperone GroEL	*Seriatopora* sp.	37848	-	-
B-cell receptor CD22	*Seriatopora hystrix*	8775	-	-
calsyntenin-1-like	*Seriatopora hystrix*	41581	-	-
uncharacterized protein	*Seriatopora hystrix*	54301	g9654	-
major yolk protein/melanotransferrin	*Seriatopora hystrix*	12216	-	-
hypothetical protein	*Seriatopora hystrix*	83695	g8985	-

Table 2.4. Final list of 32 *S. pistillata* SOM proteins, after re-analysis of LC-MS/MS spectra against *Stylophora pistillata*, *Seriatopora* sp., and *Seriatopora hystrix* gene models, and with stringent culling of potential contaminants.

Protein #	Name	Reference Species	Reference Gene ID	Previous *Seriatopora* sp. Gene ID	*A. millepora* Gene ID	Signal Peptide?
1	protocadherin Fat 4 isoform	*Stylophora pistillata*	975	g11108/g11107 /g10811/9861	JT011093	Y
2	hypothetical protein	*Stylophora pistillata*	8932	g12510/g9951/ g810/g11674	JT016638	no N terminus
3	hypothetical protein	*Stylophora pistillata*	17591	g18472	JR972076	no N terminus
4	mucin-like	*Stylophora pistillata*	20241	g6918	JR987773	no N terminus
5	hypothetical protein	*Stylophora pistillata*	15729	g2385	-	Y
6	collagen alpha	*Stylophora pistillata*	13704	g810	JT016638	no N terminus
7	integrin alpha	*Stylophora pistillata*	7948	-	-	no N terminus
8	CARP4/CARP5	*Stylophora pistillata*	16791	g11187/g1532	JT001945/ JR991407	no N terminus
9	cubulin-like	*Stylophora pistillata*	5078	-	-	no N terminus
10	MAM and LDL-receptor class A domain-containing protein	*Stylophora pistillata*	8833	g1714/g13890/ g6066	JT011118/ JR994474	no N terminus
11	hypothetical protein	*Stylophora pistillata*	16744	-	-	N
12	otoancorin-like	*Stylophora pistillata*	1774	g11702	-	N
13	neural cell adhesion molecule	*Stylophora pistillata*	19889	-	-	N
14	complement component 3	*Stylophora pistillata*	5083	-	-	Y
15	pancreatic lipase-related protein	*Stylophora pistillata*	5106	-	-	no N terminus
16	hemicentin-1	*Stylophora pistillata*	3888	-	JT016638	Y
17	hypothetical protein	*Stylophora pistillata*	16743	-	-	Y
18	sporulation-specific protein/viarl A-type inclusion protein	*Stylophora pistillata*	4520	g9861	-	N
19	otoancorin	*Stylophora pistillata*	1773	g11702	-	Y
20	low-density lipoprotein receptor-related protein	*Stylophora pistillata*	18934	-	-	no N terminus
21	predicted protein	*Stylophora pistillata*	8073	-	JT016638	no N terminus
22	protein kinase C-binding protein	*Stylophora pistillata*	15964	g5540	-	Y
23	collagen alpha	*Stylophora pistillata*	8774	-	JT016638	no N terminus
24	major yolk protein/melanotransferrin	*Seriatopora* sp.	10942	g9654	-	N

25	vitellogenin-like	*Seriatopora* sp.	11941	g15888/g1441	-	N
26	contactin-associated/neurexin	*Seriatopora hystrix*	11636	g20420/g20041	JR980881	Y
27	STPCA2	*Seriatopora hystrix*	50892	g7349	JR998014	Y
28	ependymin-like precursor	*Seriatopora hystrix*	52650	-	-	no N terminus
29	CUB and zona pellucida-like domain	*Seriatopora hystrix*	47732	g18277	JN631095	Y
30	neuroglian isoform	*Seriatopora hystrix*	96486	-	JR993827	no N terminus
31	-	*Seriatopora hystrix*	19619	-	-	no N terminus

Figure 2.3. Corals used for SOM proteome sequencing. (A) *Stylophora pistillata* parent colony from which skeletons were obtained for SOM protein sequencing. (B & C) *Seriatopora* sp. parent colonies from which DNA was obtained for genome sequencing; nubbins were grown in separate systems as backup, hence the variable coloring and morphology. (D) *Seriatopora hystrix* colony. Note how, morphologically, *Seriatopora* sp. parent colony resembles *S. pistillata* rather than *Seriatopora hystrix*.


A

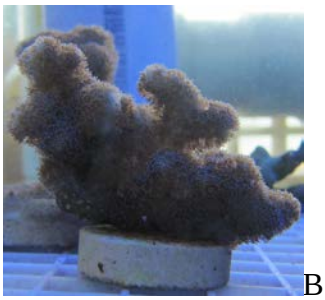
B


C


D

Figure 2.4. Phylogenetic trees of (A) COI-1 and (B) ITS, placing the parent colony for the Rutgers-based coral genome sequencing ('Tali') within the genus *Seriatopora* sp. Skeleton used for skeletal proteome sequencing falls within *S. pistillata* Clade 1 from Australia **('Brown_Stylophora').** Trees generated in RAxML by Ehud Zelzion using sequences available from (Keshavmurthy et al. 2013) and novel sequences from PCR amplification by Tali Mass and Jeana Drake, with sequencing by GeneWiz, Inc.

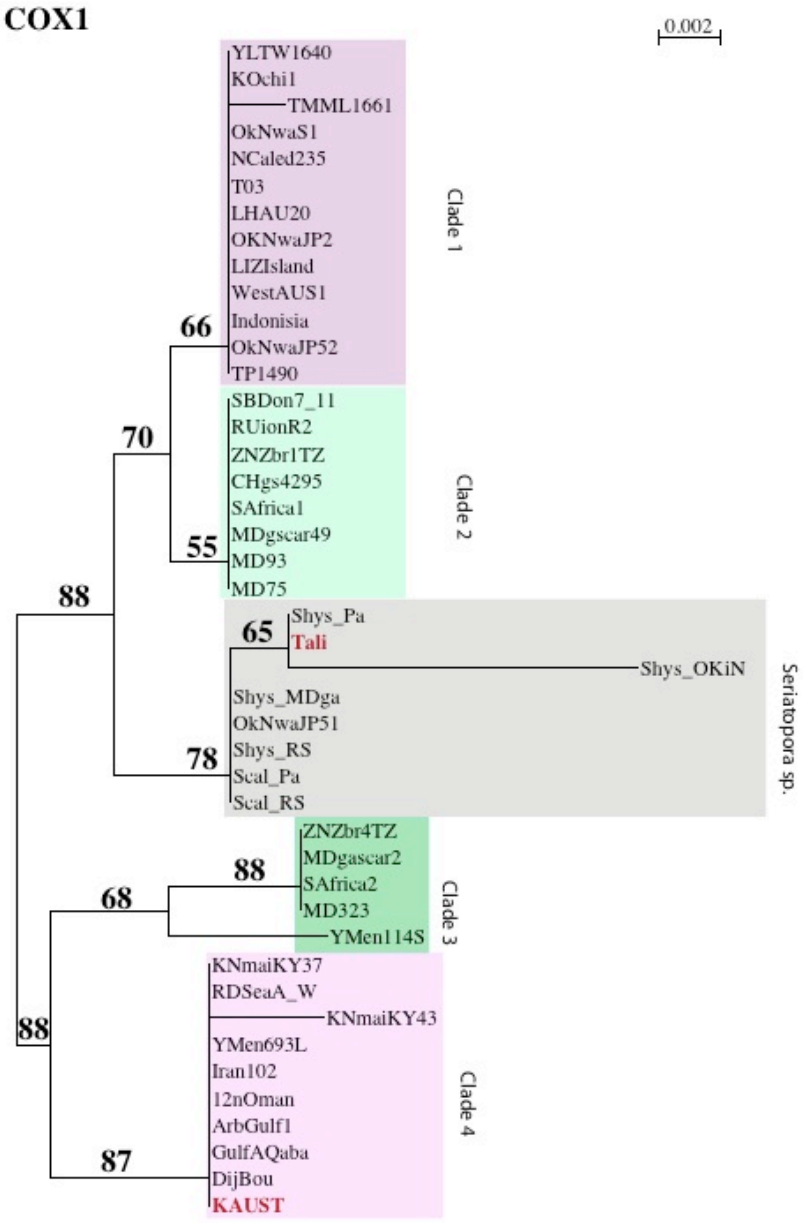

A

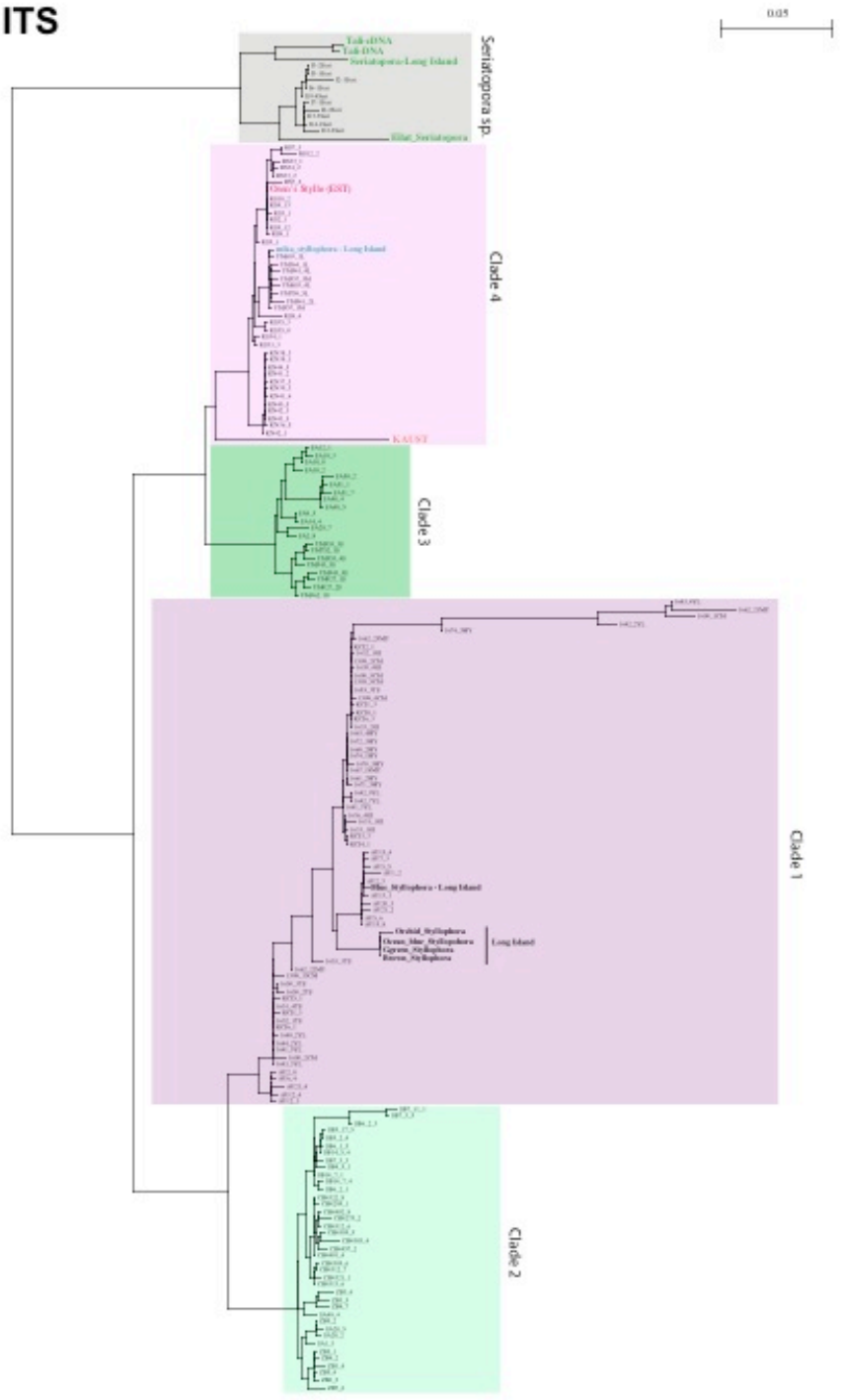
ITS
0.05
Tali rDNA
Tali DNA
Seriatopora sp.
Clade 4
Clade 3
Clade 1
Clade 2
Long Island

B

Chapter 3: The evolution and future of carbonate precipitation in marine invertebrates: Witnessing extinction or documenting resilience in the Anthropocene?

Abstract

Morphological and phylogenetic analyses suggest that the ability to precipitate carbonates evolved several times in marine invertebrates in the past 600 million years. Over the past decade, there has been a profusion of genomic, transcriptomic, and proteomic analyses of calcifying representatives from three metazoan phyla: Cnidaria, Echinodermata, and Mollusca. Based on this information, we compared proteins intimately associated with precipitated calcium carbonate in these three phyla. Specifically, we used a cluster analysis and gene ontology approach to compare ~1500 proteins, from over 100 studies, extracted from calcium carbonates in stony corals, in bivalve and gastropod mollusks, and in adult and larval sea urchins to identify common motifs and differences. Our analysis suggests that there are few sequence similarities across all three phyla, supporting the independent evolution of biomineralization. However, there are core sets of conserved motifs in all three phyla we examined. These motifs include acidic proteins that appear to be responsible for the nucleation reaction as well as inhibition; structural and adhesion proteins that determine spatial patterning; and signaling proteins that modify enzymatic activities. Based on this analysis and the fossil record, we propose that biomineralization is an extremely robust and highly controlled process in metazoans that can withstand extremes in pH predicted for the coming century, similar to their persistence through the Paleocene-Eocene Thermal Maximum (~55 Mya).

Keywords: biomineralization, metazoan, ocean acidification

3.1 Introduction

The cumulative and continuing emissions of anthropogenic emissions of CO_2 since the beginning of the industrial revolution are projected to decrease the pH of the surface oceans between 0.24 and 0.55 pH units by the year 2100 (2007), leading to a nearly 50% drop in carbonate ion concentration (Feely et al. 2009). It has also been suggested that the average pH decrease and overall diel pH variability could be even more pronounced in specific areas, such as coastal seas (Jury et al. 2013, Melzner et al. 2013). The change in carbonate chemistry potentially could result in a decreased ability for marine organisms to precipitate $CaCO_3$ (Doney et al. 2009), and has been experimentally correlated with reduced calcification rates as well as changes in ecosystem structure (Gazeau et al. 2007, Anthony et al. 2008, Cohen et al. 2009, Sheppard Brennand et al. 2010). However, the effects of ocean acidification on calcifying marine invertebrates are not consistent and suggest a degree of physiological acclimation and potential genetic adaptation (Fine et al. 2007, Ries et al. 2009, Kelly et al. 2013, Shamberger et al. 2014). One suggested mechanism for the retention of biological calcification is low-pCO_2 refugia (Tittensor et al. 2010, Manzello et al. 2012). While processes responsible for carbonate precipitation in marine invertebrates are not completely understood, we suggest that a specific suite of proteins allows biomineralization to persist in these organisms even under low pH conditions.

Although biomineralization is a common phenomenon across the tree of life, it is difficult to reduce the process to simple, general principles (Lowenstam et al. 1989, Dove et al. 2003, Müller 2011). By far, the most common biominerals produced in the contemporary ocean are calcium carbonates, especially aragonite and calcite. Although the two ingredients required to produce these mineral forms, calcium and bicarbonate

ions, are present in seawater in excess of 10 and 2 mM, respectively, $CaCO_3$ does not spontaneously precipitate in the contemporary ocean. The precipitation reaction requires catalysis by living organisms to overcome kinetic barriers.

The carbonate structures formed by metazoans are often well preserved in the fossil record. Their elemental and isotopic compositions have been extremely helpful in reconstructing the thermal and chemical history of the ocean. Carbonates themselves have been examined at different stages of the biomineralization process in marine invertebrates. For more than 50 years, it has been generally understood that the precipitation and organization of biominerals is modulated by specific biomolecules, especially proteins (Müller 2011). However, how the proteins function to facilitate the precipitation of minerals in marine invertebrates is poorly understood.

Over the past decade there has been a proliferation in the number of genomes and transcriptomes of mineralizing invertebrates (Jackson et al. 2006, Sea Urchin Genome Sequencing Consortium et al. 2006, Joubert et al. 2010, Shinzato et al. 2011, Traylor-Knowles et al. 2011, Takeuchi et al. 2012). These data sets have allowed numerous studies of the proteomes of sea urchin teeth and spicules, mollusk shells, and most recently coral skeletons (e.g., (Mann et al. 2008, Mann et al. 2008, Mann et al. 2010, Marie et al. 2010, Marie et al. 2011, Marie et al. 2011, Zhang et al. 2012, Drake et al. 2013, Marin et al. 2013, Ramos-Silva et al. 2013)). We are poised to compare the evolutionary history of biomineralizers in the fossil record (Knoll 2003) with this developing biochemical and molecular biological understanding of how the minerals are formed by the animals.

Here we review over 100 studies in a search for similarities between marine invertebrate carbonate organic matrix (COM) proteins that have been identified through genomics, transcriptomics, and proteomics. We focus on stony corals (Cnidaria), bivalve and gastropod mollusks (Mollusca), and sea urchins (Echinodermata), thereby covering representatives from three widely divergent metazoan phyla. We first outline the physiology and known biomineralization processes in each phylum, then detail the COM protein groups conserved, if not in sequence, then in function. Finally, we discuss the effects of impending ocean acidification on both the function of some of these COM proteins as well as the continuation of these organisms.

3.2 Background and context for biomineralization in the three invertebrate phyla

Despite their shared use of $CaCO_3$, evolutionary evidence suggests that biomineralization evolved independently several times across the tree of life (Knoll 2003, Murdock et al. 2011). Over the ~700 million years during which Cnidaria, Mollusca, and Echinodermata diverged from shared ancestors (Erwin et al. 2011), biomineralization was selected to support several functions. The first is as a substrate for growth. In modern stony corals, precipitation of aragonite allows for growth of the thin film of animal on a hard, continuous substrate. The process begins when larvae settle and colonies adhere to a benthic matrix. In contrast, bivalve and gastropod mollusks precipitate aragonite and/or calcite shells as a protective wall surrounding soft tissues. These structures are very effective in defending against predators. In sea urchins, calcitic spines are also a deterrent to predators, but being relatively light, they do not interfere with motility of the animal.

3.2.1 Body plan and calcifying tissues

Coral

Stony corals in the phylum Cnidaria are some of the earliest known metazoans to precipitate calcium carbonate (Knoll 2003). Cnidaria also contain Order Alcyonacea, or soft corals, which, unlike stony corals, produce small internal sclerites, or ~ mm-sized calcite plates. In Paleozoic time, stony coral structures appear to have been formed primarily from the precipitation of calcite, whereas over the past ~ 250 Ma, with the appearance of Scleractinian corals, these organisms have evolved a *de novo* aragonite precipitation process (Porter 2010). This period also broadly corresponds to their transition as host animals to symbiotic photosynthetic dinoflagellates of the genus *Symbiodinium* (Stanley et al. 2009, Tchernov et al. 2012). While some corals that lack symbionts can produce $CaCO_3$ skeletons, the builders of the relatively rapidly accreting massive reefs observable from space are hermatypic, or symbiont-containing.

Up to 90% of the carbon requirement of the coral host is translocated in the form of glycerol and/or glucose from *Symbiodinium* spp. (Falkowski et al. 1984, Burriesci et al. 2012); additionally, corals can obtain nitrogen and phosphorus by feeding on dissolved and particulate matter from the overlying water supply (reviewed byHoulbrèque et al. 2009). Some of the energy in the translocated carbon is suggested to support biomineralization, a phenomenon termed ‘light enhanced calcification’ (Kawaguti et al. 1948, Goreau 1959, Rinkevich et al. 1984)– although the mechanism(s) remain unclear (reviewed byTambutté et al. 2011).

Stony corals precipitate an extracellular skeleton in the form of aragonite under their calicoblastic ectodermal layer (Figures 3.1A & B). Recently, there have been suggestions of an amorphous phase through atomic force microscopy and synchrotron-

based XANES (Cuif et al. 2008, Falini et al. 2013). Planulae begin to precipitate aragonite only upon settling. Proteins related to adhesion have been localized toward the aboral end immediately prior to settlement (Hayward et al. 2011). Growth rate depends strongly on environmental factors, including irradiance and temperature, with some corals showing gross precipitation as high as 10 kg m^{-2} yr^{-1} (Milliman 1993). Several N-terminal sequences have been obtained from proteins associated with soft coral calcitic sclerites, but the vast majority of research on COM proteins from corals has focused on the tropical symbiotic stony corals.

Mollusks

Mollusks, the oldest extant biomineralizing bilaterians (reviewed byKnoll 2003), encompass a far more advanced and varied body plan than stony corals. Generally, the interior of the body with defined digestive organs is protected from the exterior environment by one or two $CaCO_3$ shells (although in some classes this protection is much reduced or absent) (Marin et al. 2012). The shell is generally covered with a thin organic layer, the periostracum, which not only separates the shell from the overlying water, but also plays a role in the biomineralization process. While some gastropod and bivalve mollusks contain endosymbiotic *Symbiodinium* spp., the majority are filter feeders, particularly when sessile, or scrape off algae from surfaces when motile (Klumpp et al. 1992).

In larval gastropods and bivalves, a protein-rich layer, the periostracum, is secreted from a gland in the shell prior to onset of biomineralization (Figure 3.1). Ancestral mollusks have been proposed as solely aragonite producers (Porter 2010), but in modern species the mineral is often amorphous calcium carbonate (ACC), though

occasionally is calcite or aragonite (Weiss et al. 2002). In adults, the periostracum is secreted by cells in the mantle folds and is maintained throughout the life of the mollusk, thus providing a barrier between the mineral $CaCO_3$ and the environment (Marin et al. 2012) (Figure 3.1C & D). Additionally, the periostracum serves as a preliminary scaffold on which the organism lays down $CaCO_3$ (Checa 2000). Together the periostracum and mantle provide a distinct area, the extrapallial space, in which calcification occurs in the presence of COM composed of chitin and proteins (Nudelman et al. 2006, Marin et al. 2012) (Figure 3.1D). The COM proteins, polysaccharides, and lipids secreted by the mantle guide nucleation, elongation, and finally termination of aragonite and or calcite crystals in well-defined locations and morphologies (reviewed byMarin et al. 2004)). Additionally, specific COM proteins, such as Asprich, stabilize the ACC (Politi et al. 2007) and influence the mechanical properties of the biomineral (reviewed byWeiner et al. 2011). Vesicles containing mineral precursors are also exported from specific cells within the animal and aid in facilitating biomineralization in some mollusks (reviewed byAddadi et al. 2006)).

Echinoderms

Although echinoderms display radial symmetry as adults, they evolved from a bilaterian ancestor shared with mollusks and display bilateral symmetry as embryos (Hyman 1955). Echinoderms have a defined digestive tract consisting of mouth, pharynx, esophagus, stomach, intestine, and anus. While some echinoderms are carnivorous, sea urchins – currently the only echinoderm with a sequenced genome (Sea Urchin Genome Sequencing Consortium et al. 2006) – are predominately herbivores. They use calcified

spicules for motility, protection, and to preserve body shape, and five polycrystalline magnesium calcite teeth for foraging (Ma et al. 2008).

Larval planktonic sea urchins secrete $CaCO_3$ spicules and juveniles produce a calcified test and spines, while adults construct these features plus magnesium-enriched calcite teeth, pedicellariae, and ossicles in their tube feet, all in close proximity to mineralizing cells (Killian et al. 2008). Larval sea urchins begin to create $CaCO_3$, guided by COM from primary mesenchyme cells, prior to settling (Figure 3.1E & F). As is often the case with bivalve and gastropod mollusks, it appears that this $CaCO_3$ precipitation begins in the form of amorphous calcium carbonate (ACC) but within days changes to calcite (Politi et al. 2008). Conversion of ACC to calcite is also known in adult urchins (Politi et al. 2004, Killian et al. 2009), and has been suggested as a general tactic in biomineralization, to have mineral precursors ready for crystallization (reviewed byGilbert et al. 2011).

3.2.2 Biomineralizing Proteins

The concept of biologically controlled mineralization is widely accepted (Mann 2001). In stony corals, the "biomineralome" contains an organic component that is 0.1 to 5% by weight with respect to that of the total biomineral and contains a high preponderance of acidic residues in the skeletal proteins (Young 1971, Cuif et al. 2004, Mass et al. 2012). The proteome of coral COM contains an assemblage of adhesion and structural proteins as well as highly acidic proteins (Drake et al. 2013, Ramos-Silva et al. 2013). These highly acidic proteins exhibit pKas of < 5 and a high relative composition ($\geq 28\%$) of the acidic amino acids, aspartic (Asp) and/or glutamic (Glu) acid. Four coral-acid rich proteins (CARPs), one of which was found in both coral skeleton proteomic studies (Drake et al. 2013, Ramos-Silva et al. 2013), were individually cloned and purified. All

four proteins precipitate calcium carbonate *in vitro* in artificial seawater at ambient carbonate concentrations at pH 8.2 and 7.6 (Mass et al. 2013). These results have led to the proposal of a nucleation mechanism in corals in which clusters of Asp and/or Glu residues coordinately bind Ca^{2+} ions, potentially leading to a Lewis acid displacement of protons in bicarbonate anions (Mass et al. 2013). The resulting reaction alters the mineralizing environment below the calicoblastic ectoderm such that the pKa of the local environment on the protein surface decreases and carbonate crystals are precipitated on the protein matrix, even at relatively low ambient pH (Mass et al. 2013).

As with stony corals, the organic component of the bivalve and gastropod mollusk shell minerals generally comprises between 0.01 to 5% by weight, with many of the (glyco)proteins containing a high proportion of Asp residues and/or post-translational decorations of sulfate groups (Lowenstam et al. 1989). As in corals, these proteins are highly acidic. Initially much of the focus on biomineralizing proteins in mollusks focused on these highly acidic proteins and their possible template-specific roles in nucleating precipitation, with distances between acidic residues in -sheet conformation corresponding to distances between Ca^{2+} ions in both calcite and aragonite (Weiner et al. 1975). More recently, the role of highly acidic proteins in mollusk and echinoderm mineralization has grown to encompass the inclusion of these proteins in a hypothesized organic gel, the potential stabilization of a transitional amorphous calcium carbonate step, and the binding and inhibition of growing crystal growth faces (reviewed byMarin 2007)). Additionally, a number of proteomic comparisons have shown that COM proteins include many of unknown function as well as those specific to aragonite *versus* calcite (e.g., (Jackson et al. 2006, Marie et al. 2010, Marie et al. 2012, Marin et al.

2013)). Of the proteins with known function, many are involved in maintenance of the extrapallial environment and in reworking of calcium carbonate.

Analyses of the proteins in COM from spicules, tests, and teeth of sea urchins have yielded a non-redundant list of over 200 individual molecules (Mann et al. 2008, Mann et al. 2008, Mann et al. 2010). While some of these proteins appear to be specific to one type of mineral or structure (spines versus teeth, etc.), many overlaps are observed (reviewed byGilbert et al. 2011)). Some of these proteins have been localized to larval primary mesenchyme cells, but other cells, potentially secondary mesenchyme cells, are more likely responsible for biomineralization in adult animals (Killian et al. 2008). Although highly acidic proteins are also found in sea urchin biominerals (George et al. 1991, Illies et al. 2002, Mann et al. 2008), non-acidic proteins that control either the mineralizing environment or activity of other proteins are also appreciated as essential (example is SM30 family (e.g.;Wilt et al. 2013)).

3.3 Comparison of carbonate organic matrix proteins across marine invertebrate phyla

3.3.1 Evolution of the acidic proteins

The term ‘acidic’ protein has a variety of definitions, but ultimately describes a protein that possesses a net negative charge on some or all of the primary sequence or through post-translational modification. In an attempt at clarity, we compiled a list of the ‘acidic’ proteins and their gene accession numbers in Table 3.1. It is clear from a phylogenetic analysis that these proteins arose independently several times in the evolution of animals through convergent evolution, with gene fusion potentially conferring additional roles to these peptides (Miyamoto et al. 1996, Mass et al. 2013). These proteins appear to be essential for biomineralization. We conducted a protein sequence similarity analysis,

using > 1500 non-redundant coral, mollusk, and sea urchin mineral-derived proteins reported in the literature. Through these analyses, we found only one case of cross-phyla sequence similarity among any of the acidic biomineralization proteins for which sequences are available. Prismalins, shematrins, and some shell matrix proteins from mollusks show 30 to 40% similarity with several collagens from echinoderms and corals (Figure 3.2, SI Table 3.1); this is likely due to the high glycine content of shematrins (Yano et al. 2006) similar to the primary structure of collagens.

Within corals, several acidic proteins show sequence similarity across Orders Scleractinia and Alcyonacea. These include stony coral CARPs 4 and 5 (Drake et al. 2013), SAARPs 1 and 2, SOMP, and Amil-SAP2 (Moya et al. 2012, Ramos-Silva et al. 2013) and the soft coral protein ECMP-67 (Rahman et al. 2011) (SI Table 2). Although not yet analyzed in *Acropora digitifera* and *Pocillopora damicornis* skeleton, CARP4 homologues are found in transcriptomes of these species as well (Shinzato et al. 2011, Vidal-Dupiol et al. 2013). The CARP4 sub-family has been shown to be both highly conserved across and limited to stony corals (Drake et al. 2013), and now the N-terminal sequence from the soft coral, *Lobophytum crassum*, may be assigned to this family based on sequence alignment (Figure 3.3).

Stony corals precipitate aragonite whereas soft corals form calcite, suggesting that the CARP4 sub-family arose in Anthozoa prior to divergence between Scleractinia and Alcyonacea. However, because Actiniarians, or sea anemones, which lack the CARP4 subfamily, diverged from Scleractinia after Alcyonacea (Berntson et al. 1999), they may have lost the gene. It has been proposed that ECMP-67 encourages the precipitation of only calcite (Rahman et al. 2011), despite its similarity to the aragonite-associated

CARP4 and SAARP1 (Figure 3.3). Interestingly, several mollusk proteins have also been suggested to function in both aragonite and calcite precipitation (MS17; (Feng et al. 2009)) or in polymorph control (Aspein; (Takeuchi et al. 2008)). Additionally, Aspein, Asprich, and Pif, which all are components of molluscan shells, share 30% sequence similarity (SI Table 2; (Tsukamoto et al. 2004, Gotliv et al. 2005, Suzuki et al. 2009). Thus although the acidic proteins are independently derived, this sequence comparison suggests a common mechanism of $CaCO_3$ precipitation by acidic proteins in the three marine invertebrate phyla.

Some of the biomineralizing proteins appear to have dual functions. For example, perlwapin, prismalin, molluscan shell prism nacre protein, shematrins, and several collagens, are all implicated in organization and structural support of the bioinorganic matrix. These are called 'other' gene ontology (GO) terms in Figure 3.2 due to equal distribution of collagen, membrane, and extracellular GO assignments. These proteins may also serve a dual role as terminators of biomineralization and are not the only COM proteins, both acidic and non-acidic alike, shown to have crystallization inhibition activities (e.g.;Ma et al. 2007, Politi et al. 2007, Feng et al. 2009). A dual nature of a biomineralizing protein is also observed for the mollusk protein, nacrein, which exhibits both internal acidic regions and carbonic anhydrase activity (Miyamoto et al. 1996). In sea urchins, SpP16 is an acidic protein with a transmembrane region, suggesting that it is anchored to the primary mesenchyme cells to which it has been localized; while its precise mechanism in calcitic spicule formation remains to be determined, it shows some similarities to other calcium binding proteins to regulate calcium transport, again suggesting dual function (Illies et al. 2002).

Carbonic anhydrases, which interconvert CO_2 and HCO_3^-, are integral within carbonate-based biominerals (Bertucci et al. 2013). Their use in biomineralization has been suggested to date back to the earliest calcifying metazoans (Jackson et al. 2007). Gene duplication events and further mutations since the Paleozoic have resulted in a wide variety of the enzyme, many of which are localized within the bioinorganic matrix. Our proteomic analysis revealed representatives of divergent carbonic anhydrases in the biomineral matrix in each of the three invertebrate phyla (Table 3.2). These proteins reinforce their functional necessity in the evolution of the precipitation of extracellular calcium carbonate in each of the three metazoan phyla. Indeed, multiple carbonic anhydrases are found in COM of each phylum, suggesting a level of redundancy for the biomineralization process.

Just as bicarbonate is required for the biomineralization mechanism, so is Ca^{2+}. In animals, Ca^{2+} is transported into and out of cells by plasma membrane-bound Ca-dependent ATPases. These enzymes are widely distributed in mollusks, sea urchins, and corals (Zoccola et al. 2004, Wang et al. 2008, Todgham et al. 2009). However, of the more than 100 reports of COM, only one identified a Ca-ATPase in a 'biomineralome' (Joubert et al. 2010). An additional mechanism for Ca^{2+} transport in corals is the translocation of calcium from the bulk water to the site of mineralization (Gagnon et al. 2012) by a so-called "paracellular" pathway (Tambutté et al. 2012). However, without a chelating or trapping molecule, this mechanism would not concentrate calcium ions. Finally, proton pumps not associated with mitochondrial ATPases, an additional method to modify the saturation state of the mineralizing environment (Corstjens et al. 2001), were not observed in COM by the authors of any of the studies used in our bioinformatics

analysis. Additionally, none of the 295 non-redundant proteins conserved across phyla returned molecular function GO terms associated with non-mitochondrial proton pumps.

3.3.2 Conserved non-acidic proteins across phyla

A number of non-acidic COM proteins are either conserved by sequence (Figure 3.2) or function (Table 3.2). For heuristic purposes, we have aggregated these proteins by function into major groups: (i) proteins that participate in adhesion of cells to their substrates and/or provide a scaffold for organizing the biomineral, and (ii) proteins that signal and regulate biomineralization. Our list is not exhaustive (see SI Table 3.2). However, it is useful in providing a framework for comparing similarities and differences in COM proteins across the three phyla.

Adhesion and Microstructure

Actins and beta-tubulin, cytoskeletal proteins that work as polymerization molecular motors, are present in COM of stony corals and in sea urchins (Figure 3.2). Although they could be contaminants from the animal component (i.e., not truly part of the COM; (Mann et al. 2008), physiological and genomic data suggest they are part of the biomineralization "toolkits" for both corals and sea urchins. Inhibition of these proteins significantly reduces organic matrix synthesis and calcification in corals (Allemand et al. 1998). While similar studies have not been conducted on sea urchin biomineralization, actin is crucial to the primary mesenchyme cell ingression stage just prior to onset of embryonic biomineralization, with actin inhibition resulting in loss of ingression (Wu et al. 2007). Secondly, biomineralization in paralogue organisms such as diatoms, which precipitate amorphous silicate, involves actins and tubulins (Hildebrand et al. 2008).

A number of proteins that adhere to or interact with actin and tubulin are found in COM across marine invertebrate phyla, but are not conserved by amino acid sequence,

and therefore are assumed to be independently evolved (Table 3.2). For example, laminins, a family of glycoproteins, along with fibronectins and integrins, serve as structural support in mollusks, echinoderms, and corals, respectively (Table 3.2). Peroxidasins and thrombospondins (in corals and sea urchins) may also serve as extracellular structural and adhesive proteins (Table 3.2; (Péterfi et al. 2009).

Finally, collagens, which provide a flexible framework and confer structural support for biominerals, appear to be widely distributed in corals and sea urchins (Figure 3.2, Table 3.2). It is unclear whether collagens are actually found in mollusks (Blank et al. 2003, Xuan Ri et al. 2007). Alternatively, chitin, a potential structural replacement for collagen is found in mollusks (reviewed by (reviewed byEhrlich 2010). In this case, chitin, like collagen, can provide a highly structured scaffold on which COM proteins can bind (reviewed by (Falini et al. 2004). It has been suggested to have a more direct role in polymorph control (Falini et al. 1996). Chitin synthase (Joubert et al. 2010) and a chitin-binding protein (Mann et al. 2012) have been detected in mollusk shell proteomes; they do not show cross-phyla sequence similarities in our analysis (SI Table 2).

3.3.3 Signaling and Regulation

Low-density lipoprotein (LDL) receptors are ancient proteins that aid in signal transduction across cell membranes and are responsible for cell specification and axis patterning in cnidarians and sea urchins (Wikramanayake et al. 2004, Lee et al. 2006, Lee et al. 2007). Notch proteins, which contain an epidermal growth factor domain (EGF), are calcium-binding transmembrane signal transduction pathway proteins that interact with LDL receptors (Baron 2003). In sea urchins, they direct secondary mesenchyme cell development and spiculogenesis (Suyemitsu et al. 1990, McClay et al. 2000).

Several of these proteins, with ‘membrane’ GO terms assigned, are reported in sea urchin and coral COM (Figure 3.2).

Bone morphogenic proteins (BMPs) are responsible for signal gene regulation in apatite producing cells (reviewed byCanalis et al. 2003) and up-regulate Notch signaling genes in osteoblast precursor cells (de Jong et al. 2004). BMPs are reported in COM from all three phyla (Table 3.2) but, as ‘extracellular’ GO terms, are only conserved between mollusks and sea urchins (Figure 3.2). As signal transduction pathway proteins, BMPs from corals and mollusks induce mesenchyme cell differentiation and osteogenesis (Zoccola et al. 2009, Takami et al. 2013) and are involved in sea urchin cell specification and axis patterning (Angerer et al. 2000). They have also been immunolocalized to calicoblastic ectodermal cells in corals (Zoccola et al. 2009) and a novel protein that shows structural (from structure prediction) but not sequence similarity to the BMP inhibitor Noggin was recently observed in coral COM (Drake et al. 2013).

In addition to cell signaling, reworking of individual COM proteins is important to the function of the complex. Matrix metalloproteinases (MMPs) are specific extracellular matrix degradation enzymes that require cations for their catalytic activity. COM MMPs, as extracellular proteins, show sequence similarity between corals and sea urchins (Figure 3.2). MMPs affect sea urchin spicule elongation but not nucleation (Ingersoll et al. 1998) and regulate extracellular matrix in humans (reviewed byWoessner 1991, Birkedal-Hansen et al. 1993). They are found in mollusk hemolymph and an MMP inhibitor has been extracted from mussel pearls (Mannello et al. 2001, Jian-Ping et al. 2010), suggesting that they may be present in mollusk COM as well.

Ubiquitin is a protein that attaches to and signals other proteins for degradation or relocation, or inhibits protein binding or activity. It is highly conserved in COM proteins across all three phyla and is generally assigned a 'membrane' cellular component GO term (Figure 3.2). Ubiquitylated proteins are reported from the prismatic layer of mollusks; removal of ubiquitin decreased the ability of these proteins to inhibit calcium carbonate mineralization (Fang et al. 2012). Hazelaar et al. (Hazelaar et al. 2003) proposed that, in diatoms, ubiquitin may signal templating proteins for degradation as the cell walls develop pores; a similar role in invertebrate calcium mineralization has yet to be examined.

3.3.4 Summary of Conservation of Biomineralizing Proteins

Morphological, phylogenetic, and now proteomic evidence indicates that marine $CaCO_3$ precipitation is a convergent evolutionary process. Coral, mollusks, and sea urchins have all evolved their own suites of acidic proteins to catalyze the nucleation of $CaCO_3$ (Illies et al. 2002, Gotliv et al. 2005, Drake et al. 2013) and co-opted a number of adhesion, structural, signaling, and regulation proteins to provide structure and environmental stability to the calcifying regions (Marin et al. 2004, Zhang et al. 2006, Allemand et al. 2011). This convergence suggests that there are general roles for biomolecules in the biomineralization process and that, although biomineralization toolkits may not be conserved across phyla, the requirements to have these biological roles fulfilled is. Further, the precise macroscopic morphologies of skeleton, shell, and spicule/teeth, etc. may then be driven by those proteins or other biomolecules that are functionally individual not only to each phylum, but also often to specific minerals. Examples of these functionally individual proteins, which in some cases have been reviewed elsewhere, are lysine-rich matrix proteins and amorphous calcium carbonate binding

proteins in mollusks (Zhang et al. 2006, Ma et al. 2007), galaxins in corals (Fukuda et al. 2003), and the mesenchyme specific cell surface glycoproteins in sea urchins (Leaf et al. 1987, Killian et al. 2008).

3.4 Future of marine invertebrate biomineralizers

Estimates of CO_2 emissions and the projected effects on upper ocean ecosystems over the next 100 years are dire, especially for marine calcifiers that will face the combined issues of warming and ocean acidification (Raven 2005, Feely et al. 2009, Ries et al. 2009, Hoegh-Guldberg et al. 2010, Pandolfi et al. 2011). Models of the average calcite saturation state ($\Omega_{calcite}$) in the surface ocean projects a decrease from 5 to 2 in the next 100 years (Doney et al. 2009, Norris et al. 2013). Studies of biomineralizing marine invertebrates indicate a variety of potential responses to ocean acidification, from potential decreased calcification rates (Ries et al. 2009, Holcomb et al. 2010, Kroeker et al. 2010) to ecosystem shifts (Anthony et al. 2008, Crook et al. 2012). Additionally, each of the marine invertebrate mineralizers discussed here have representatives that naturally persist in waters with low calcium carbonate saturation (i.e., > 1000 m depth or in regions of upwelling, high respiration rates, or rainwater runoff; e.g., (Anagnostou et al. 2011, Shamberger et al. 2014)). However, in addition to examining the responses of current marine biomineralizers, it is useful to consider both the micro- and macroscopic effects of increased atmospheric CO_2, particularly as it pertains to ocean acidification.

As detailed above, several highly acidic coral proteins function at ambient and low pH (Mass et al. 2013). This capacity suggests that while crystal growth rate and morphology can be dependent of the saturation state of the medium (Holcomb et al. 2009), the pKas of these and likely other highly acidic proteins are three orders of

magnitude lower than seawater. Thus, in spite of the fact that pH may decline by up to 0.5 pH units in the coming century, the reactivity of these proteins in the precipitation of carbonates will remain virtually unchanged. This built-in molecular resilience will likely allow the nucleation reaction to continue. Although this resilience does not address the physiological response of marine biomineralizers to a surrounding medium whose pH is stressful to processes beyond the nucleation of minerals (Lannig et al. 2010, Stumpp et al. 2011, Moya et al. 2012), these organisms are not static and there is evidence of genetic and transcriptional adaptation to low pH conditions (Moya et al. 2012, Hüning et al. 2013, Kelly et al. 2013).

Given the inevitable acidification of the contemporary ocean in the coming decades it is potentially also instructive to examine the geological record of analogues. One possible analogue is the Paleocene Eocene Thermal Maximum (PETM) (Norris et al. 2013). This period, 55.5 to 55.9 million years ago, was characterized by a 4 to 5^{o} C increase in sea surface temperatures in the tropics (Zachos et al. 2003) and nearly 1000 ppm increase in CO_2 in the atmosphere (Beerling et al. 2011). While the PETM corresponds with a dramatic reduction in $CaCO_3$ in the geologic record (Zachos et al. 2005) and a decrease in the coverage of coral reefs (reviewed byNorris et al. 2013)), all marine invertebrate taxa discussed here survived through this extraordinary period. Indeed, some experienced rapid radiation and diversification in the Eocene (e.g.;Stanley 2003)).

The survival of the major carbonate-precipitating marine invertebrates in the face of ocean acidification is likely because (i) the site of biomineralization is removed from the surrounding medium, (ii) the proteins responsible for the precipitation of carbonates

function at low pH, and (iii) genetic adaptation allows the organisms to persist, albeit perhaps not optimally, in their new environments. Additionally, recent research suggests that these organisms are able to modify their mineralizing environment in response to pH stress (Yuen et al. 2006, Venn et al. 2013). This ability suggests that the biomineralization processes will almost certainly persist throughout the Anthropocene. It appears that these organisms are far more resilient than is often acknowledged. However, from a molecular biology perspective, significant research remains toward understanding 1) the expression rates of known COM proteins under variable environments, as well as the biochemical cascades responsible for any changes; 2) the interactions of the COM proteins with each other to regulate the initiation, elongation, and termination steps of mineralization; and 3) how signals of COM protein evolution, which also guided biomineralization in the past, may be retained in fossil minerals.

Data Accessibility Statement: All data were taken from publically available datasets. Original sources and accession numbers of all sequences are noted in Table S2.

Table 3.1. Proteins from coral, mollusk, and sea urchin carbonate organic matrices that have been characterized as 'acidic'. The gene accession number is given along with the primary reference to the work describing the proteins.

Characteristic	Coral	Mollusk	Sea urchin
Aspartic acid-rich regions	CARP4 (KC493647) and CARP5 (KC493648) (Drake et al. 2013) SAARP1 (JT001945), SAARP2 (JT991407), Amil-SAP2 (JR983041) (Ramos-Silva et al. 2013) EMCP-67 (no accession #) (Rahman et al. 2011)	Aspein (AB094512) (Tsukamoto et al. 2004) Asprich (AAU04807-15) (Gotliv et al. 2005) Pif (AB236929) (Suzuki et al. 2009) Prismalin (AB159512) (Suzuki et al. 2004) Nacrein (Q27908) (Miyamoto et al. 1996) MSI60 (O02402) (Sudo et al. 1997) AP7 (AF225916) (Michenfelder et al. 2003)	
Low pI, serine-rich regions		Mucoperlin (AF145215) (Marin et al. 2000)	P16 (AF519415) (Illies et al. 2002)
Glutamic acid-rich regions		MSI31 (O02401) (Sudo et al. 1997)	P19 (AF519413) (Illies et al. 2002)
Tyrosine-rich regions		N14 (Q9NL39) (Kono et al. 2000) Pearlin (O97048) (Miyashita et al. 2000) N16 (AB023067) (Samata et al. 1999)	
Aspartic and glutamic acid-rich regions		AP24 (AF225915) (Michenfelder et al. 2003)	
Serine- and aspartic acid-rich regions		MSP-1 (Q95YF6) (Sarashina et al. 2001)	
Phosphorylated			34 phosphoproteins (*) (Mann et al. 2010)

* See reference cited for the available 34 sequence ID numbers and to download sequences from publisher.

Table 3.2. Proteins of shared function, but not shared sequence, found in carbonate organic matrices across the three marine invertebrate phyla. Protein classifications follow those found in their original publications unless they grouped with another classification during similarity clustering. The gene accession numbers are provided.

Protein Name	Coral	Mollusk	Sea urchin
Bone morphogenic protein *	*Acropora* sp. (EU785982) (Zoccola et al. 2009) *Stylophora pistillata* (EU78981) (Zoccola et al. 2009)	*Pinctada margaritifera* (90c_1652_1) (Joubert et al. 2010)	*Strongylocentrotus purpuratus* (NP_999820) (Mann et al. 2010)
C-type lectin	-	*P. margaritifera* (90c_3116_2, 298867_2192_0444_6) (Joubert et al. 2010)	*S. purpuratus* (XP_003726084, XP_003726239, XP_793473, AF519418) (Illies et al. 2002, Mann et al. 2008, Mann et al. 2010)
Carbonic anhydrase	*S. pistillata* (EU532164, ACE95141, ACA53457) (Moya et al. 2008, Bertucci et al. 2011, Drake et al. 2013) *Acropora millepora* (JR995761, JR973601, JR998380, JT002659, JT014542, JR989434, JT018935, JR979146, JR996464, JR990087, JR998014) (Moya et al. 2012, Ramos-Silva et al. 2013)	*P. margaritifera* (90c_299_1) (Joubert et al. 2010) *Crassostrea gigas* (EKC19847.1) (Zhang et al. 2012) *Lottia gigantea* (lotgi66515, lotgi205401) (Mann et al. 2012)	*S. purpuratus* (XP784796, XP_003726289, XP_784328_ABE27963) (Mann et al. 2008, Mann et al. 2010, Stumpp et al. 2011)
Collagen *	*A. millepora* (JR991083,) (Ramos-Silva et al. 2013) *S. pistillata* (KC479166, KC479163, KC342195, KC342197) (Drake et al. 2013)	*Haliotis asinina* (GT274423) (Marie et al. 2010) *C. gigas* (EKC3725.1) (Zhang et al. 2012) *L. gigantea* (lotgi123902) (Mann et al. 2012)	*S. purpuratus* (SPU009076, SPU015708, SPU003768, SPU022116, NP_999676, (Todgham et al. 2009, Mann et al. 2010)
Fibronectin *		*Mytilus californianus* (P86861) (Marie et al. 2011) *C. gigas* (EKC41461.1 – EKC41463.1) (Zhang et al. 2012)	*S. purpuratus* (XP_003729283) (Mann et al. 2010)
Hemicentin/ Thrombospondin *	*A. millepora* (JT016638, JR989905) (Moya et al. 2012, Ramos-Silva et al. 2013) *S. pistillata* (KC342189, KC150884) (Drake et al. 2013)	-	*S. purpuratus* (XP_794971, XP003727369, XP003728681, XP784935, XP_780466, XP001198520, XP_786756) (Mann et al. 2008, Mann et al. 2010)
Integrin	*S. pistillata* (KC479167) (Drake et al. 2013)		*S. purpuratus* (XP_794080) (Mann et al. 2010)
Laminin/ Neurexin	*A. millepora* (JR980881) (Ramos-Silva et al. 2013) *S. pistillata* (KC342198, KC479169) (Drake et al. 2013)	(receptor) *P. margaritifera* (90c_665_4) (Joubert et al. 2010) *L. gigantea* (lotgi203487) (Mann et al. 2012)	*S. purpuratus* (XP781951, XP_003726434, XP_780725.3, XP_001197577.1) (Mann et al. 2008, Mann et al. 2010)

- Indicates that some sequences show sequence similarity across phyla. See SI Table 1.

Figure 3.1. Schematic drawings of three biomineralizing marine invertebrates. (A–B) Four cell layers separate the external aragonite skeleton from overlying seawater (after;Allemand et al. 2004). (C–D) Mollusk aragonite, calcite, and/or ACC are precipitated in the extrapallial space between the periostracum and mantle (after;Marin et al. 2004). (E–F) Primary mesenchyme cells precipitate larval sea urchin ACC and/or calcite (after;Urry et al. 2000).

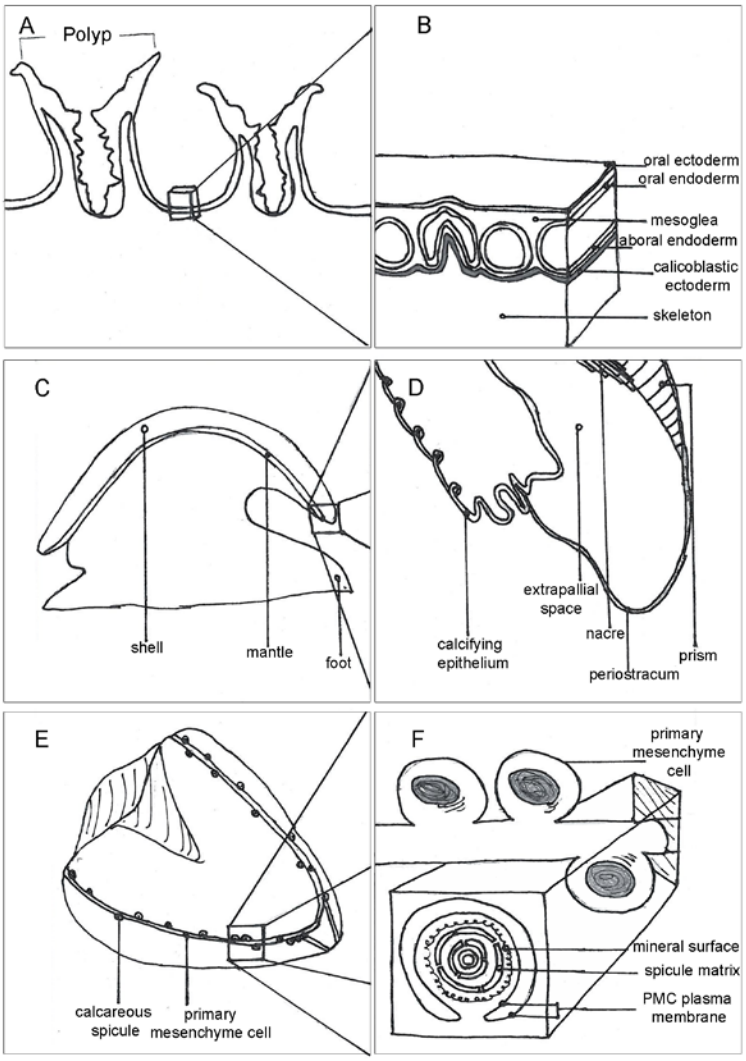

Figure 3.2. Cellular component ontology of COM proteins conserved across phyla. Sequences from over 100 biomineral proteome studies were grouped by hierarchical clustering using the CD-HIT suite web server (Li et al. 2006, Huang et al. 2010) (http://weizhong-lab.ucsd.edu/cd-hit/) and assigned GO terms using Blast2Go software (Conesa et al. 2005). Although 1531 proteins reduced to 1051 clusters at 30% similarity, only 64 clusters showed sequence similarity across phyla. Studies published from the 1990s through June 2013, using N-terminal and mass spectrometry COM sequencing, RT-PCR, or GO and KEGG annotation of genomic and transcriptomic data sets are included. Mass spectrometry sequences were excluded if the experimental data were compared with gene models from a different species.

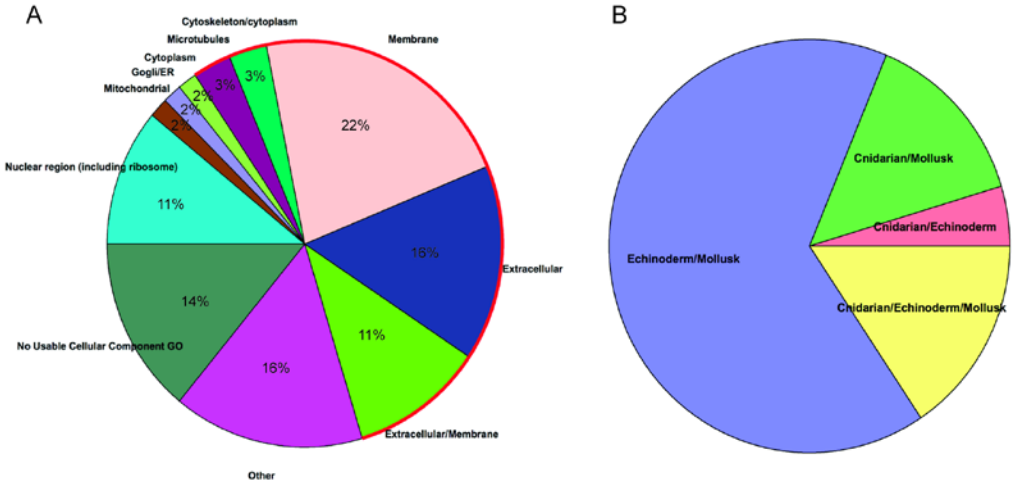

Figure 3.3. Multiple sequence alignment of CARP4 sub-family homologues. Alignment of homologues from four stony corals places a previously un-aligned soft coral N-terminal sequence into this family. The CARP4 subfamily is not found in sea anemones even though anemones diverged from stony corals after the soft coral divergence.

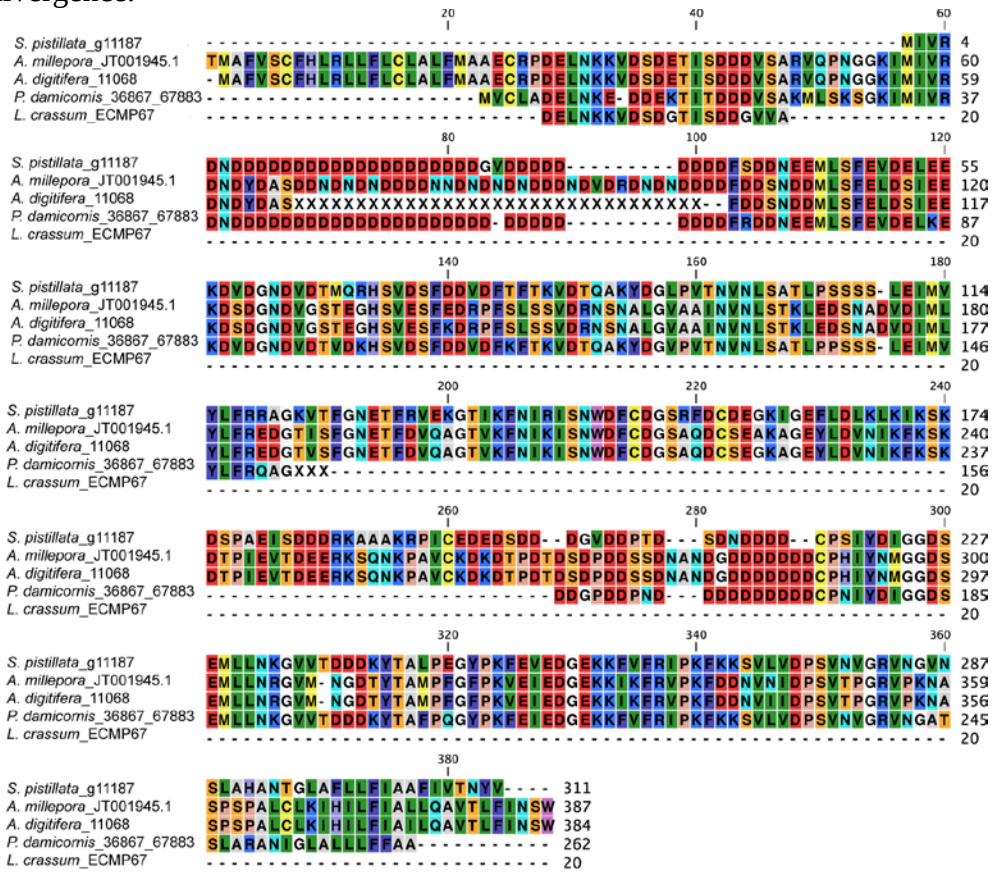

3.5 Supplementary Material

Supplementary material is available from the publisher at http://dx.doi.org/10.12952%2Fjournal.elementa.000026.

Table S1. Protein sequences with >=30% sequence similarity between phyla. Cross-phyla clustering of non-redundant carbonate organic matrix proteins from N-terminal and mass spectrometry COM sequencing, RT-PCR, or GO and KEGG annotation of genomic and transcriptomic data sets (from over 100 studies) grouped by hierarchical clustering using the CD-HIT suite web server (http://weizhong-lab.ucsd.edu/cd-hit/). The gene accession numbers are included. 1531 proteins reduced to 1051 clusters at 30% or greater similarity, although only 64 clusters showed sequence similarity across phyla. Studies published from the 1990s through June 2013 are included. Clusters with the same name have been combined. Note: Mass spectrometry sequences were excluded if the experimental data were compared with gene models from a different species. * indicates that non-homologous proteins with similar function were also observed. See Table 2 in main document.

Table S2. Proteins from coral, mollusk, and sea urchin COM sequencing, RT-PCR, or GO and KEGG annotation. 1076 proteins, including redundancy when noted by multiple sources, reduced to 1031 non-redundant sequences.

Chapter 4: The influence of CO_2 on calcification in coral cell cultures

Abstract

Understanding the cellular and molecular responses of stony corals to ocean acidification is key to predicting their ability to maintain calcification under high CO_2 conditions. Biomineralization toolkit proteins have been proposed for several corals and elucidating the connection between expression of these genes and calcification will allow a better understanding of their roles in the mineralization process. We used cell cultures of the Indo-Pacific stony coral, *Stylophora pistillata* to test the effects of increased CO_2 on the calcification process at the cellular and molecular levels. After rearing cell cultures for up to nine days in four CO_2 conditions and two glucose treatments, we analyzed samples by microscopy, qPCR, western blot, FIRe, and mass spectrometry. *S. pistillata* grown at low (400 ppm) and moderate (700 ppm) CO_2 re-aggregate into proto-polyps and precipitate $CaCO_3$. When grown at high and very high CO_2, (1000 and 2000 ppm, respectively) *S. pistillata* cells up-regulate several highly acidic genes as well as a carbonic anhydrase, but down-regulate long-term cadherin production and minimize proto-polyp formation; this coincides with cessation of measurable $CaCO_3$ precipitation. These results suggest that compensatory molecular adjustments allowing cells to deal with ocean acidification are successful only up to a point, beyond which these mechanisms cannot compete with local chemical conditions unfavorable to biomineralization.

4.1 Introduction

As precipitators of an aragonitic skeleton, stony corals are thought to be under considerable stress from increasing atmospheric pCO_2 (e.g.; Smith et al. 1992, Leclercq et al. 2002, Pandolfi et al. 2011). A variety of studies have shown that calcification rate (e.g.; Anthony et al. 2008, Drenkard et al. 2013, Strahl et al. 2015) as well as photosynthetic (Anthony et al. 2008) and other metabolic processes (e.g.; Edmunds et al. 2014) are depressed in experimentally increased CO_2 treatments for some corals. However, the effects of increased CO_2 on coral calcification are not negative for all corals (Ries et al. 2009, Comeau et al. 2013, Strahl et al. 2015), and some taxa persist in naturally high CO_2 environments such as near volcanic or karst vents (Fabricius et al. 2011, Crook et al. 2012) or in bays that experience low aragonite saturation due to high calcification and respiration (Shamberger et al. 2014). They also exhibit differential responses to increased pCO_2 when fed (e.g.; Drenkard et al. 2013, Houlbrèque et al. 2015).

Elemental and isotopic information from fossil coral skeletons have been used as proxies for paleo-environmental conditions. In particular, boron isotopes are used to calculate pH of ancient seawater (Honisch et al. 2004). A number of assumptions must be made for these proxies including that the precipitation reaction proceeds with no or minimal biological control. However, corals have a strong direct control over both the mineralization process and the chemical make-up of the mineralizing interface (Lowenstam et al. 1989, Falini et al. 2013, Venn et al. 2013, Holcomb et al. 2014). For these reasons, it is necessary to understand how coral biomineralization happens at the cellular level.

For many years, model organisms have been used to understand biomineral formation at the cellular level; one such marine example is sea urchin larval studies (e.g.; Beniash et al. 1999). Although a similar model system does not exist for stony corals, there has been success in maintaining coral cell bundles (Domart-Coulon et al. 2001) or re-aggregated cells as proto-polyps for up to one month (Helman et al. 2008, Mass et al. 2012). In these systems, coral cells secrete an extracellular matrix that adheres them to the substrate and precipitate extracellular aragonite crystals on 'proto-polyps'. However, rate of calcification or of skeletal organic matrix (SOM) protein expression in these systems have not been examined to date. Neither have they been used to study the cellular-level effects of environmental stressors on corals.

SOM proteins retained in coral skeleton from corals in the families Pocilloporidae and Acroporidae have recently been sequenced (Drake et al. 2013, Ramos-Silva et al. 2013). These include proteins of known function such as the adhesive cadherin and a carbonic anhydrase, as well as uncharacterized and highly acidic proteins. Several of these SOM proteins have been immunolocalized to the calicoblastic cell layer and at the nano-scale within skeleton (Mass et al. 2014).

Marine invertebrate calcifiers share a variety of related SOM proteins of known functions including membrane-associated and extracellular proteins (Drake et al. 2014). However, the highly acidic proteins evolved independently. In stony corals, soluble acidic proteins (SAPs) have only been found in Acroporid skeletons, while the coral acid rich proteins (CARPs) or secreted acidic Asp-rich proteins (SAARPs) have been found in both Acroporid (Ramos-Silva et al. 2013) and Pocilloporid (Drake et al. 2013, Mass et al. 2014) aragonitic skeleton and in soft coral calcitic sclerites (Rahman et al. 2011).

Additionally, several CARPs/SAARPs have been shown to precipitate calcium carbonate from seawater, potentially by a Lewis acid mechanism (Mass et al. 2013).

In this study, we grew *Stylophora pistillata* cell cultures in growth media manipulated from 400 to 2000 ppm pCO_2 and in 0.1 and 0.2 mM glucose to examine the effects of ocean acidification and nutrition, respectively, on both mineral and SOM protein production. Previous studies have examined the effects of pCO2 and heterotrophy on coral spat (Drenkard et al. 2013) and nubbins (Edmunds 2011) and show that corals recover some degree of mineralization ability under heterotrophic conditions. In contrast to other studies using nubbins, our cultures allow us to focus on cellular rather than organismal processes and produce new $CaCO_3$ uncontaminated by parent mineral. Here, we highlight the cellular response to ocean acidification to detail, through molecular, biochemical, and elemental analysis, the direct control of coral cells on the biomineralization process.

4.2 Methods

4.2.1 Experimental Setup and Conditions

Experimental growth medium was prepared at 400, 700, 1000, and 2000 (±30) ppm CO_2 in an incubator (Percival Scientific) at 26ºC. 1 L artificial seawater (ASW) was mixed to achieve a salinity of 40; this salinity was chosen because the ASW was eventually diluted in growth medium to a final salinity of 34 (Appendix Table 4.1). ASW was sterile-filtered to 45 μm and bubbled in a standard algae bubbling system consisting of an autoclaved plastic Erlenmeyer flask, stopper, and tubing plus sterile serotological pipette and sterile 0.45 μm one-time-use syringe filters. This bubbling system was opened only in a UV hood next to a flame. The above precautions were employed to eliminate external bacterial contamination of the cultures. Sealed sterile ASW was bubbled with

air ambient to the incubator in the dark until TOC and pH measurements stabilized. Initial and stabilized samples were also taken for alkalinity titrations.

At each CO_2 level, ASW was mixed with Dulbecco's Modified Eagle Medium (DMEM, Sigma D5030) plus additives to achieve the following: 12.5% DMEM (at 8.3 g/L containing 0.578 g/L L-glutamine, 0.05 g/L taurine), 20 mg/L aspartic acid, 50mg/L ascorbic acid, 2% heat-inactivated fetal bovine serum (Invitrogen), 0.1 mM glucose, and 1% anti-biotics/mycotics cocktail (GIBCO). Growth medium was filtered and bubbled as above until TOC and pH measurements stabilized; alkalinity titrations were also performed.

DIC was measured on a TOC analyzer (Shimadzu) with a bicarbonate standard curve, and certified reference material (CRM; Batch 132) from the Dickson lab at UC San Diego as an internal standard. Alkalinity titrations of initial ASW mixtures were conducted on a Metrohm Titrando 888 against NIST pH standards and using the CRM noted above as an internal standard. CO_2 was maintained in the incubator using CO_2 gas (Airgas; bone dry) and soda lime; manufacturer specifications state that output accuracy is ±20 ppm + 2% of the reading which tended to fluctuate ±20 ppm of the set CO_2 concentration. pH of equilibrated seawater was calculated from incubator CO_2 setting, DIC, and alkalinity in CO2sys (Pierrot et al. 2006). pH of equilibrated DMEM+ASW was measured on a Fisher Scientific Accumet pH meter against NIST standards. Chemical parameters of growth medium are given in Table 4.1.

Cell cultures of the zooxanthellate Indo-Pacific coral, *Stylophora pistillata*, were produced from nubbins contained in an in-house 800-L aquaria as previously described with the following modifications (Mass et al. 2012). Initial 4-hr incubations in calcium-

free seawater plus 3% anti-biotics/mycotics (GIBCO) and 20 μg/L chloramphenicol, during which cell adhesion is disrupted, were conducted at ambient CO_2 and room temperature for nubbins used in all treatments. Secondary incubations, during which cells spontaneously dissociate from the skeleton, were conducted in sterile DMEM+ASW described as above but made with ASW stabilized at ambient CO_2. These secondary incubations were maintained for 1.5 days at room temperature in a non-sterile humidified incubation chamber at ambient light:dark cycle. Dissociated *S. pistillata* cells and tissue were gently pipetted away from the skeleton and centrifuged at 3000 rpm for 10 minutes at room temperature. The pellet was re-suspended in medium bubbled to the appropriate CO_2, as described above, and filtered on 20 μm nylon mesh into Primaria culture dishes to a total volume of 3 ml bubbled medium. An additional volume of glucose was added to half of the cultures to bring their final glucose concentration to 0.2 mM. Cultures were maintained in a sealed, ethanol sterilized, humidified incubator for up to 9 days. The incubator was opened only to remove culture wells for sample collection. Medium was replaced in 9 d cultures after 5 d. We have previously shown that $CaCO_3$ does not precipitate in cultures that (1) contain medium but no cells, and (2) contain cells killed with sodium azide (Mass et al. 2012).

4.2.2 Sample Collection

S. pistillata cell cultures were cultivated in triplicate immediately upon set-up and at 4 hr, 1 d, 5 d, and 9 d. All wells were examined on an inverted IX71 epifluorescent microscope (Olympus) to monitor proto-polyp formation. Due to incompatibility of methods of processing, each of the analyses below received its own triplicate of samples at each time point.

4.2.3 SOM Protein Expression

qPCR

Triplicate samples for qPCR were cultivated at each time point by scraping each well with a rubber policeman and centrifuging the contents at 13,000 g for 3 minutes; pellets were stored in 0.55 ml TRI Reagent (Life Technologies) at -80^{o}C. RNA was extracted per the manufacturer's protocol and treated with TURBO DNase (Ambion) to remove DNA. Within 48 hours of extraction, RNA was converted to cDNA using SuperScript III (Invitrogen) by manufacturer's methods. All samples were analyzed by PCR with a primer set for CARP1 that amplifies a 160 bp product from cDNA and a ~300 bp product from DNA (Appendix Table A2) to ensure that only genomic DNA-free cDNA was used for qPCR.

S. pistillata cell culture cDNA was amplified on a Stratagene MX300P qPCR thermal cycler. Primers specific to CARPs 3 and 4 and STPCA2 were used (Appendix Table A2 (Bertucci et al. 2011)). Before use, efficiency of primers was confirmed to be 100% ±10% and amplicon sequences were confirmed (Genewiz Sequencing Service). The housekeeping gene was the *S. pistillata*-specific 18S (Appendix Table A2 (Kvitt et al. 2011)). All reactions contained 0.1-04 μg template, 0.5 μM of each primer, and 1X Power SYBR Green PCR Master Mix (Life Technologies). Thermal profiles comprised: initial denaturing at 94^{o}C for 10 minutes; then 40 cycles of 94^{o}C for 30 seconds, primer-specific annealing temperature for 30 seconds, and 72^{o}C for 30 seconds; followed by final extension at 72^{o}C for 5 minutes with a 37-cycle dissociation curve. As per standard $\Delta\Delta C_T$ protocol, C_Ts of genes of interest were standardized to those of the HKG and then to those of 400 ppm CO_2 T_0 samples before natural log transformation.

Western Blot

Total protein was cultivated at each time point as described above; cell pellets were stored at -80^{o}C. Protein was resuspended in phosphate buffered saline (PBS) and quantified by bichronoic acid assay (Thermo Scientific) with bovine serum albumin as a standard. Equal total protein amounts were loaded onto TGX Stain-Free precast gels (Bio-Rad); known amounts of a peptide from the *S. pistillata* SOM cadherin (accession number AGG36361.1) were also loaded on each gel. Separated proteins were transferred to PVDF membrane using the Trans-Blot Turbo Transfer System (Bio-Rad). After blocking with 4% bovine serum albumin in 0.05% Tween-20 in PBS, blots were incubated for one hour in a *S. pistillata* cadherin-specific primary antibody at room temperature (Mass et al. 2014), rinsed copiously, incubated in goat-anti-rabbit-HRP (Santa Cruz) secondary antibody, and rinsed again. Blots were imaged on a Chemi-Doc (Bio-Rad) using Lumigen TMA-100. Images were analyzed in PHOTOSHOP; intensity of cadherin bands in sample lanes were quantified against band intensity in standard lanes.

4.2.4 Calcification Rate

We developed a novel method to approximate calcification rate in *S. pistillata* cell cultures using Sr. Radiogenic Ca can be useful to measure calcification on coral nubbins, where inorganic Ca greatly exceeds Ca bound to contaminating organic material adhered to skeleton (Goreau 1959, Moya et al. 2006). However, in our system, the majority of the solid contents of cell culture wells is organic with a large pool of bio-bound Ca. In contrast, Sr is minimally bioactive (Pors Nielsen 2004).

Media was removed from each well by pipetting, and wells were rinsed three times with 1 ml NH_4OH-infused MilliQ water for one minute with minimal agitation to remove residual media without dissolving $CaCO_3$. Rinses were removed by pipetting

with a fresh, water-rinsed tip and discarded. Wells were then incubated in 0.5 ml 0.05 M acetic acid (Optima, Trace Metal clean) for 30 minutes at room temperature, after which the acid was pipetted from the well using water- and acid-rinsed tips into acid-leached eppendorf tubes. Acid samples were centrifuged at 13,000 g for 3 minutes and 0.4 ml of the supernatant was transferred by water- and acid-rinsed tip to fresh acid-leached eppendorf tubes. Samples were stored at 4^{o}C until further processing.

Samples were analyzed for Sr content on a Finnigan Element XR analyzer against an in-house-made seawater standard optimized for coral skeleton samples. Matrix standards were included in each run and all samples included In and Sc spikes as a secondary test of matrix effects and instrument drift. Data were blank- and then drift-corrected. Calcification rates were calculated by first converting ^{86}Sr in low resolution detection mode to $CaCO_3$ assuming a Sr/Ca partitioning coefficient of $8.81 * 10^{-3}$ at 26^{o}C (Ferrier-Pages et al. 2002), then standardizing to total protein content of cultures cultivated for quantitative cadherin Western blotting.

4.2.5 Variable Fluorescence

Variable fluorescence of *S. pistillata* cell cultures was measured using a custom-built fluorescence induction and relaxation (FIRe) system with external probe (Gorbunov et al. 2004). Only single turnover flash data were collected. Briefly, blue light emitting diodes (450 nm with 30 nm bandwidth) induce red fluorescence (measured at 680 nm with 20 nm bandwidth) from chlorophyll a caused by reduction of the plastoquinone (PQ) pool on the acceptor side of Photosystem II (Kuzminov et al. 2013). A fully oxidized PQ pool yields F_o, or minimal fluorescence while a fully reduced PQ pool yields F_m, or maximum fluorescence. After dark adaption, the variable fluorescence, $(F_m-F_o)/F_o$, is the maximum

quantum yield of photochemistry; however, *S. pistillata* cell cultures were not dark adapted in these experiments.

4.2.6 Statistical Analysis

Statistical analyses were performed in IBM SPSS Statistics. F_v/F_m, calcification rate, and cadherin production rate data were analyzed by Independent Samples t Test performed pairwise between timepoints, CO_2 treatments, and glucose treatments. $p < 0.05$ was chosen as the significance cutoff.

4.3 Results

Stylophora pistillata cell cultures formed proto-polyps as in previous experiments (Mass et al. 2012), but size was affected by CO_2 treatment. At 400 and 700 ppm CO_2 (hereafter referred to as low and moderate, respectively), large proto-polyps greater than 10 cells in diameter formed; however, at 1000 and 2000 ppm CO_2 (hereafter referred to as high and very high, respectively), proto-polyps were generally less than 10 cells across (Figure 4.1). Additionally, at the two higher CO_2 treatments many cells remained suspended in the medium rather than adhering to the growth plate. No difference in proto-polyp size, cell adhesion, or occurrence of bacteria was observed between glucose treatments.

We followed the expression, through time, of four skeletal organic matrix proteins – two CARPs, a carbonic anhydrase, and a cadherin (Drake et al. 2013, Ramos-Silva et al. 2013, Mass et al. 2014). CARPs 3 and 4 were chosen for their ability to precipitate $CaCO_3$ in vitro (Mass et al. 2013) and their localization to less-soluble growth layers of intact skeleton (Mass et al. 2014). STPCA-2 is not only a highly active form of carbonic anhydrase (Bertucci et al. 2011), but is also currently the only carbonic anhydrase sequenced from coral skeleton (Drake et al. 2013, Ramos-Silva et al. 2013). The final protein of interest, a protocadherin fat-like protein, was chosen due to its ubiquitous

immunolocalization throughout the skeleton as well its consistently high e-value in *S. pistillata* skeletal proteome sequencing, suggesting that it is relatively abundant (Drake et al. 2013, Mass et al. 2014).

Expression of SOM genes examined in this study was affected by CO_2 treatment, glucose addition, and age of cultures (Figure 4.2). Both CARPs 3 and 4 were up-regulated under increased CO_2, in 0.2 mM glucose, and in older cell cultures. CARP3 expression persisted at a >2.5 fold increase even at very high CO_2, regardless of glucose treatment (Figure 4.2a). In contrast, CARP4 was down-regulated at very high CO_2, and with added glucose early in the experiment (Figure 4.2b). However, added glucose resulted in increased CARP4 expression at low, moderate, and high CO_2 later in the experiment.

Transcription of the highly active carbonic anhydrase, STPCA-2 (Bertucci et al. 2011), was upregulated later in the experiment, under increased CO_2, and with glucose addition (Figure 4.2c). Cultures ≤1 day old exhibited severely down-regulated STPCA-2 expression, but transcription recovered by 5 days. It is noteworthy that STPCA-2 expression in the highest CO_2 treatment decreased by an order of magnitude relative to initial samples, but showed a trend toward recovery when additional glucose was added.

Cadherin protein production was negatively impacted by CO_2 treatment, but positively impacted by glucose addition (Figure 4.2d). In fact, no cadherin was detected by western blotting later in the experiment at high CO_2 or at any time point for samples grown at very high CO_2 (Figure 4.3). In contrast, early in the experiment at high CO_2, cadherin production was significantly higher after 4 hours than initially ($p < 0.05$), and

had recovered to initial levels by 9 days at low and moderate CO_2, with no effect of glucose addition.

$CaCO_3$ precipitation by coral cells in culture was detected only in low and moderate CO_2 treatments, particularly after 5 days (Figure 4.4). After 5 days, there was no difference in $CaCO_3$ precipitation between glucose or CO_2 treatments. However, at 9 days, cultures reared at moderate CO_2 precipitated $CaCO_3$ at a nearly 20x higher rate than those reared at low CO_2 (average 130 ng $CaCO_3^{-1}$ μg $protein^{-1}$ d^{-1} versus 7 ng $CaCO_3^{-1}$ μg $protein^{-1}$ d^{-1}), with no significant difference between glucose addition treatments. In fact, glucose addition did not significantly affect calcification rate, positively or negatively, in coral cell cultures at any point in the experiment.

Photosynthesis and calcification were decoupled in our cell culture system. After a delay likely induced by preparation of the culture, symbiotic dinoflagellates' variable fluorescence (F_v/F_m) was optimized at moderate and high CO_2 (Figure 4.5). In fact, recovery of F_v/F_m was strongest after 5 days in cultures grown at high CO_2, which was significantly higher than any other CO_2 treatments ($p < 0.05$), but was not significantly different between glucose treatments. At 9 days, cultures grown at moderate and high CO_2 recovered an F_v/F_m of 0.5 – 0.7. At this time point, there was no difference between glucose treatments. However, F_v/F_m was significantly and nearly significantly higher in moderate versus high pCO_2 treatments at 0.1 and 0.2 mM glucose ($p = 0.02$ and 0.09, respectively). In contrast, when grown at low or very high CO_2, variable fluorescence did not recover over the course of the experiment.

4.4 Discussion

This study was designed to test the effect of increased CO_2 on biomineralization-related gene expression and calcification rates of coral cell cultures, and potential amelioration of

negative responses by increased nutrition. CO_2 effects on calcification by juvenile and adult stony corals has been studied in both field and laboratory experiments, often over the course of weeks, and with varying organismal responses (e.g.; Drenkard et al. 2013, Rodolfo-Metalpa et al. 2015, Strahl et al. 2015). Additionally, differential expression of biomineralization-related genes has been studied in juvenile and adult corals subject to a variety of stressors (e.g.; Moya et al. 2012,Moya, 2014 #1020, Carreiro-Silva et al. 2014, Maor-Landaw et al. 2014). In order to elucidate the more immediate effects of increased CO_2 on a stony coral, the current experiments addressed short-term responses of *Stylophora pistillata*, specifically at the cellular level. In these experiments, we focused on expression of two coral-specific highly acidic genes, a highly active carbonic anhydrase, and an abundant cadherin. By using coral cell cultures, we show how separated cells of the *S. pistillata* holobiont respond within hours to days to altered CO_2.

One advantage of our cell culturing system over intact nubbins is that in the culture system, there is no difference in chemical composition, specifically CO_2, between the calicoblastic interface of tissue and skeleton and the overlying medium because the 3-dimensional structure of the organism has been removed. In previous studies, micro-electrodes and dies have been used to show that intact nubbins can alter the chemistry of the calicoblastic interface (Al-Horani et al. 2003 , Venn et al. 2013, Holcomb et al. 2014). Using the present cell culture method, we are able to assess more directly the cellular responses to altered CO_2. Specifically, we are able to examine the direct effects of specific CO_2 concentrations on biomineralization gene expression and calcification or dissolution without the organism moderating CO_2 in a separated calcifying interface

(McCulloch et al. 2012, Vidal-Dupiol et al. 2013). Additionally, the cell culture system generates new $CaCO_3$ uncontaminated by parent skeletal material (Mass et al. 2012).

Total SOM protein production has recently been shown to increase under acidified medium conditions (Tambutte et al. 2015). Additionally, in newly settled *Acropora millepora* polyps reared for three days at 380, 750, and 1000 ppm CO_2, approximately 40% of examined SAPs are up-regulated at moderate and high CO_2; (Moya et al. 2012). In contrast, expression of the acidic proteins 'secreted protein acidic and rich in cysteine' and aspein in mussels is not affected or is down-regulated, respectively, by increased CO_2 (Liu et al. 2012, Hüning et al. 2013). Like the coral SAPs, *S. pistillata* CARPs 3 and 4 in the current experiments were up-regulated as CO_2 increased in the low glucose treatment. These two proteins are able to precipitate $CaCO_3$ from unamended seawater (Mass et al. 2013), and appear to be incorporated into the less-soluble growth skeletal layers as in-fillers of a mold (Mass et al. 2014). Hence, our results suggest that *S. pistillata* cells will retain a molecular ability to grow their aragonite crystals as ocean pH decreases because CARPs should remain deprotonated and therefore functional at pHs below those predicted for the ocean. However, the effect of increased CO_2 on production of nucleation-specific proteins and on preservation of the mineral remain to be determined.

By catalyzing the reversible conversion of CO_2 to HCO_3^-, carbonic anhydrases (CAs) are proposed to be integral to the biomineralization process not only in corals, but in other carbonate producers as well (Heathfield 1970, Medakovic 2000) (reviewed byBertucci et al. 2013). While many CAs have intracellular roles related to homeostasis, several representatives have been found in mineralizing marine invertebrate shell, test,

and skeleton (Mann et al. 2008, Zhang et al. 2012, Drake et al. 2013, Ramos-Silva et al. 2013). However, although the role of these proteins is conserved across phyla, the sequences are not (Drake et al. 2014). Interestingly, STPCA-2, the only CA found to date in coral skeleton is an α-CA that both was originally immunolocalized to the cytosol of *S. pistillata* and clusters at the base of a group of intracellular CAs (Bertucci et al. 2011, Drake et al. 2013, Ramos-Silva et al. 2013). In contrast, STPCA, an α-CA immunolocalized to the calicoblastic epithelium has not been detected in coral skeleton (Moya et al. 2008). The K_{cat} of STPCA-2 is nearly twice that of STPCA and is higher than many comparable human CAs (Bertucci et al. 2011). Therefore, as a part of the biomineralization toolkit, it is expected that STPCA-2 should be quite effective at dealing with an increase in H^+ associated with increased CO_2 or resulting from the production of $CaCO_3$.

In the present study, STPCA-2 transcription increased as a function of culture age, CO_2 concentration, and glucose addition. Up-regulation of α-CAs thought to be involved in coral biomineralization have been noted in a cold-water coral (Carreiro-Silva et al. 2014) and a mussel (Hüning et al. 2013) in response to induced ocean acidification, whereas in warm-water corals, CA expression is differentially expressed under similar treatments depending on the length of exposure, the species, and the CA of interest (Moya et al. 2012, Ogawa et al. 2013). While it should be noted that STPCA-2 was not included in these previous studies of the effects of altered pH on CA expression, there are likely multiple CAs involved in the coral biomineralization process. The localization of the original STPCA specifically to the calicoblastic epithelium in *S. pistillata* suggests that it is responsible for transporting DIC to the site of calcification, even if it is not

directly involved in at the site of calcification and therefore is not retained in the skeleton (Moya et al. 2008). Additionally, broad-spectrum CA inhibitors induce a general decrease in calcification (Tambutte et al. 1996, Furla et al. 2000). Therefore, although STPCA-2 is the only CA presently known in coral skeleton, it is likely that many CAs have a role in biomineralization.

Expression of cadherin, a cell-cell and cell-substrate adhesion protein, may be linked to later phases of proto-polyp formation, although its production does not appear to be a successful compensatory mechanism to continue such formation under high CO_2 (Figure 4.1). For example, cadherin expression at high CO_2 was initially strongly up-regulated; however, this was insufficient to maintain proto-polyps adhered to substrate. This suggests that despite the localization of the protein at cell junctions in nubbin epithelia (Mass et al.), production of this particular cadherin is not a guarantee of cell-cell or cell-substrate adhesion in *S. pistillata* cell cultures stressed by increased CO_2. Disintegration of the coenosarc and separation of polyps has been observed in a related Pocilloporid coral, *Pocillopora damicornis*, in response to acidified growth medium (Kvitt et al. 2015). Therefore, reduction in cell or tissue adhesion appears to be a stress response to increased CO_2 and may be mediated by cadherin production at moderate CO_2, but not at high CO_2. This may correspond to reduced calcification. Indeed, knockdown of genes involved in cell adhesion pathways has been shown to lead to reduced calcification in sea urchins and mice (Barron et al. 2008, Rho et al. 2011).

Strong up-regulation of cadherin after one day of exposure to increased CO_2 suggests that this protein may be a good indicator of initial CO_2 stress. In contrast, cadherin expression was strongly down-regulated at very high CO_2; in fact, no cadherin

protein was detected by western blotting for any timepoints of cultures grown at 2000 ppm CO_2. This pattern is similar to decreased cell bundle formation coincident with decreased E-cadherin expression in malignant tumor cells grown at 8000 ppm CO_2 and higher (Ma et al. 2009).

Links between cadherin and mineral production have previously been shown in other systems. Cadherin knockdown results in decreased vesicle adhesion and otolith assembly in zebrafish (Clendenon et al. 2009). Similarly, cadherin-11 null mutant mice cell cultures exhibit reduced calcification (Kawaguchi et al. 2001). In our *S. pistillata* cultures, severely down-regulated cadherin expression from Day 5 onward was observed coincident with loss of $CaCO_3$ production or preservation at high (1000 ppm) and very high (2000 ppm) CO_2. Although this work does not resolve the precise role for cadherin specific to coral biomineralization, it does show the integral nature of this protein.

Symbiodinium spp. in *S. pistillata* cells lost the ability to photosynthesize in our culture system, as determined by variable fluorescence, F_v/F_m, at 'modern' (400 ppm) and very high (1000 ppm) CO_2 , but recovered this ability at moderate and high CO_2. With seasonal variation, *S. pistillata* F_v/F_m tends to range from 0.55 to 0.7 (Winters et al. 2006), which was obtained by our cell cultures at 5 days when grown at high CO_2 (1000 ppm), and 9 days when grown at moderate CO_2 (700 ppm). A significant increase in net photosynthesis has been observed in some corals grown in naturally high CO_2 environments (Strahl et al. 2015) and under experimental conditions (Anthony et al. 2008). In contrast, *S. pistillata* and *Seriatopora caliendrum* have shown no difference in net photosynthesis or F_v/F_m from low to very high CO_2 (Houlbrèque et al. 2012, Wall et al. 2014). In our culture system, within each glucose treatment, there was no difference

in F_v/F_m at moderate versus high CO_2 (700 versus 1000 ppm, respectively). It is unknown at this time why F_v/F_m did not recover at low or very high CO_2 (400 versus 2000 ppm, respectively).

Stylophora pistillata calcification rates, when examined on the order of weeks, have been shown to be maintained at the CO_2 concentrations similar to the low, moderate, and high treatments in the present study (Marubini et al. 2008, Venn et al. 2013). Other Pocilloporid (Comeau et al. 2013, Strahl et al. 2015) and temperate (Ries et al. 2009) corals have shown the same pattern of maintenance of calcification up to 1000 ppm CO_2, while some coral families such as Acroporidae, Agariciidae, and Favidae (Comeau et al. 2013, Drenkard et al. 2013, Strahl et al. 2015) appear to show sensitivity to increased CO_2 at lower concentrations than do the Pocilloporid. It should be noted that because no calicoblastic interface exists in our culture system, there can be no delineated zone of pH up-regulation or Ca supersaturation observed for intact nubbins (Al-Horani et al. 2003 , Venn et al. 2013). Hence, calcification response by *S. pistillata* cells in culture is not directly translatable to calcification by intact corals. Instead, our data show that coral cells maintain calcification up to 700 ppm CO_2, but not at higher concentrations.

In the case of release by nutrition of CO_2 effects on calcification, it is thought that the added energy of heterotrophy contributes in multiple ways. When delivered as zooplankton, feeding may provide nutrients to *Symbiodinium* spp. photosynthesis that may use some of the additional DIC (Holcomb et al. 2010), or may support an increase in biomass, although how this allows to corals to maintain calcification is not understood (Edmunds 2011). Additionally, in *S. pistillata*, feeding allows increased energy storage as lipid under temperature stress (Borell et al. 2008). In contrast, a degree of recovery in

calcification is observed in *Favia* sp. under heterotrophic conditions without a coincident increase in lipid content (Drenkard et al. 2013). In our system, the growth medium is already rich in inorganic nutrients in excess of that which allows recovery of calcification under moderate CO_2 concentrations (Holcomb et al. 2010), replicating well-fed conditions.

In our study, a doubling of glucose resulted in increased transcription and production of genes of interest, but this did not translate to increased calcification, even when photosynthesis did not occur at low CO_2. This reinforces the important role of a fixed carbon source in allowing SOM protein production, whose synthesis may be perturbed under increased CO_2 (Edmunds et al. 2014). However, previous studies have shown that addition of fixed carbon as glucose or glycerol leads to increased calcification (Holcomb et al. 2014); this was not observed in our cell cultures. Clearly, additional processes are at play in that SOM protein production did not translate to increased calcification.

Net accumulation of $CaCO_3$ requires not just precipitation but also preservation. Because of a potential cellular diffusion layer of ~1.5 μm (Karlsson et al. 1991), any mineral that extended more than this distance from the cultured cells would no longer receive the micro-environment changing benefits of enzymes such as carbonic anhydrase, reducing that mineral's preservation under raised CO_2. Therefore, the coral cell cultures may have continued to nucleate and extend $CaCO_3$ that was subsequently dissolved in the growth medium >1.5 μm away from the cell, in a process that likely does not occur in an intact coral's calicoblastic interface. Future experiments using, among other things, a more sensitive method to detect calcification may help to resolve this.

4.5 Conclusions

Coral skeleton formation is under direct biological control suggesting a mechanism for maintenance of mineral production under moderately acidified ocean conditions. Our results suggest that cell adhesion to form protopolyps, mediated by cadherin, is integral to the calcification process. Once proto-polyps are formed, a localized mineralizing milieu can be biochemically modified by proteins such as STPCA-2 to create conditions favorable for mineralization to commence under low and moderate CO_2 concentrations, and $CaCO_3$ framing can be filled in by CARPs and other proteins. However, this biological control is insufficient to overcome the role of carbonate chemistry of the calcifying medium at high CO_2 (1000 ppm), or is spatially restricted to a zone near the coral cells and is unable to provide mineral preservation, and apparent calcification drops off precipitously. Therefore, we propose that biological controls allow coral cells to continue to calcify in simulated ocean acidification conditions proposed for the remainder of the 21st century. However, the ability of cells to precipitate and preserve $CaCO_3$ appears to be detrimentally affected when the calcifying cells encounter $\geq$1000 ppm CO_2.

Table 4.1. Artificial seawater and growth medium chemical parameters.

	400 ppm CO_2	**700 ppm CO_2**	**1000 ppm CO_2**	**2000 ppm CO_2**
ASW Calculated pH	8.06	7.89	7.72	7.45
ASW Equilibration DIC (mM)	2.387	2.432	2.368	2.375
ASW Alkalinity (μmol/kg)	2597	2800	2537	2559
Medium Equilibrated pH	7.95	7.87	7.61	7.3
Medium Equilibration DIC (mM)	1.287	1.545	1.468	1.611
Medium Alkalinity (μmol/kg)	3067	3461	3370	3231
ASW Salinity	40			
Medium Salinity	34			
All Temperature (ºC)	26			
All Light (μmol quanta/m^2/s) (L/D)	100 (12:12)			

Figure 4.1. Light micrographs of *S. pistillata* cell cultures reared at 400 ppm (A) and 1000 ppm (B) CO_2. Formation of proto-polyps greater than 10 cells in diameter was observed in cultures reared at low and moderate CO_2, but no proto-polyps greater than 5 cells in diameter were observed at high or very high CO_2. No feeding effect was observed in formation of proto-polyps. Images acquired at 200x magnification.

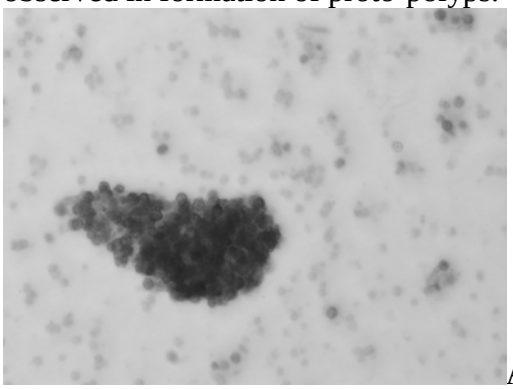

A

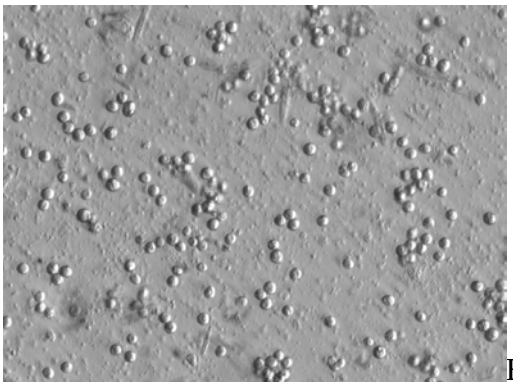

B

Figure 4.2. Expression fold change of skeletal organic matrix genes by *S. pistillata* cell cultures through time at four CO_2 and two feeding treatments. CARP3 (A), CARP4 (B), and STPCA-2 (C) gene expression was determined by qPCR by the $\Delta\Delta C_T$ method. Cadherin (D) protein expression was quantified by Western blot. At all time points, fold change is relative to expression at 400 ppm CO_2 at T_0. All samples were collected in triplicate. Brighter green and red correspond to greater up- and down-regulation, respectively.

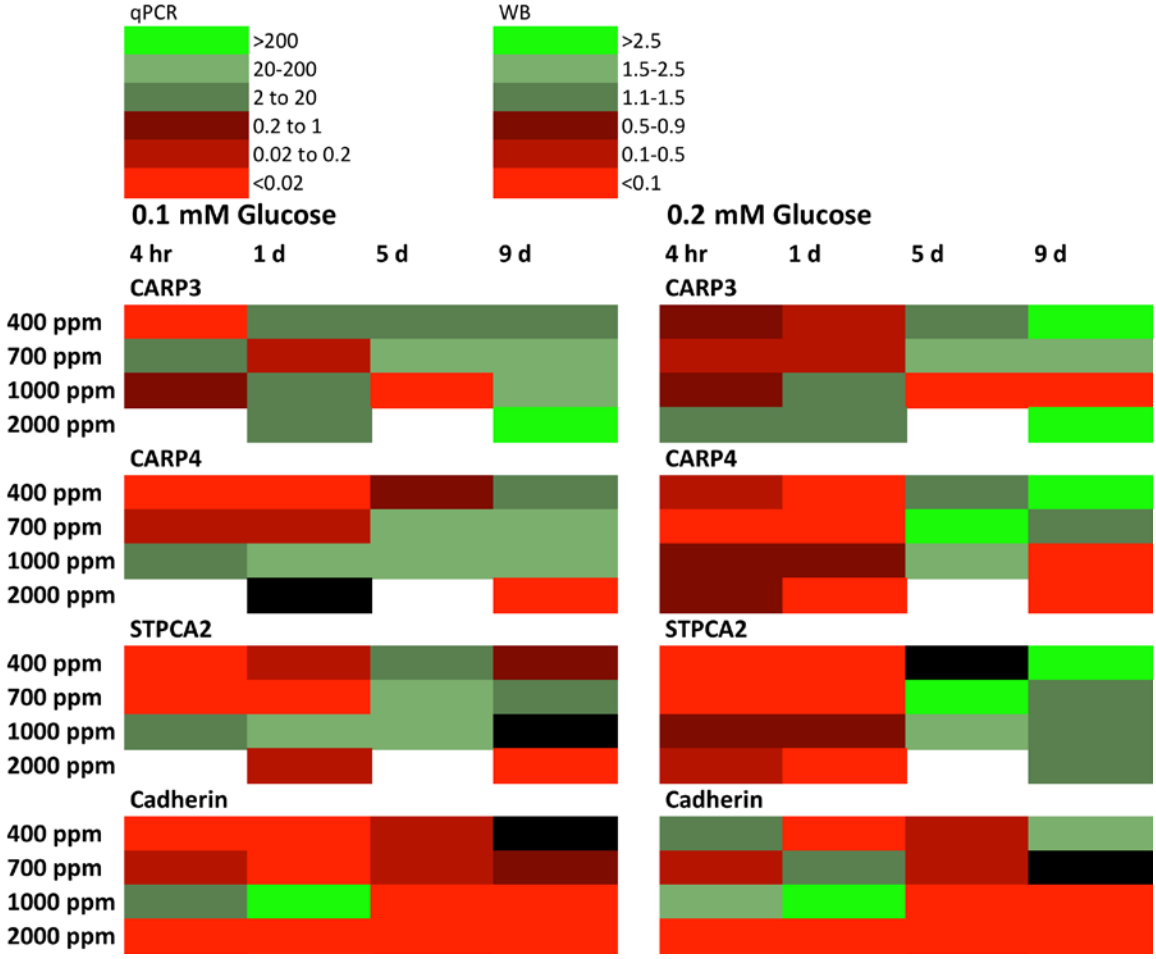

Figure 4.3. Cadherin protein expression quantified by western blot.

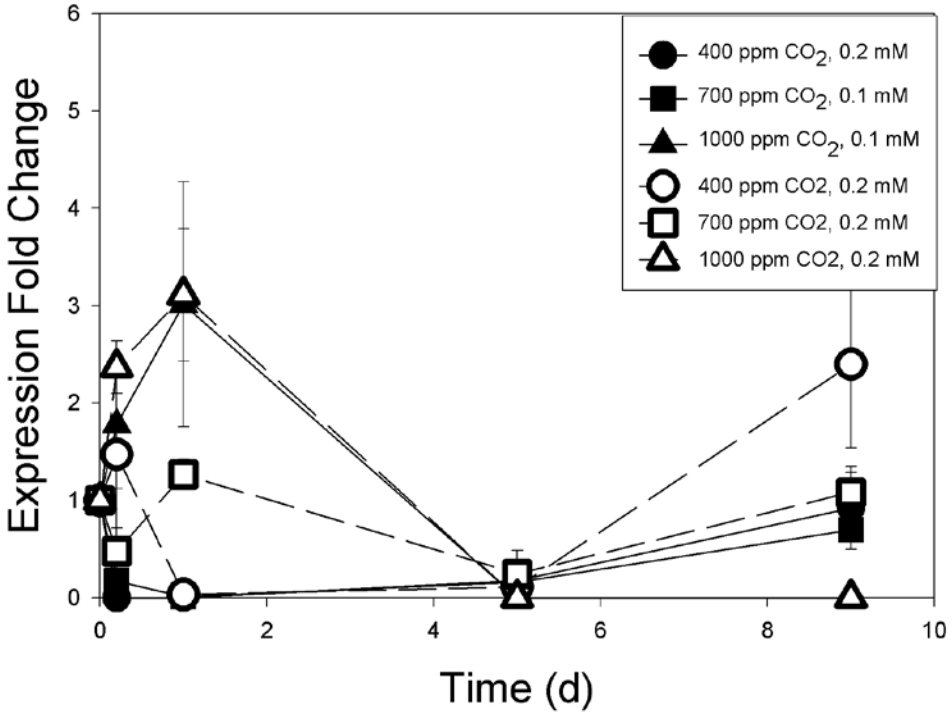

Figure 4.4. Calcification rate of *S. pistillata* cell cultures at 400 and 700 ppm CO_2 based on Sr incorporation. No appreciable $CaCO_3$ was detected at 1000 or 2000 ppm CO_2.

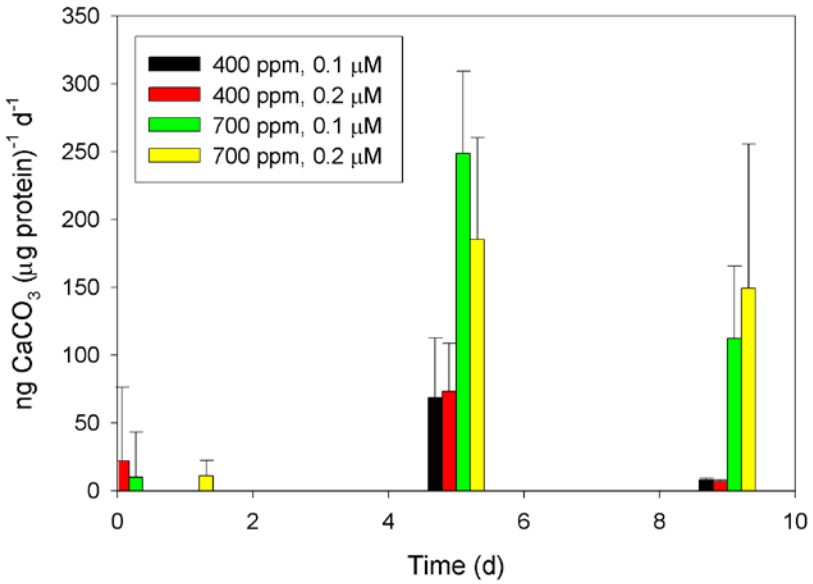

Figure 4.5. Variable fluorescence of *S. pistillata* cell cultures through time at four CO_2 and two feeding treatments. Solid symbols and lines denote 0.1 mM glucose treatments; empty symbols and dashed lines denote 0.2 mM treatments. All readings were collected on four individual wells.

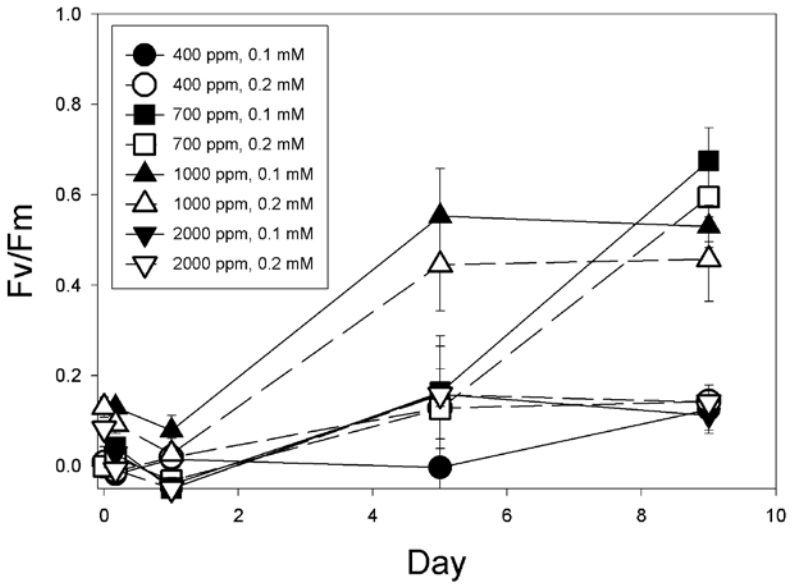

Chapter 5: A NanoSIMS study on the mechanisms of calcification in coral cells

Abstract

Localization of biomineralization proteins to tissues and mineral has greatly expanded our understanding of the process. However, the roles of these proteins remain elusive, particularly because the spatial relationship, at the nano-scale, between the functional domains of these proteins and the growing mineral is unknown. Cell cultures of the stony coral, *Stylophora pistillata*, grown in the presence of ^{15}N-aspartic acid, were examined by electron microscopy and NanoSIMS to develop these tools for understanding coral calcification. Our findings to date show that proteins containing a high proportion of this amino acid, such as the coral acid rich proteins (CARPs), have both intra- and extracellular roles in mineral formation. Intracellularly, CARPs appear to concentrate Ca, potentially for export from the cell to sites of calcification. Extracellularly, CARPs adhere cells to their neighbors and secure newly formed $CaCO_3$ nano-particles to cells and the substrate. These results show that combining cell cultures and NanoSIMS will be a very useful tool to understand the roles of highly acidic proteins in coral calcification.

5.1 Introduction

Coral biomineralization is a highly controlled process, yet it remains poorly understood. Recent advances have been made in the areas of skeletal proteomics (Drake et al. 2013, Ramos-Silva et al. 2013), transcriptome analysis (Moya et al. 2012, Mass et al. 2013, Vidal-Dupiol et al. 2013, Mass et al. in review), and cellular physiology (Zoccola et al. 2004, Moya et al. 2008, Zoccola et al. 2009, Bertucci et al. 2011, Laurent et al. 2013), and suggest that multiple types of proteins are required for specific steps of the

calcification mechanism. Many of these proteins are transmembrane or secreted proteins with catalytic function, such as K^+-dependent Na^+/Ca^{2+} exchangers, calcium ATPases (Zoccola et al. 2004), and carbonic anhydrases (Bertucci et al. 2011). Additionally, a group of coral-specific proteins, termed coral acid rich proteins (CARPs), with unique sequence structure and $CaCO_3$-precipitating ability has recently been described (Mass et al. 2013). Soluble acidic proteins (SAPs) and secreted acidic Asp-rich proteins (SAARPs) have also been identified by genome (Shinzato et al. 2011) and skeletal proteome (Ramos-Silva et al. 2013) studies although their functions are unknown.

The presence of highly acidic proteins is well-established in biominerals precipitated by many organisms (Lowenstam et al. 1989, Dove et al. 2003). Although some proteins are made acidic by post-translational modifications such as phosphorylation (Mann et al. 2010), many of the proteins contain a domain with a high proportion of aspartic or glutamic acids. At physiological pH, the carboxyl group on both of these amino acids is de-protonated, giving them a net negative charge. It was discovered that if separated by a single amino acid, these negative charges could produce an environment with negative charges at distances comparable to the distances between calcium atoms in $CaCO_3$ crystals (Weiner et al. 1975). Recently however, polymer-induced liquid-precursor (PILP) phases (Olszta et al. 2003), amorphous particle accretion processes (Gal et al. 2014), and a Lewis acid reaction involving specifically CARPs (Mass et al. 2013) have been proposed as more likely mechanisms for $CaCO_3$ precipitation.

CARPs and SAARPs are coral-specific proteins that contain >30% and >20%, respectively, aspartic and/or glutamic acids (Mass et al. 2013, Ramos-Silva et al. 2013).

They possess N-terminal signal peptides and, along with Amil-SAP-1 and -2, have been localized to the skeleton by both proteomic (Drake et al. 2013, Ramos-Silva et al. 2013) and immunohistochemical (Mass et al. 2014) analyses. The CARP-based $CaCO_3$ precipitation reaction has been proposed to be a Lewis acid process whereby CARP carboxylate-localized Ca ions lead to a micro-environmental pKa decrease, whereupon Ca is released from the carboxylates in favor of bicarbonate which is deprotonated by the acidic amino acid (Mass et al. 2013). The CARPs (and SAPs and SAARPs) ultimately remain trapped within the mineral they have induced, leading to an amino acid signature biased heavily in favor of aspartate/asparagine and glutamate/glutamine (Young 1971, Mass et al. 2012).

CARP4 is an interesting highly acidic coral protein. It was the first such protein sequenced, by Edman degradation, from coral skeleton (Puverel et al. 2005) and is one of few sequenced by mass spectrometry (Drake et al. 2013, Ramos-Silva et al. 2013). It has been immunolocalized to early mineralization zones (Mass et al. 2014) suggesting that it is involved in the initial nucleation reaction (Cuif et al. 1998). However, it is also found embedded in crystals thought to infill a skeletal mold during the day (Mass et al. 2014). In primary structure, the protein is comprised of a repeated pattern of an acidic region followed by a phylogenetically conserved non-acidic region (Drake et al. 2013). The first highly acidic region contains a string of >20 consecutive aspartic acid residues. Like other CARPs, CARP4 precipitates $CaCO_3$ from unamended seawater in vitro (Mass et al. 2013).

Nanoscale Secondary Ion Mass Spectrometry (NanoSIMS) is now a well-established technology used to determine major and trace element and isotope

distributions in both biological (Clode et al. 2007, Kopp et al. 2013) and mineral (Domart-Coulon et al. 2014, Gothmann et al. 2015, Rollion-Bard et al. 2015) samples, as well as interfaces of the two in non-coral systems (e.g.;Mueller et al. 2013). Element and ratio information is obtained with a resolution of 1 μm or less (Meibom et al. 2008). However, a limiting factor to NanoSIMS' usefulness is instrumental constraints against obtaining positive and negative ion information simultaneously. For instance, $^{15}N/^{14}N$ is typically determined as $^{15}N/^{12}C^-$ and $^{14}N^{12}C^-$ using a Cs^+ beam while Ca abundance is obtained as a cation using an O- beam. This issue can be circumvented by using the anion forms of alkali and alkaline earth metals, such as $^{24}Mg^{16}O^-$, $^{40}Ca^{16}O^-$ (Paris et al. 2014), and potentially $^{40}Ca^-$.

Here I analyzed ^{15}N-aspartic acid (hereafter '^{15}N-Asp') labeled cell cultures of the stony coral, *Stylophora pistillata*, by SEM and NanoSIMS to identify regions of potential co-localization of CARPs and calcium carbonate. Results indicate at least two roles for CARPs: concentrating intracellular Ca stores and adhesion of cells both to other cells and to extracellular $CaCO_3$. These roles may explain why some CARPs, notably CARP4, are found ubiquitously in coral skeleton.

5.2 Methods

5.2.1 Cell Culture Preparation

The Indo-Pacific stony coral, *Stylophora pistillata*, was chosen for these experiments due to its frequent use in ecological and physiological studies of hermatypic corals (Keshavmurthy et al. 2013), and because several recent analyses focusing on coral SOM proteins have employed this species (Drake et al. 2013, Mass et al. 2014) (Chapter 3). Cell cultures were generated from *S. pistillata* nubbins obtained from an in-house

aquarium facility according to previously a published protocol (Mass et al. 2012). Briefly, nubbins were incubated for four hours in calcium-free seawater containing 3% antibiotics/mycotics cocktail (GIBCO) and 20 mg/L chloramphenicol while gently rocking at room temperature to disrupt cell-cell adhesion. Nubbins were then transferred to a nutrient-rich growth medium prepared as follows. Dulbecco's Modified Eagle Medium (Gibco11966-025; at 8.3 g/L with added 0.578 g/L L-glutamine, 0.05 g/L taurine, and 25 mM HEPES buffer) was diluted to 12.5% in Instant Ocean with a 20 μg/L aspartic acid, 50 μg/L ascorbic acid, 2% heat-inactivated fetal bovine serum (Invitrogen), 0.1 mM glucose, and 1% antibiotics/mycotics cocktail. Final salinity of the growth medium was 34. The medium was brought to a pH of 8.2 with sodium hydroxide and then filtered on a 0.22 μm PES membrane (Nalgene). Nubbins in diluted growth medium were gently rocked overnight at room temperature during which time cells spontaneously dissociated from each other and from the skeleton. Dissociated cells were pelleted at 3000 rpm for 10 minutes, gently resuspended in fresh growth medium, and filtered through a 20 μm nylon mesh into Primary 6-well culture plates containing 10 mm glass slides to a total volume of 3 ml per well.

5.2.2 Choosing Sampling Timepoints

S. pistillata cell cultures transcribe increasing amounts of CARP 3 and 4 genes from initial culture creation to 9 days (Chapter 3). However, ^{15}N-Asp additions should begin only once both $CaCO_3$ precipitation has commenced and CARP4 production significantly exceeds background levels. I focused on CARP4 because it is the only CARP family to date sequenced from *S. pistillata* and *Acropora millepora* skeleton (Drake et al. 2013, Ramos-Silva et al. 2013) and because CARP4 contains a region of >20 consecutive Asp

residues (*S. pistillata* CARP4 accession number AGG36357.1). *S. pistillata* cell cultures were generated as described above (without glass slides) and pelleted in triplicate at 1, 3, 5, 6, 9, and 10 days. Pellets were stored in TRI Reagent (Life Technologies) at -80^{o}C until RNA extraction per the manufacturer's protocol. RNA was treated with TURBO DNase (Ambion) to remove DNA and, within 48 hours of extraction, converted to cDNA using SuperScript III (Invitrogen) by manufacturer's methods. All samples were analyzed by PCR with a primer set for CARP1 (F-AGGTCATTTCTCTGATGATG; R-CTCCGTCATTGTTGGATTAT; T_{anneal} = 57^{o}C), that amplifies a short CARP1 intron, to ensure that only genomic DNA-free cDNA was used for qPCR.

cDNA was analyzed by qPCR on a Stratagene MX300P thermal cycler using gene-specific primers for the CARP4 (F-AGACCCATTTGTGAAGAC; R-CGGTAACCACTCCTTTATT; T_{anneal} = 5^{0o}C) and 18S (F-AACGATGCCAACTAGGGATCA; R-GGTTTCCCATAAGGTGCCAAA; T_{anneal} = 56^{o}C (Kvitt et al. 2011)) genes as previously described (Chapter 4). Thermal profiles were initial denaturing at 94^{o}C for 10 minutes; then 40 cycles of 94^{o}C for 30 seconds, primer-specific annealing temperature for 30 seconds, and 72^{o}C for 30 seconds; followed by final extension at 72^{o}C for 5 minutes with a 37-cycle dissociation curve. Relative gene expression of CARP4 was determined by the standard $\Delta\Delta C_T$ method; C_Ts of the gene of interest (CARP4) were standardized to those of the housekeeping gene (18S), then to those of Day-1 samples, before conversion to 'fold change' as $2^{-\Delta\Delta Ct}$. Fold-changes were determined to be statistically different from zero by Student's t-test.

5.2.3 ^{15}N-Asp Additions

12.5% DMEM was prepared as described above except that the unlabeled aspartic acid was replaced with ^{15}N-Asp (Aldrich). 1-ml of this labeled growth medium was exchanged for the unlabeled medium at 5, 9, and 12 days. Cultures were allowed to grow for 30 minutes in this labeled medium; this length of time was chosen as corals show minimum catabolism of aspartic acid (Allemand et al. 1998, Swanson et al. 1998, Roberts et al. 1999, Kopp et al. 2013) coincident with incorporation of the amino acid into protein in this time window (Paulsson et al. 1983, Allemand et al. 1998). After 30 minutes, labeled growth medium was discarded and cultures were rinsed with unlabeled medium three times for three minutes each. Cultures were then allowed to grow either for an additional hour in unlabeled medium before termination and fixation, or until the next time point.

5.2.4 Sample Fixation

After 1-hour incubations in culture medium to clear un-incorporated ^{15}N-Asp samples were collected and fixed at 5, 9, and 12 days. Glass slides in the wells were gently transferred from the growth medium to 2% glutaraldehyde in 0.22 μm-filtered phosphate buffered saline (PBS) adjusted to pH 8.2 with sodium hydroxide. Cells were fixed in glutaraldehyde for four hours without rocking so as not to dislodge cells from the slides. Glutaraldehyde was the gently replaced with ethanol in a 5-step dehydration series from 50-100% molecular grade ethanol in MilliQ, with stationary incubations at each step for 20 minutes and a second 100% ethanol step. Cells on glass slides were then stored at -20^{o}C in 100% ethanol for ≤10 days before critical point drying with CO_{2liq}. Dried samples were immediately coated in 10 nm Au.

^{15}N enrichment was confirmed for cell pellets by Elemental Analysis – Isotope Ratio Mass Spectrometry (EA-IRMS) in the laboratory of Bess Ward at Princeton University. Cells adhered to the culture dish were dislodged with a rubber policeman, transferred to eppendorf tubes, pelleted at 10,000 g for 3 minutes, rinsed with filtered PBS, and stored at -80^{o}C. Pellets were resuspended in PBS to determine protein concentration by bichronoic acid assay (Thermo Scientific) against bovine serum albumin, then analyzed by EA-IRMS against a 3-point urea standard (Sigma) checked against high purity N_2 gas with signal calibration performed regularly using L-glutamic acid reference material (USGS40), with tin cup and PBS blanks were included in the analysis. As sample sizes were very small and did not allow replication for EA-IRMS, data were interpreted as positive- or no-signal and were not meant to be quantitative. Additionally, the control sample 'dropped' with a labeled sample so that we could not confirm by EA-IRMS that the control was ^{15}N -unlabeled.

5.2.5 Protopolyp Imaging

It has previously been shown that *S. pistillata* protopolyps produce extracellular $CaCO_3$ after 10 days (Mass et al. 2012). To confirm that the present protopolyps were indeed producing extracellular calcium carbonate, Au-coated glass slides were imaged on a Phenom Pro X with energy dispersive spectroscopy (EDS). Protopolyps >3 cells in diameter were point-analyzed by energy dispersive spectroscopy (EDS) on cells, aggregations of nano-particles, and background to detect regions containing Ca. Of interest was the Ca Kα peak at 3.6-3.8 keV, and the Mg and Na Kα peaks at 1.15-1.35 and 0.91-1.13 keV, respectively. EDS spectra were blank corrected to the signal at 5 keV and standardized to the signal at 3.9 keV to visualize small Ca peaks.

5.2.6 NanoSIMS

S. pistillata protopolyps were analyzed on the California Institute of Technology Microanalysis Center's Cameca NanoSIMS 50-L. Samples were coated with an additional 30 nm gold to increase conductivity. Protopolyp samples exhibited strong charging; hence the electron gun was employed negating acquisition of secondary ion images. Select protopolyp regions of interest (ROIs) were pre-sputtered with a positive primary beam (Cs^+; ~1 pA) beam for five minutes and then 14 or 27.5 ms/pixel dwell times for sample analysis. Each ROI was analyzed as up to 7 layers for secondary ions of $^{16}O^-$, $^{12}C_2^-$, $^{14}N^{12}C^-$, $^{15}N/^{12}C^-$, $^{32}S^-$, $^{40}Ca^-$, and $40Ca^{16}O^-$ (Table 5.1). Because the ionization of Ca to negative ions is low, the $^{40}Ca^-$ peak was checked against a calcite standard. ROIs were 8x8 to 18x18 μm and were analyzed as a 256x256-point grid, resulting in spot sizes of ~30-70 nm. Following SIMS analysis, each sample was re-imaged by SEM with elemental point-analysis by EDS.

5.2.7 NanoSIMS Image Processing

Pixel counts for $^{15}N/^{12}C^-$, $^{14}N^{12}C^-$, and $^{40}Ca^-$ were analyzed using Poisson counting statistics. Standard deviation, σ_x, of all non-zero counts for each mass were computed as

$$\sigma_x = \sqrt{\mu_x}$$

where μ_x is the mean of all non-zero counts within an assigned mass window, x. As this is also the Poisson noise, $2\sigma_x$ was used as the cutoff for significant total counts per pixel. Isotope and element ratios for $^{15}N/^{12}C^-/^{14}N^{12}C^-$ and $^{40}Ca^-/^{14}N^{12}C^-$were generated using OpenMIMS open-source software in ImageJ at these cutoffs for individual relevant masses and for each plane of analysis. Because enrichment of ^{15}N is used here as a proxy for presence of highly acidic proteins, a cutoff of 0.0036 $^{15}N/^{12}C^-/^{14}N^{12}C^-$, or $\delta^{15}N$ natural

abundance, was applied to the $^{15}N/^{14N}$ ratio images. $^{40}Ca^-/^{14}N^{12}C^-$ was also calculated to distinguish non-cellular inorganic Ca (high $40Ca/^{14}N^{12}C^-$) versus cellular Ca (low $40Ca/^{14}N^{12}C^-$).

5.3.8 CARP4 Transmembrane Prediction

To aid in understanding the localization of $^{15}N/^{14}N$ enrichment, the potential for CARP4 anchoring in cell membranes was examined. Consensus transmembrane predictions for CARP4 (Genbank Accession No. Agg36357.1) were generated in TMpred, TMHMM, and DAS TMfilter servers (Hofmann et al. 1993, Krogh et al. 2001, Cserzo et al. 2002).

5.3 Results

CARP4 expression, as fold change, increased from cell culture creation to 10-days' growth, and is described equally well by $\log_{10}$ and ln functions (Figure 5.1A, B). Expression statistically exceeded a fold-change of zero after 5 days of *S. pistillata* cell culture incubation. This also coincides with detectable calcification (as Sr incorporation into the acetic acid-soluble phase; see Chapter 4) and previous observations of cell cultures. Hence, 5-day incubations were chosen as the first timepoint for ^{15}N-Asp additions.

Nano-balls of apparently amorphous $CaCO_3$ were observed by SEM on protopolyps at all timepoints (Figure 5.2). These nano-balls contained Ca and were depleted in Na/Mg relative to cellular or background locations (Table 5.2). They were only observed on or near *S. pistillata* cells. No aragonite crystals were observed on protopolyps in any of the samples.

Ca, in both inorganic and cellular forms, was detected by NanoSIMS in samples aged 5- and 12-days ('5d-12' and '12d-12', respectively; Figure 5.3A-D). Average non-

zero $^{40}Ca^-$ relative to non-zero $^{14}N^{12}C^-$ locations of detection within each ROI was marginally higher in 12-d samples compared with 5-d samples (Table 5.3), suggesting that protopolyps were calcifying over the 12-day incubations. However, $^{14}N^{12}C^-$ counts/pixel were nearly an order of magnitude lower in 5-day samples compared with 12-d samples, so all further comparisons using these samples must be made with great care.

Absolute values of EA-IRMS analysis of $\delta^{15}N$ should be used with caution as total N content of cell pellets was very low and samples were not analyzed in replicate. Instead, EA-IRMS values should be considered as indication of whether enrichment was achieved. With this caveat, 9-day and 12-day samples appear to be labeled with ^{15}N, but 5-day samples were minimally labeled (Table 5.3). As noted above, the sample to which ^{15}N-Asp was added and the samples collected both on the fifth day, accidentally 'dropped' with the Control sample during EA-IRMS analysis; therefore, the extent of actual labeling is unknown. Additionally, the samples for which ^{15}N-Asp was added only on the fifth day, but were allowed to grow until 12 days, appeared by EA-IRMS to not be ^{15}N -enriched (Table 5.3).

Minimal $^{15}N/^{12}C^-/^{14}N^{12}C^- >0.0036$ and few total $^{15}N/^{12}C^-$ counts above the Poisson noise cutoffs suggest that 5-day samples were not ^{15}N -labeled effectively for NanoSIMS detection (Table 5.3; Figure 5.4). NanoSIMS count data show that while 0.3% 14N12C—containing pixels exhibited $^{15}N/^{12}C^-/^{14}N^{12}C^- >0.01$ in Control samples, 5-day samples displayed $^{15}N/^{12}C^-/^{14}N^{12}C^- >0.01$ in <0.05% of $^{14}N^{12}C^-$-containing pixels. This supports the EA-IRMS results (Table 5.3). In contrast, 12-day samples exhibited $^{15}N/^{12}C^-/^{14}N^{12}C^-$ >0.01 in 3.1% of 14N12C—containing pixels.

Although the samples to which ^{15}N-Asp was added on both day 5 and day 9 ('9d-12' and '9d-9') appear to be enriched in ^{15}N (Table 5.3), detection of $^{15}N^{12}C^-$ and $^{40}Ca^-$ was minimal. In fact, maximum counts per pixel were 3 and 5, respectively for $^{15}N^{12}C^-$ and $^{40}Ca^-$. This was likely a function of both shorter dwell time compared with the Control and 12-day samples (14 ms versus 27.5 ms), and that the NanoSIMS was set up to run both a 5-day and a 9-day sample overnight with auto-optimization. Therefore, 9-day ROIs cannot be used in the current $^{15}N/^{14}N$-versus-Ca analysis.

S. pistillata cultured protopolyps, to which ^{15}N-Asp was added on days 5, 9, and 12, ('12d-12') exhibit sufficient labeling (Table 5.3) and experienced manually optimized NanoSIMS time so as to acquire a relatively large number of ion counts per pixel within each ROI (Figure 5.5). Although a background of low-level enrichment ($^{15}N/^{14}N < 0.008$) is observed ubiquitously on and in cells in all 12-day ROIs, aggregation of ^{15}N labeling is evident on the edges of cells and at cell junctions, as well as on non-cellular material (Figure 5.5).

$^{40}Ca^-$ matches well with material that, by SEM, appears to be non-cellular, although it occurs both extra- and intracellularly (Figure 5.3 C and F). SEM resolution does not allow for distinguishing different morphological features of areas that correspond only to $^{40}Ca^-/^{14}N^{12}C^-$ versus areas that correspond to $^{40}Ca^-$. However, it is clear from NanoSIMS and from post-SIMS SEM images that organically tied Ca and inorganic Ca occur as both intra- and extracellular forms.

Co-localization of enrichment of ^{15}N and $^{40}Ca^-$ in 12d-12 samples is minimal, but present, as seen in composite images of $^{15}N^{12}C^-/^{14}N^{12}C^-$ (green) and $^{40}Ca^-$ or $^{40}Ca^-/^{14}N^{12}C^-$ (blue). On each ROI of this sample, there are several areas at the cells' surfaces where

blue and bright green are observed in adjacent or shared pixels. ^{15}N enrichment, when co-localized with $^{40}Ca^{-}/^{14}N^{12}C^{-}$, is typically seen at the edges of the $^{40}Ca^{-}/^{14}N^{12}C^{-}$. Although, in these cases, $^{15}N/^{14}N$ enrichment is not significantly different from that which is not associated with $^{40}Ca^{-}/^{14}N^{12}C^{-}$, intracellular $^{40}Ca^{-}$ counts are ~5 times higher (Table 5.4). Because the samples are topographically complex and contain multiple sources of matrix effects as compared to a polished flat calcite standard, it is not possible at this time to determine the total Ca concentration of these regions.

CARP4 is predicted to have a transmembrane region at its C-terminus from amino acids 292 to 311. This anchor is predicted by all three servers queried.

5.4 Discussion

Although CARP4 transcription was relatively high by day 5, incorporation of ^{15}N-Asp during 30-minute incubations was insufficient to produce isotopic enrichment. However, samples that received ^{15}N-Asp additions at days 5 and 9, and were cultivated at day 9 were enriched above background. Therefore, it appears that transcription >500 times the initial rate of the cell cultures is necessary for ^{15}N-Asp to be incorporated into protein at a sufficient level for NanoSIMS detection. A 20-minute lag in ^{14}C-Asp incorporation into coral skeletal organic matrix has previously been observed (Allemand et al. 1998). However, after this lag, ^{14}C-Asp incorporation quickly reaches a plateau. The current experiment sought to avoid metabolism of aspartic acid (Swanson et al. 1998, Kopp et al. 2013), hence the choice of 30-minute incubations. Additionally, without the three-dimensional structure of an intact nubbin, the protopolyps may incorporate the labeled amino acid more quickly than previously observed. Therefore, 30-minute incubations

seem appropriate for this type of work, and the limiting factor is simply translation of a sufficient amount of aspartic acid-rich protein.

Acidic proteins have been implicated in cell-cell adhesion, both in terms of enhancement (Liaw et al. 1994) and limitation (Girard et al. 1996). Much of the higher enrichment of ^{15}N-Asp in 12-day *S. pistillata* cell cultures that received three pulses of label was observed at the edges of cells and at cell junctions. CARPs 1, 3, and 4 have been immunolocalized to ectodermal cell junctions in *S. pistillata* tissue sections (Mass et al. 2014). More specifically, CARP4 antibodies bind strongly to the skeletal side of desmocytes, specialized coral cells for attachment to newly formed skeleton (Muscatine et al. 1997). Hence, the localization of ^{15}N-Asp to edges of cells and cell junctions provides support for minimal metabolism of the amino acid, suggesting that ^{15}N detection is indeed specific to aspartic acid. Along with the C-terminus transmembrane prediction for CARP4, it also reinforces a role in cell-cell adhesion for CARPs.

CARPs and other acidic proteins have been shown to precipitate $CaCO_3$ and control the mineral polymorph in unamended seawater and supersaturated solution, respectively (Politi et al. 2007, Takeuchi et al. 2008, Rahman et al. 2011, Mass et al. 2013). Additionally, acidic proteins have been immunolocalized to various polymorphs and grow layers of biogenic $CaCO_3$ (Alvares et al. 2009, Suzuki et al. 2009, Mass et al. 2014). Hence, it was anticipated that there would be strong co-localization of ^{15}N-Asp with Ca in *S. pistillata* cell cultures. However, this was not the case.

Inorganic Ca (as $^{40}Ca^-/^{14}N^{12}C^-$) was observed intra-, trans-, and extracellularly in *S. pistillata* cell culture protopolyps after 12 days of growth. When co-localized, ^{15}N-Asp most frequently occurred with or adjacent to intracellular inorganic Ca. Intracellular

aragonite crystal precursors have been suggested in coral desmocytes for the past four decades (Hayes et al. 1977), although there is disagreement as to whether some of the reported membrane-associated biomineralization vesicles may actually be a product of chemical fixation (Clode et al. 2002). Overall, however, there is agreement that the calicoblastic epithelium contains small pockets of high calcium concentration (Clode et al. 2003, Marshall et al. 2007). Therefore, the present experiment supports the hypothesis of intracellularly concentrated Ca, in this case with Ca concentrations likely ~5 times higher than the background cellular, mediated by organic molecules such as CARPs, to be used for extracellular mineral production. Additionally, although the CARPs can precipitate $CaCO_3$ from seawater in vitro (Mass et al. 2013), the current results suggest a second *in vivo* role to concentrate and transport intracellular Ca to extracellular sites of calcification.

A third role for CARPs, again as adhesive, is also suggested by the NanoSIMS data. Figure 5.3 clearly shows extracellular inorganic Ca, which is, in some cases, spatially separated from ^{15}N-Asp. This inorganic Ca also appears to have extended away from the cell, but still retains some contact with the glass slide. High sequence conservation of non-acidic regions of CARP4 has led to the suggestion that these domains are involved in protein-protein interactions (Fraser et al. 2002, Aytuna et al. 2005, Mass et al. 2012 554). Hence, aspartic acid-rich CARPs may act as part of the adhesion network observed between calicoblastic cells and newly formed skeleton (Clode et al. 2003). This process is known in other biomineralization systems, with acidic regions of proteins able to bind mineral while non-acidic regions bind other proteins such

as integrin (Smith et al. 1996, Gilbert et al. 2000, Goldberg et al. 2001), which is also observed in the coral skeletal organic matrix protein complex (Drake et al. 2013).

Overall, NanoSIMS is a highly useful tool to study the interface of biomolecules and biominerals. Protopolyps at least nine days old incorporate sufficient ^{15}N-Asp so that, with sufficient ROI acquisition optimization and dwell times of ~30 seconds, reanalysis of these samples may yield interesting insights into the temporal progression of protopolyp calcification. Future experiments using coral cell cultures should incorporate both single- and multiple-exposure pulses of ^{15}N-Asp to clarify that minimal aspartic acid catabolism occurs over the incubations. However, it is clear from the present experiment that ^{15}N-Asp and $^{40}Ca^-$ co-localization is possible in this system and yields fruitful information about the spatial relationship between CARPs and newly formed $CaCO_3$.

5.5 Conclusions

S. pistillata protopolyps >9 days old incorporate ^{15}N-Asp labeling in sufficient amounts for NanoSIMS analysis. NanoSIMS confirmed the intracellular co-localization of highly acidic proteins and $CaCO_3$. This reveals that CARPs likely have a role in concentrating intracellular Ca that can be used for external calcification. CARPs also appear to support adhesion of cells to each other and to extracellular $CaCO_3$. Hence, there appear to be multiple roles for CARPs in the biomineralization process.

Table 5.1. NanoSIMS masses detected after sputtering with a Cs+ beam.

Atomic Mass Unit	**Element(s)**
15.985	$^{16}O^-$
23.960	$^{12}C_2^-$
25.924	$^{14}N^{12}C^-$
27.002	$^{15}N^{12}C^-$
31.806	$^{32}S^-$
39.798	$^{40}Ca^-$
55.787	$^{40}Ca^{16}O^-$

Table 5.2. Cation EDS peak area ratio ranges after baseline correction and standardization to the 4 keV baseline.

Sample Type	**Auto-detected Ca Peak**	**Na[1]/Mg[2] Peak Area Ratio**	**Mg[2]/Ca[3] Peak Area Ratio**
Nano-balls adhered to or near cells	Yes	1.1-2.7	1.6-3.2
Cell	No	1.4-5.8	2.0-4.7
Glass slide background	No	4.5-6.9	1.6-2.9

[1] Na peak area was integrated for the Kα peak from 0.91 to 1.13 keV.

[2] Mg peak area was integrated for the Kα□peak from1.15 to 1.35 keV.

[3] Ca peak area was integrated for the Kα peak from 3.6 to 3.8 keV.

Table 5.3. NanoSIMS counting statistics of ROIs on *S. pistillata* protopolyps.

Sample	Dwell Time (ms)	Average Maximum $^{14}N^{12}C^-$ counts per pixel	Average Maximum $^{15}N^{12}C^-$ counts per pixel	Average Maximum $^{40}Ca^-$ counts per pixel	Average # non-zero $^{14}N^{12}C^-$ counts-containing pixels	Average # non-zero $^{15}N^{12}C^-$ counts-containing pixels	Average # non-zero $^{40}Ca^-$ counts-containing pixels	$^{14}N^{12}C^-$ 2 σ cutoff	$^{15}N^{12}C^-$ 2 σ cutoff	$^{40}Ca^-$ 2σ cutoff	$\delta^{15}N$
Control	27.5	600.7	9.0	9.0	61,757	218	5,674	19	3	3	-[#]
5d-5	14	335.3	3.4	6.4	9529	389	772	5	2	3	8.25[#]
5d-12[+]											-1.26
9d-9[*]	14	84.2	4.7	3.0	11427	543	213	4	2	2	19.04
9d-12											5.13
12d-12[+]	27.5	4288.6	27.9	18.5	51909.9	1637.3	9343.2	39	5	3	12.86

[*] Only one ROI considered for 9d-9 sample.

[#] Control and 5d-5 samples 'dropped' together during EA-IRMS analysis; hence no $\delta^{15}N$ data were obtained for the Control sample, and enrichment of 5d-5 sample is diluted to an unknown degree by the Control.

[+] Sample not analyzed by NanoSIMS.

Table 5.4. NanoSIMS counts of co-localized $^{40}Ca^-$ and $^{15}N^{12}C^-/^{14}N^{12}C^-$ for 12-day-old *S. pistillata* protopolyp regions of interest (ROI). Three spots of each type were analyzed for each ROI.

ROI	$^{40}Ca^-$ and $^{15}N^{12}C^-/^{14}N^{12}C^-$ co-localized		$^{40}Ca^-$ and $^{15}N^{12}C^-/^{14}N^{12}C^-$ not co-localized	
	Average $^{40}Ca^-$ Counts	Average $^{15}N^{12}C^-/^{14}N^{12}C^-$	Average $^{40}Ca^-$ Counts	Average $^{15}N^{12}C^-/^{14}N^{12}C^-$
12d_12_3	4.9 (±2.81)[1]	0.01363 (±0.02355)	0.6 7(±1.11)	0.03094 (±0.10279)
12d_12_4	4.49 (±2.64)[1]	0.00315 (±0.00186)	0.78 (±0.95)[1]	0.00355 (±0.00046)
12d_12_5	4.56 (±2.55)[1]	0.00227 (±0.00156)	0.98 (±1.25)[1]	0.00405 (±0.00096)

[1] Indicates significant difference between co-localized and non-co-localized spots, $p<0.001$.

Figure 5.1. Expression of CARP4 throughout the 10-day growth of *S. pistillata* cell cultures is described equally well by $\log_{10}$ (A) and ln (B) functions.

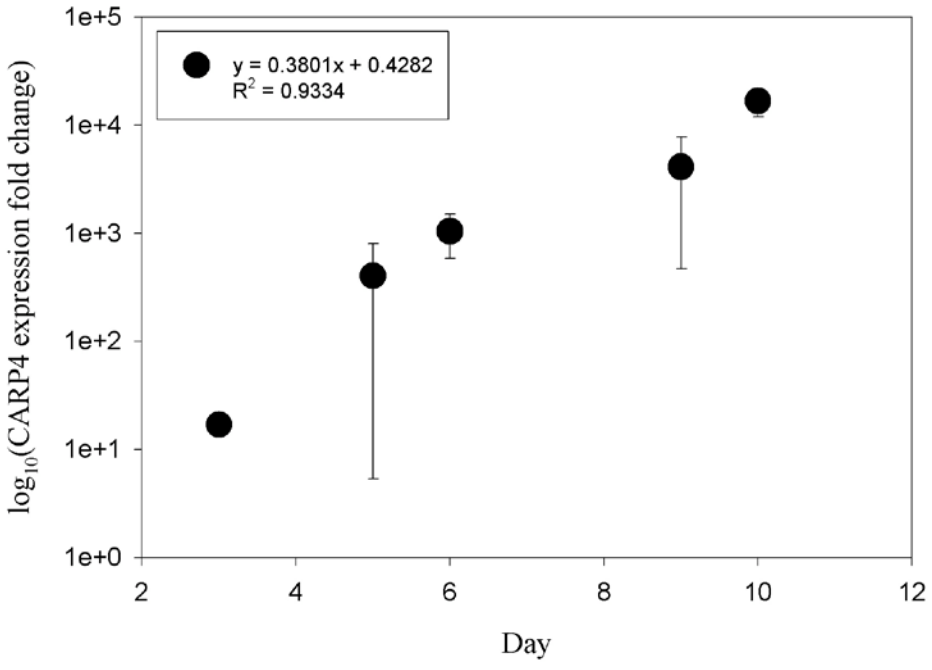

A

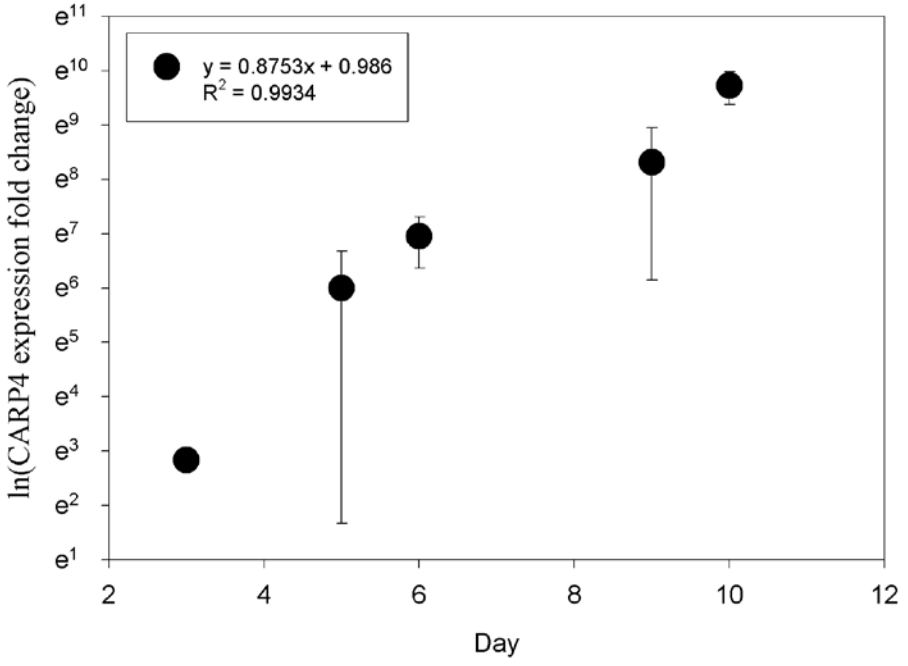

B

Figure 5.2. Formation of *S. pistillata* protopolyps and production of extracellular $CaCO_3$ nano-particles after 5- (A), 9- (B), and 12-days (C) of growth.

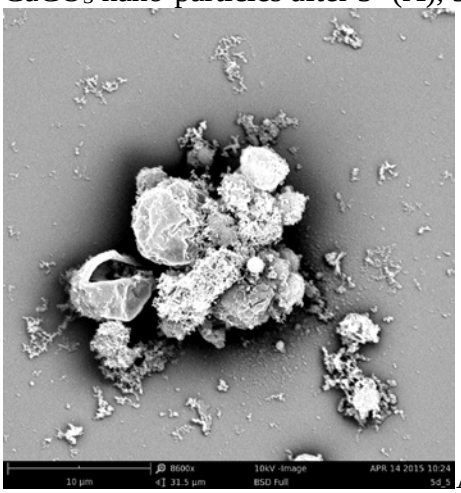

A

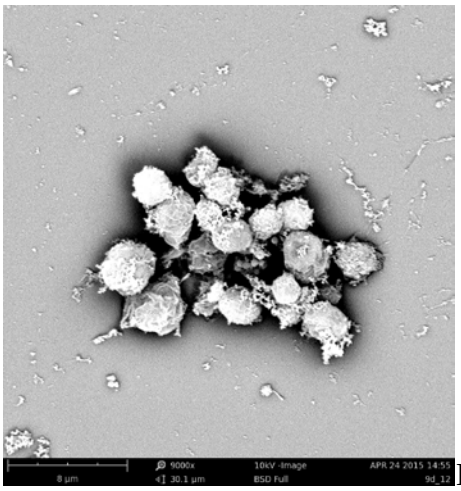

B

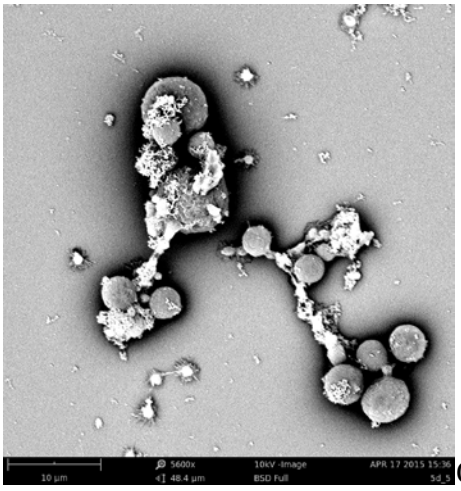

C

Figure 5.3. Intracellular and extracellular Ca in *S. pistillata* protopolyps. Highly organic-associated Ca, as $^{40}Ca^-$ (A,D); inorganic Ca (as $^{40}Ca^-/^{14}N^12C^-$ (B,E), and post-SIMS SEM-detected nano-particles (C,F) after 5-days' (A,B,C) and 12-days (D,E,F) growth. SIMS orientation is a mirror of SEM orientation.

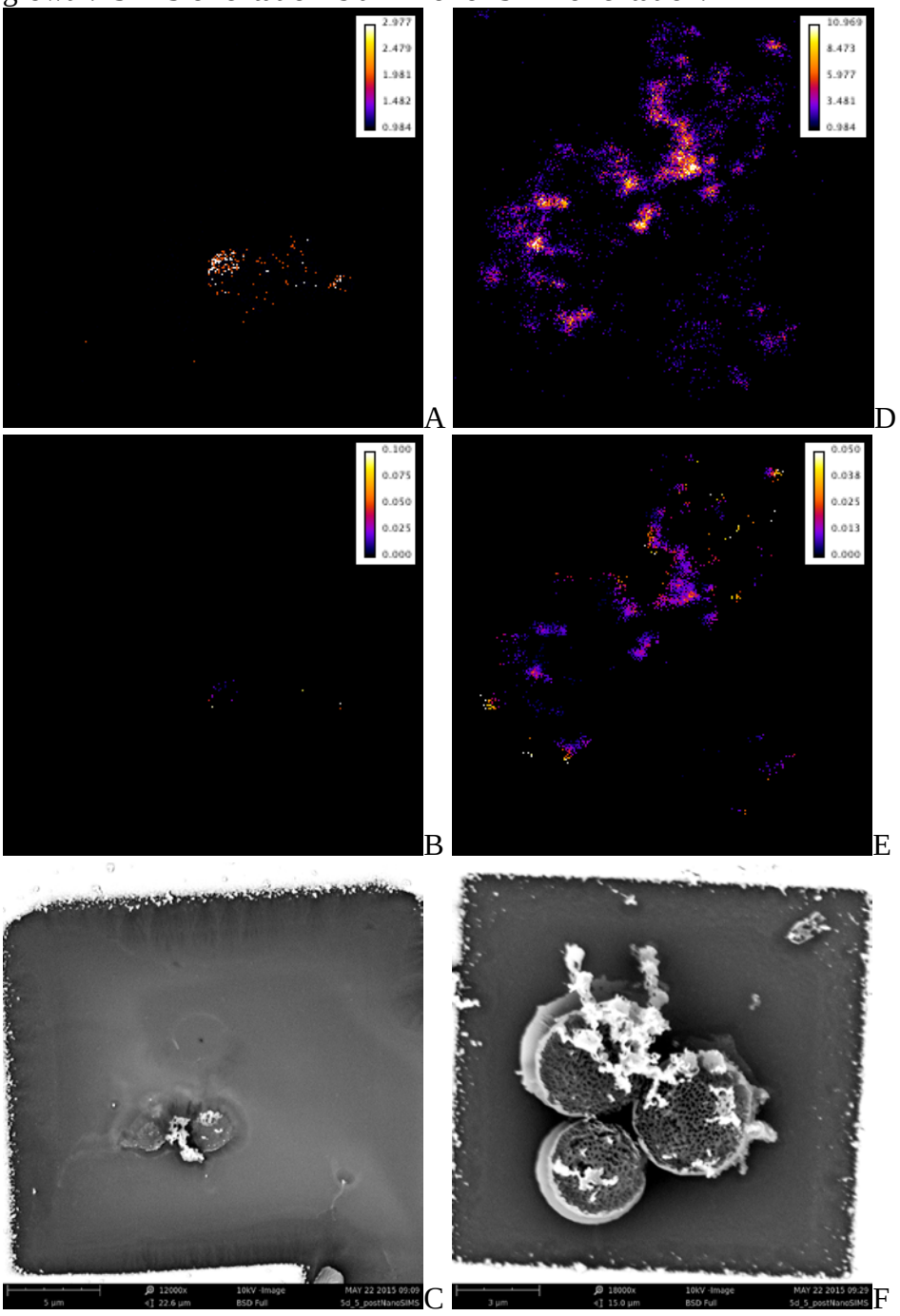

Figure 5.4. 5d-5 sample ROI. (A) ^{15}N-enrichment (green; as $^{15}N^{1}2C^{-}/^{14}N^{1}2C^{-}$ by NanoSIMS) by 5d-5 samples was insufficient for NanoSIMS analysis, despite apparent enrichment detected by EA-IRMS. (B) Post-SIMS SEM image of the same location. SIMS orientation is a mirror of SEM orientation.

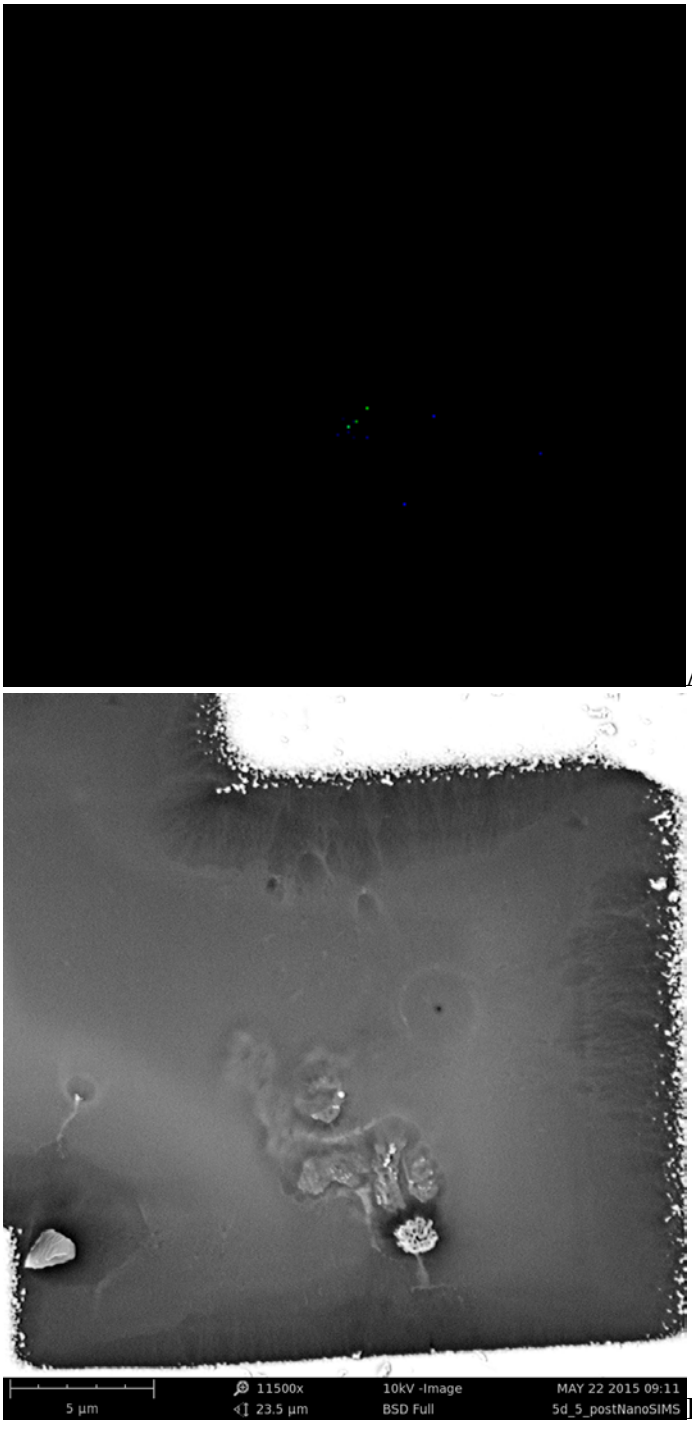

A

B

Figure 5.5. 12d-12 sample ROI. (A) ^{15}N enrichment (as $^{15}N^{1}2C^{-}/^{14}N^{1}2C^{-}$ by NanoSIMS) in 12d-12 samples was higher at cell edges and junctions. ^{15}N-Asp (green) was more closely associated with intracellular inorganic Ca (B; blue; as $^{40}Ca^{-}/^{14}N^{1}2C^{-}$) than extracellular Ca (C; blue). Yellow arrows are $\delta^{15}N$ and inorganic Ca co-localization. Nanoparticles were observed both intra- and extracellularly (see Figure 5.3F).

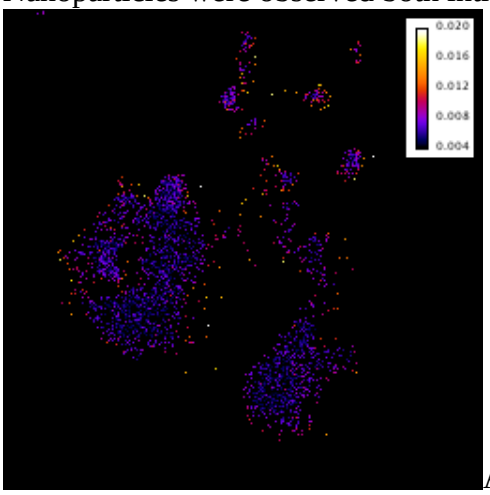

A

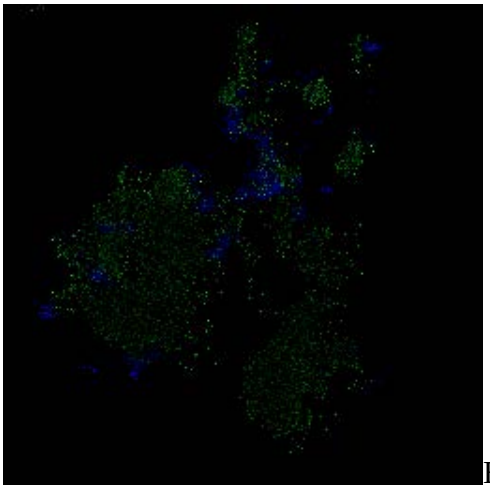
B

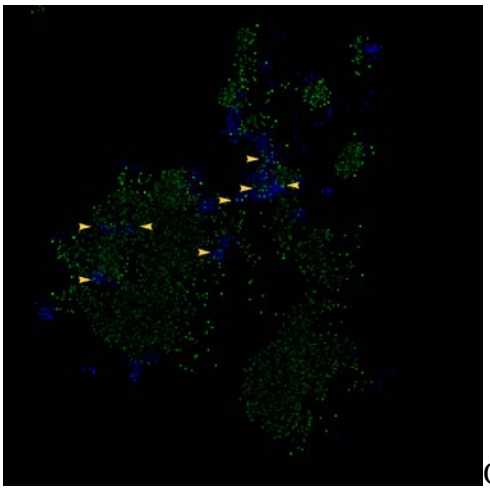
C

Chapter 6: Conclusions

This thesis constitutes the first coral skeletal proteome (Chapter 2), the first application of coral cell cultures for understanding the effects of ocean acidification on coral calcification at the cellular and molecular levels (Chapter 4), and the first use of NanoSIMS to test the co-localization of aspartic acid and newly formed aragonite in corals (Chapter 5). These findings detail the skeletal protein production response of corals to environmental perturbations and provide additional evidence for potential roles of highly acidic proteins in corals' biomineralization process. Additionally, the work in this dissertation prompts numerous areas of future research.

Corals, like mollusks, likely produce family-specific biomineral-associated protein complexes (Marin et al. 2013). In fact, while there is significant overlap in SOM proteins detected in *S. pistillata* and *A. digitifera* (Drake et al. 2013, Ramos-Silva et al. 2013), there are clearly proteins from skeleton of each species not found in the other by LC-MS/MS sequencing. An example is galaxin, a potential collagen-binding protein (Bhattacharya et al. in review) observed in *A. digitifera*, but not *S. pistillata*, skeleton. Recent sequence analysis suggests that galaxin is polyphyletic within corals (Bhattacharya et al. in review), and as such may have a diminished role in biomineralization of Pocilloporids (*S. pistillata*) compared with Acroporids (*A. digitifera*). This is not surprising given the confusion surrounding coral phylogenetics (Budd et al. 2010). Further comparative skeletal proteome analyses will be useful to resolve the evolution of the stony coral biomineralization toolkit(s).

An issue that came to light during this dissertation is the problem of coral cellular versus human contamination of SOM protein samples (Ramos-Silva et al. 2013).

Contamination of carbonate organic matrix proteins by highly conserved proteins of potential human origin are not unknown in proteomic studies (Chapter 3 and (Drake et al. 2014)). While I am confident that coral cellular contamination is not present in the *S. pistillata* SOM proteome (Drake et al. 2013), it would be useful to determine if highly conserved proteins, such as actin and ubiquitin, are derived from the coral or from a human source. Immunological localization of some of these proteins in coral skeleton thin sections is a step in the right direction (Mass et al. 2014), but does not conclusively resolve the issue.

Now that two independent coral skeletal proteomes exist (Chapter 1 and (Drake et al. 2013, Ramos-Silva et al. 2013)), future transcriptomic studies should utilize these targets to assess the ability of corals to maintain calcification during dramatic global change. Several recent studies using intact coral nubbins have missed this opportunity (Carreiro-Silva et al. 2014, Rosic et al. 2014) while others have examined expression of a few of these genes (ex; (Maor-Landaw et al. 2014). Because the three-dimensional structure of intact nubbins affects the actual pH experienced by calicoblastic cells, it will be interesting to compare CARP and cadherin expression profiles of whole corals compared with cell cultures.

Finally, the NanoSIMS analysis of *S. pistillata* cell cultures is preliminary and several 'kinks' remain to be resolved in the method. These include establishing minimum effective dwell times and marking mounts so that ROIs chosen before SIMS analysis can successfully be found in the SIMS without the aid of secondary ion images. Additionally, efforts to support the identity of SIMS-based Ca signals as $CaCO_3$, including co-localization with S (as $^{32}S^-$) or Mg (as $^{24}Mg^{16}O^-$) did not come to fruition.

$^{32}S^-$ co-localized with $^{14}N^{12}C^-$ and the mass window chosen for $^{24}Mg^{16}O^-$ turned out to fit $^{40}Ca^-$ better. Mass windows for P ($^{31}P^-$) have been used as negative ions in previous mass spectrometry studies of coral skeletons (LaVigne et al. 2010), may not be useful because of the element's biological roles in DNA and cell membranes. However, B ($^{11}B^{12}C^-$, $^{11}B^{14}N^-$, $^{11}B^{16}O^-$)(Valle et al. 2011), Fe ($^{56}Fe^{16}O^-$ or $^{57}Fe^{16}O^-$)(Byrne et al. 2010), and negatively ionized Ba and Sr should be examined for their applicability as tracers of carbonate-based, rather than cellular, Ca.

Appendix 1: Chapter 4 Supplementary Tables

Table A1. Carbonate parameters of *S. pistillata* culture medium bubbled to four CO_2 levels.

	400 ppm CO_2	**700 ppm CO_2**	**1000 ppm CO_2**	**2000 ppm CO_2**
ASW Equilibration pH	8.18	8.04	7.76	7.64
ASW Equilibration DIC (mM)	2.39	2.43	2.37	2.38
Equilibration pH	7.95	7.87	7.61	7.30
Equilibration DIC (mM)	1.29	1.55	1.47	1.61
All Salinity	34			
All Temperature (ºC)	26			
All Light (µmol quanta/m^2/s) (L/D)	100 (12:12)			
All Carbonate Alkalinity (µmol/kg)	2612.3 (±125.1)			
All Total Medium Alkalinity (µmol/kg)	3276.9 (±139.7)			

Table A2. *S. pistillata* qPCR primer information.

Primer	Sequence	Amplicon size (bp)	qPCR T_{anneal} (ºC)	Reference
CARP1	F-AGGTCATTTCTCTGATGATG R-CTCCGTCATTCTTGGATTAT	160	57	This work
CARP3	F-GTAGCTGAACCATCTGAAG R-CGTTCTCGTCAACACTATC	166	56	This work
CARP4	F-AGACCCATTTGTGAAGAC R-CGGTAACCACTCCTTTATT	142	50	This work
STPCA2	F-GCAAAGAAACTGACAAAGG R-TCTACAGCTTCTGGATCA	158	50	(Bertucci et al. 2011)
18S	F-AACGATGCCAACTAGGGATCA R-GGTTTCCCATAAGGTGCCAAA	-	56	(Kvitt et al. 2011)

Appendix 2: Additional NanoSIMS images

Figure A1. Control sample total Ca ($^{40}Ca^-$;A & E), $\delta^{15}N$ ($^{15}N^{12}C^-/^{14}N^{12}C^-$) >0.0036 (B & F), $\delta^{15}N$ >0.0036 relative to total Ca (C & G), and $\delta^{15}N$ >0.0036 relative to inorganic Ca ($^{40}Ca^-/^{14}N^{12}C^-$; D & H). Post-SIMS SEM image of the same location (I). A-D are the first ~0.5 μm-thick plane of the sample; E-H are the second ~0.5 μm-thick plane. ROI size was 12x12 μm. The sample was incubated only in un-enriched Asp and was cultivated on day 12.

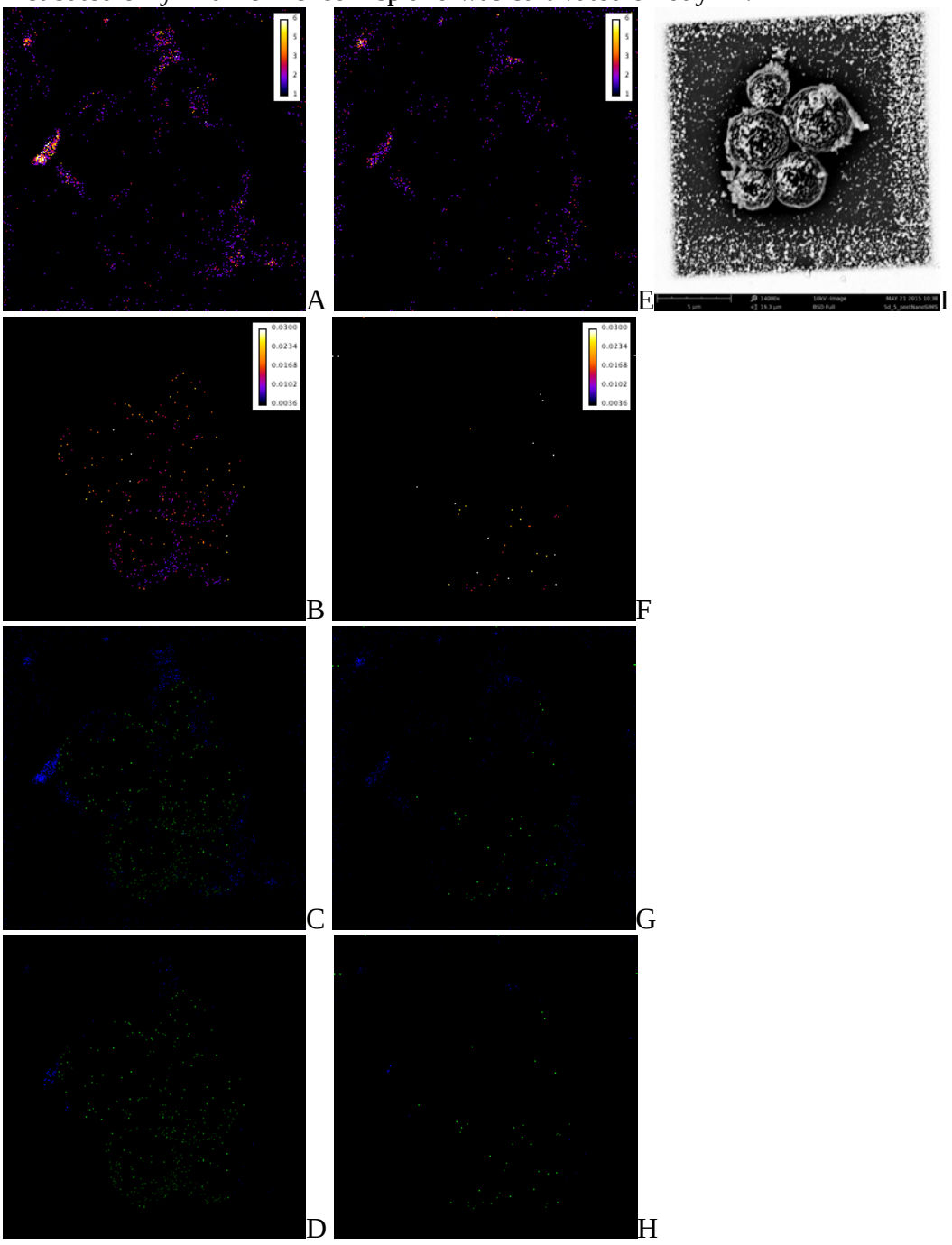

Figure A2. 5d-5 sample ROI2 total Ca ($^{40}Ca^-$;A, B, C), $\delta^{15}N$ ($^{15}N^{12}C^-/^{14}N^{12}C^-$) >0.0036 (D, E, F). A & D, B & E, and C & F are the first, third, and fifth (of seven) ~0.5 μm-thick planes of the sample, respectively. ROI size was 15x15 μm. The sample was both incubated in ^{15}N-Asp and cultivated on day 5.

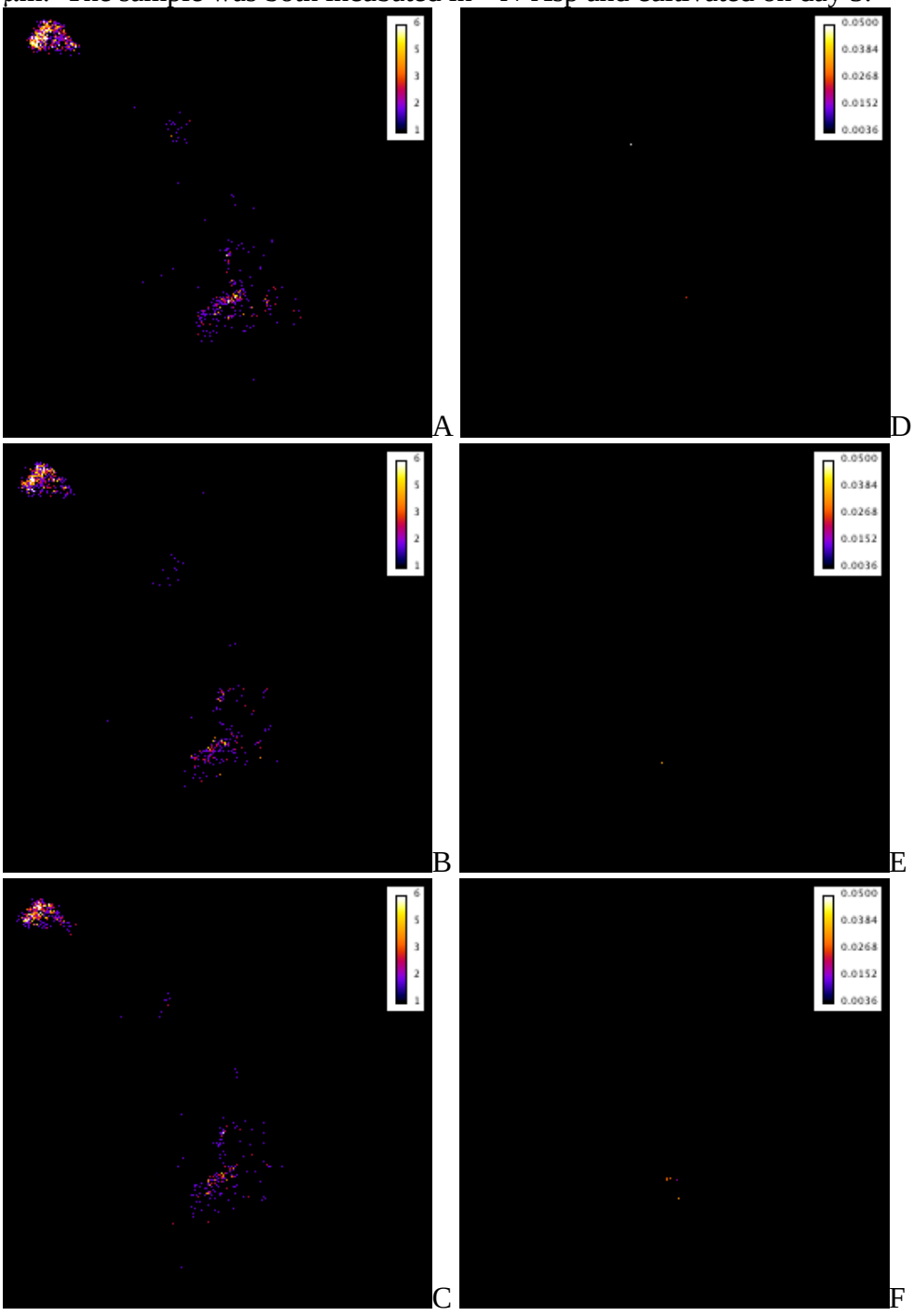

Figure A3. 5d-5 sample ROI3 total Ca ($^{40}Ca^-$;A, B, C), $\delta^{15}N$ ($^{15}N^{12}C^-/^{14}N^{12}C^-$) >0.0036 (D, E, F), $\delta^{15}N$ >0.0036 relative to total Ca (G, H, I), and $\delta^{15}N$ >0.0036 relative to inorganic Ca ($^{40}Ca^-/^{14}N^{12}C^-$; J, K, L). Post-SIMS SEM image of the same location (M). A/D/G/J; B/E/H/K, and C/F/I/L are the first, fourth, and sixth (of seven) ~0.5 μm-thick planes through the sample, respectively. ROI size was 15x15 μm. The sample was both incubated in ^{15}N-Asp and cultivated on day 5.

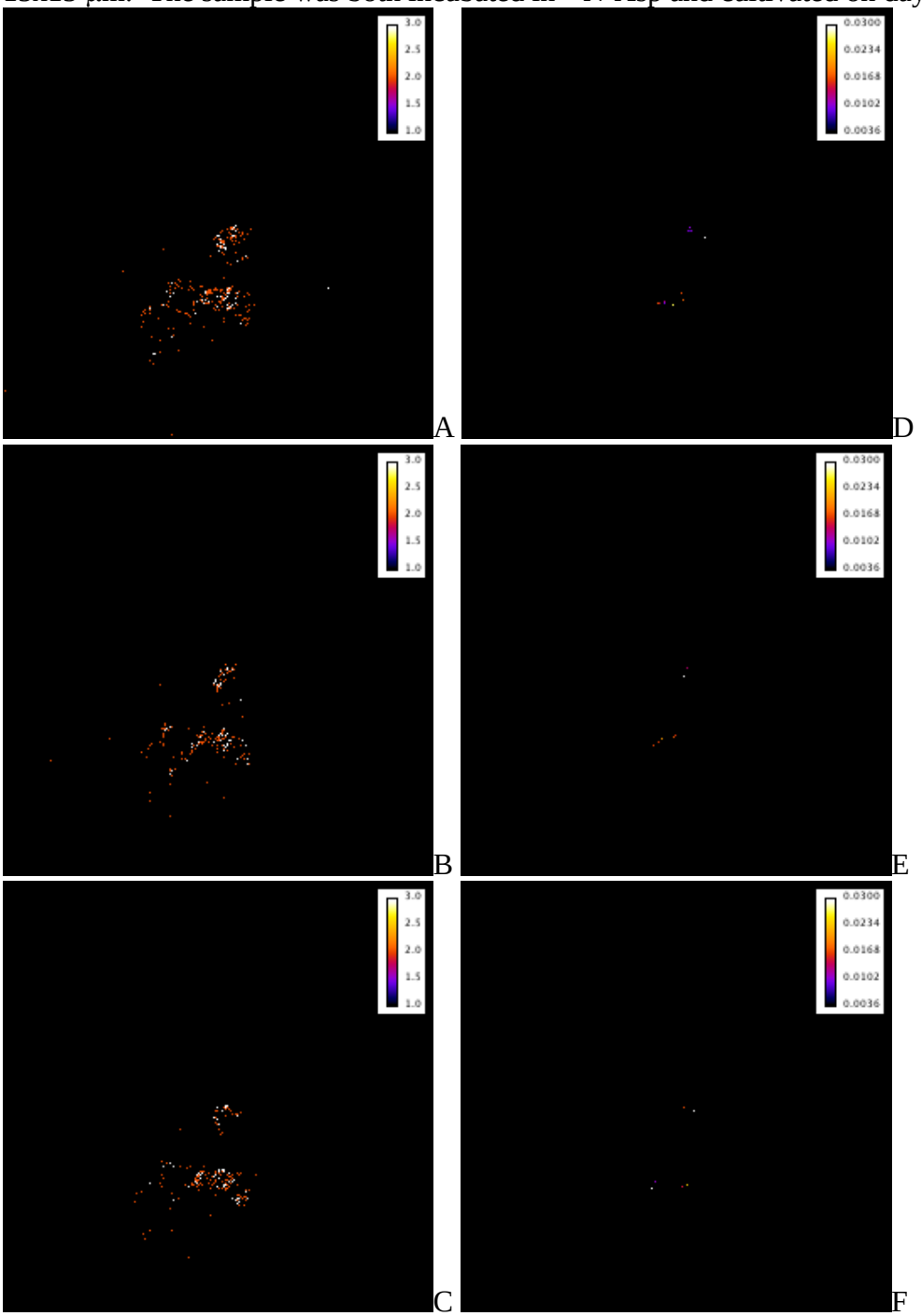

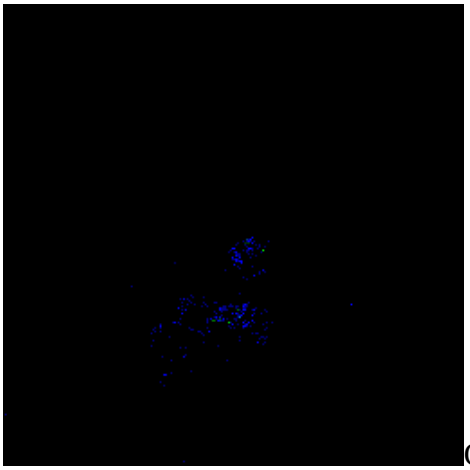
G
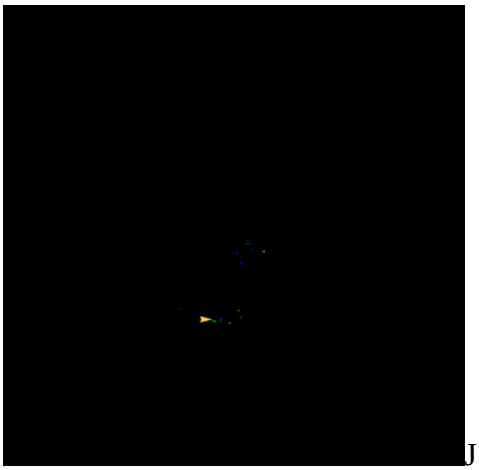
J
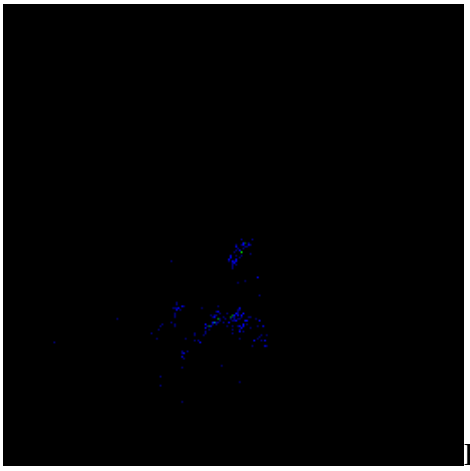
H
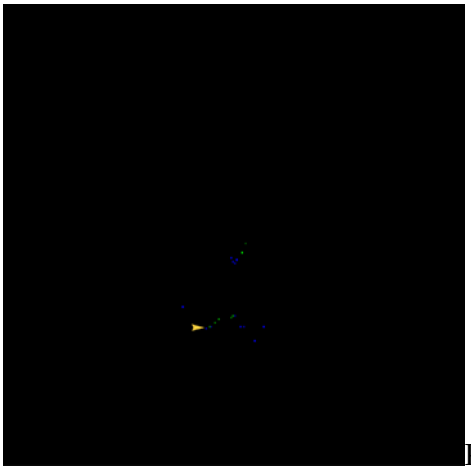
K
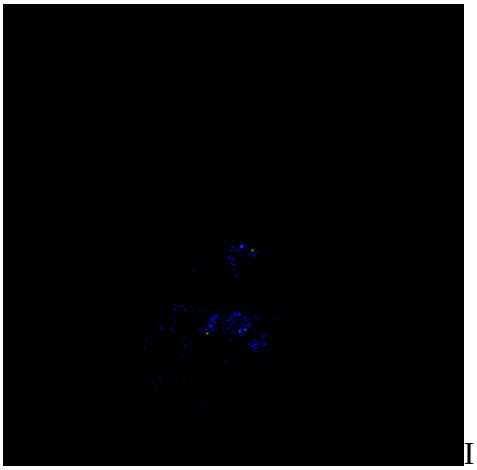
I
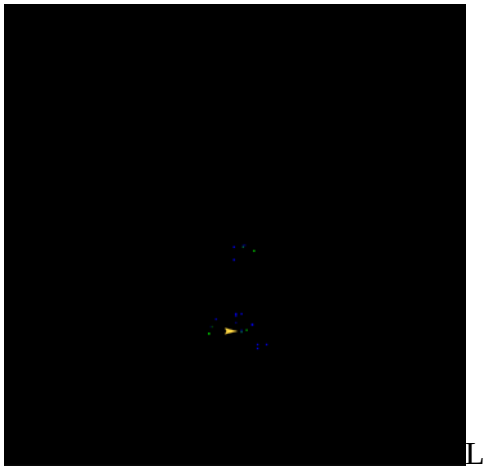
L
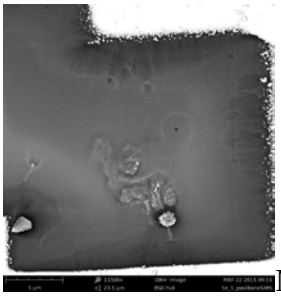
M

Figure A4. 5d-5 sample ROI4 total Ca ($^{40}Ca^-$;A, B, C), $\delta^{15}N$ ($^{15}N^{12}C^-/^{14}N^{12}C^-$) >0.0036 (D, E, F). A & D, B & E, and C & F are the first, third, and fifth (of seven) ~0.5 μm-thick planes of the sample, respectively. ROI size was 15x15 μm. Sample 5d-5 was both incubated in ^{15}N-Asp and cultivated on day 5.

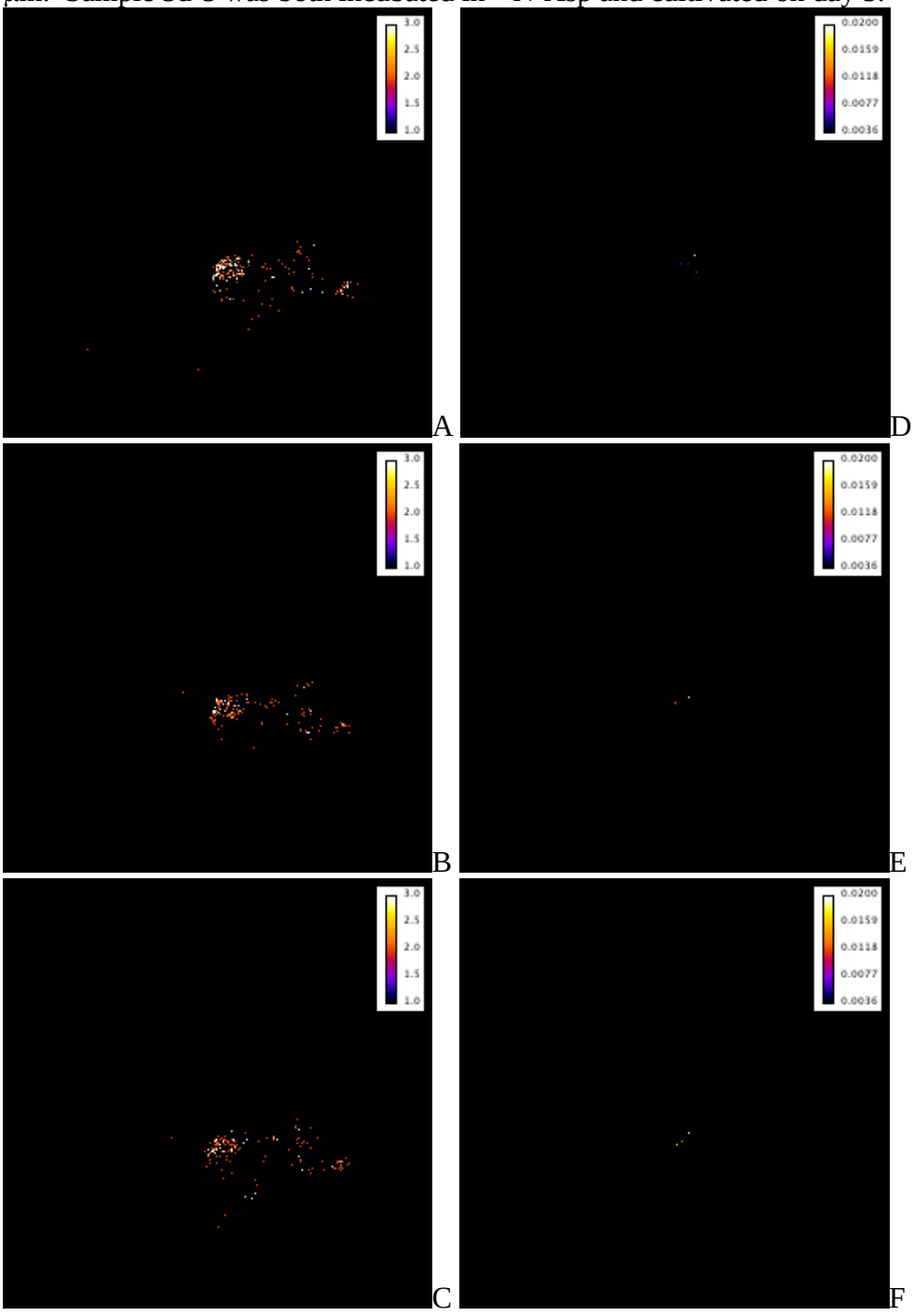

Figure A5. 12d-12 sample ROI2 total Ca ($^{40}Ca^-$;A & E), $\delta^{15}N$ ($^{15}N^{12}C^-/^{14}N^{12}C^-$) >0.0036 (B & F), $\delta^{15}N$ >0.0036 relative to total Ca (C & G), and $\delta^{15}N$ >0.0036 relative to inorganic Ca ($^{40}Ca^-/^{14}N^{12}C^-$; D & H). Post-SIMS SEM image of the same location (I). A-D are the first ~0.5 µm-thick plane of the sample; E-H are the second ~0.5 µm-thick plane. ROI size is 8x8 µm. Arrows in D and H indicate areas of $\delta^{15}N$ and inorganic Ca co-localization. The sample was incubated in ^{15}N-Asp on days 5, 9, and 12, and cultivated on day 12.

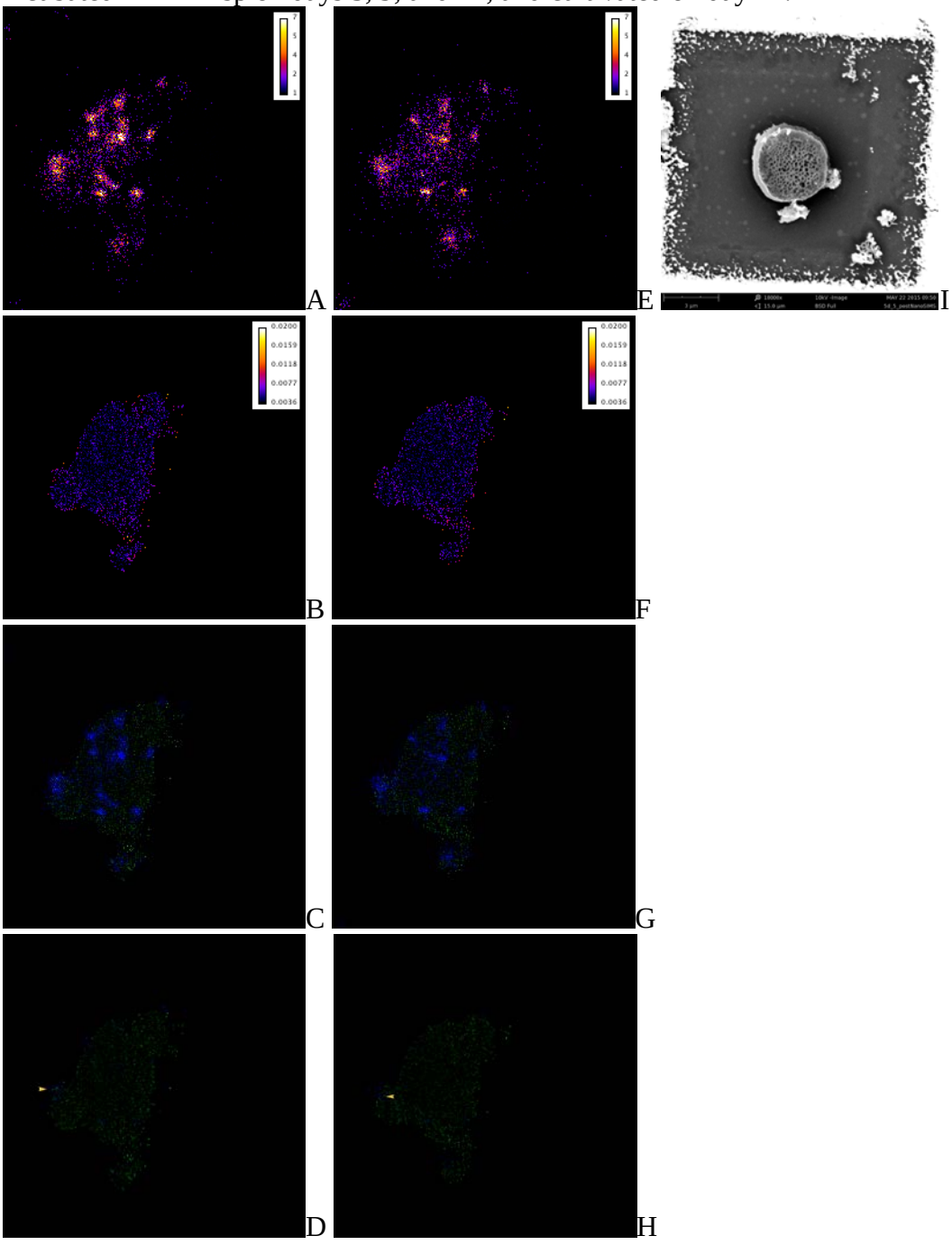

Figure A6. 12d-12 sample ROI3 total Ca ($^{40}Ca^-$;A & E), $\delta^{15}N$ ($^{15}N^{12}C^-/^{14}N^{12}C^-$) >0.0036 (B & F), $\delta^{15}N$ >0.0036 relative to total Ca (C & G), and $\delta^{15}N$ >0.0036 relative to inorganic Ca ($^{40}Ca^-/^{14}N^{12}C^-$; D & H). Post-SIMS SEM image of the same location (I). A-D are the first ~0.5 µm-thick plane of the sample; E-H are the second ~0.5 µm-thick plane. ROI size is 18x18 µm. Arrows in D and H indicate areas of $\delta^{15}N$ and inorganic Ca co-localization. Sample 12d-12 was incubated in ^{15}N-Asp on days 5, 9, and 12, and cultivated on day 12.

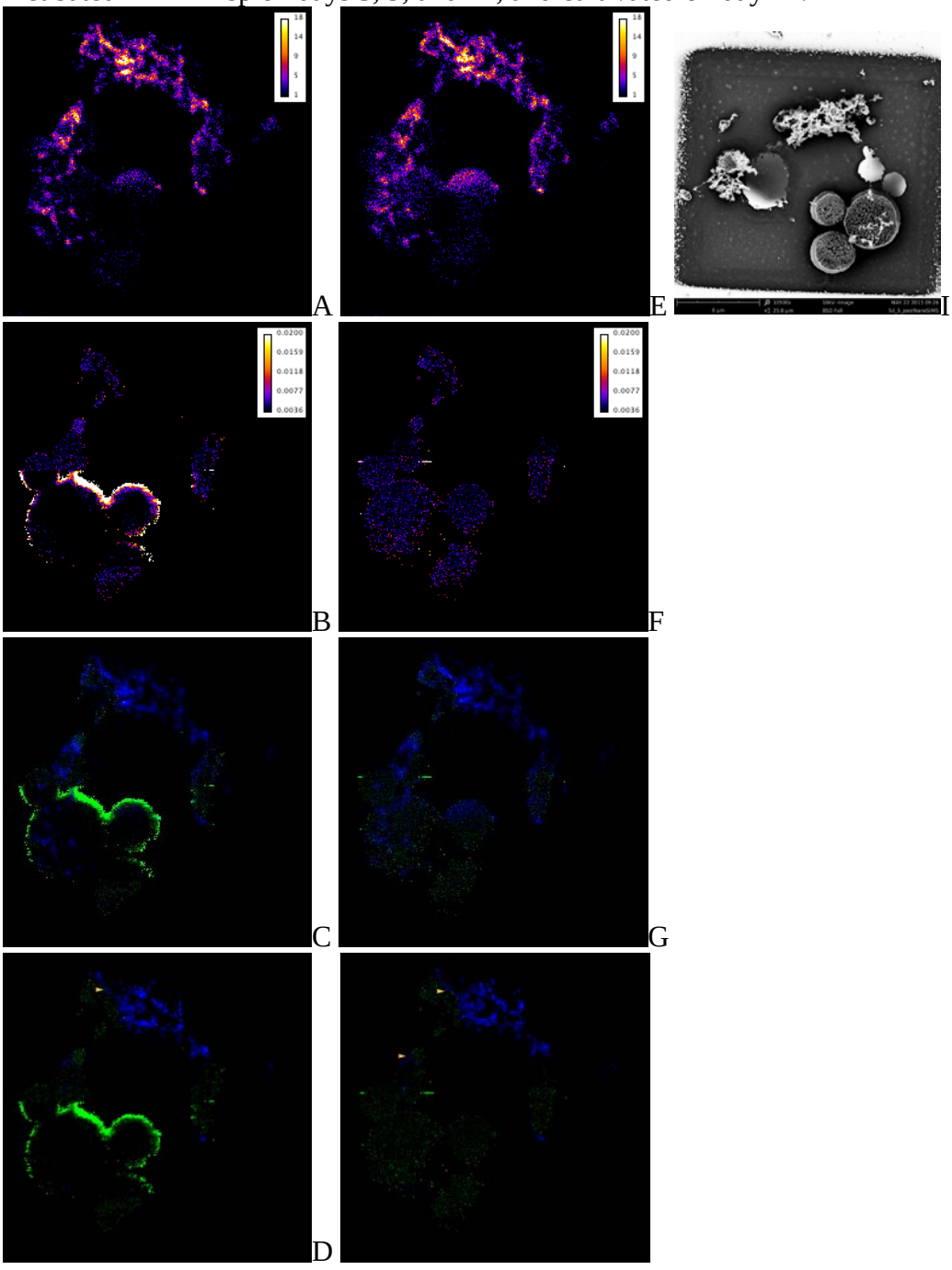

Figure A7. 12d-12 sample ROI4 total Ca ($^{40}Ca^-$;A & E), $\delta^{15}N$ ($^{15}N^{12}C^-/^{14}N^{12}C^-$) >0.0036 (B & F), $\delta^{15}N$ >0.0036 relative to total Ca (C & G), and $\delta^{15}N$ >0.0036 relative to inorganic Ca ($^{40}Ca^-/^{14}N^{12}C^-$; D & H). Post-SIMS SEM image of the same location (I). A-D are the second ~0.5 μm-thick plane of the sample; E-H are the fourth ~0.5 μm-thick plane. ROI size is 11x11 μm. Arrows in D and H indicate areas of $\delta^{15}N$ and inorganic Ca co-localization. Sample 12d-12 was incubated in ^{15}N-Asp on days 5, 9, and 12, and cultivated on day 12.

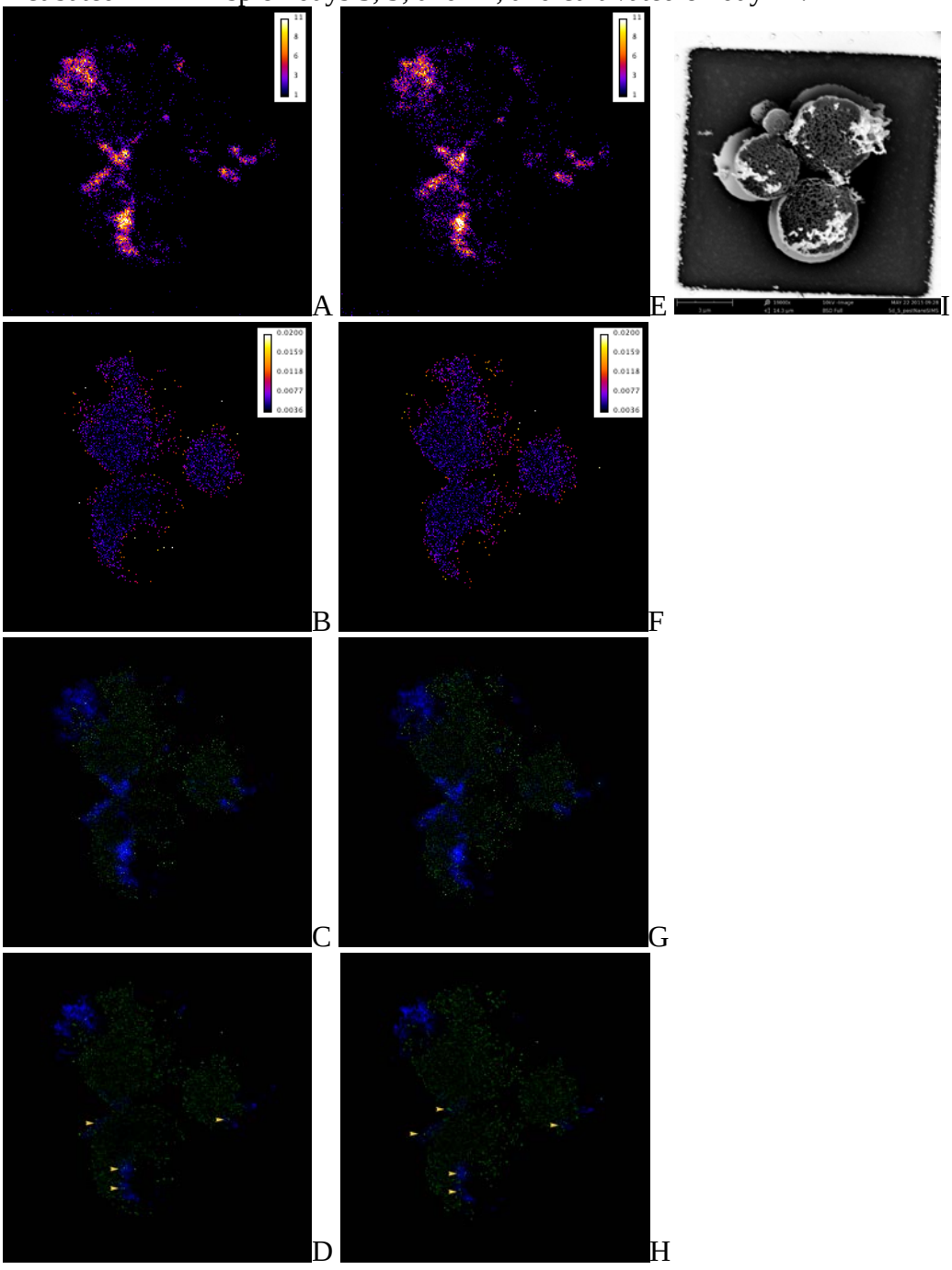

Figure A8. 12d-12 sample ROI5 total Ca ($^{40}Ca^-$;A & E), $\delta^{15}N$ ($^{15}N^{12}C^-/^{14}N^{12}C^-$) >0.0036 (B & F), $\delta^{15}N$ >0.0036 relative to total Ca (C & G), and $\delta^{15}N$ >0.0036 relative to inorganic Ca ($^{40}Ca^-/^{14}N^{12}C^-$; D & H). Post-SIMS SEM image of the same location (I). A-D are the second ~0.5 μm-thick plane of the sample; E-H are the fourth ~0.5 μm-thick plane. ROI size is 10x10 μm. Arrows in D and H indicate areas of $\delta^{15}N$ and inorganic Ca co-localization. Sample 12d-12 was incubated in ^{15}N-Asp on days 5, 9, and 12, and cultivated on day 12.

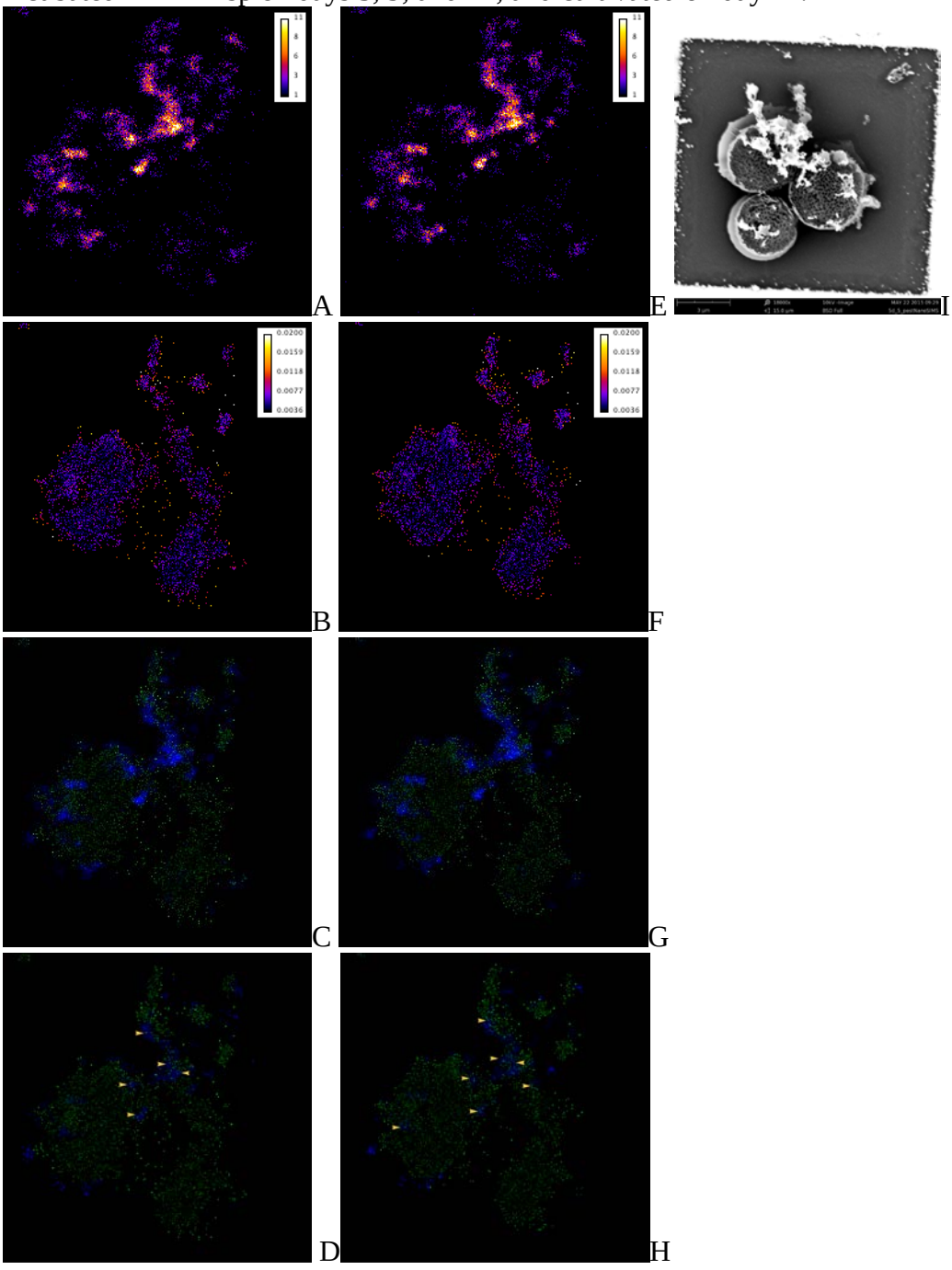

References

Addadi, L., D. Joester, F. Nudelman and S. Weiner (2006). "Mollusk shell formation: a source of new concepts for understanding biomineralization process." Chemical European Journal **12**: 980-987.

Al-Horani, F. A., S. M. Al-Moghrabi and D. de Beer (2003). "The mechanism of calcification and its relation to photosynthesis and respiration in the scleractinian coral *Galaxea fascicularis*." Marine Biology **142**(3): 419-426.

Allemand, D., C. Ferrier-Pagès, P. Furla, F. Houlbrèque, S. Puverel, et al. (2004). "Biomineralisation in reef-building corals: from molecular mechanisms to environmental control." Comptes Rendus Palevol **3**(6–7): 453-467.

Allemand, D., E. Tambutte, J.-P. Girard and J. Jaubert (1998). "Organic matrix synthesis in the scleractinian coral *Stylophora pistillata*: Role in biomineralization and potential target of the organotin tributyltin." Journal of Experimental Biology **201**: 2001-2009.

Allemand, D., E. TambuttE, J. Girard and J. Jaubert (1998). "Organic matrix synthesis in the scleractinian coral *Stylophora pistillata*: Role in biomineralization and potential target of the organotin tributyltin." Journal of Experimental Biology **201**(13): 2001-2009.

Allemand, D., É. Tambutté, D. Zoccola and S. Tambutté (2011). Coral calcification, cells to reefs. Coral reefs: an ecosystem in transition, Springer**:** 119-150.

Alvares, K., S. N. Dixit, E. Lux and A. Veis (2009). "Echinoderm phosphorylated matrix proteins UTMP16 and UTMP19 have different functions in sea urchin tooth mineralization." Journal of Biological Chemistry **284**(38): 26149-26160.

Anagnostou, E., R. M. Sherrell, A. Gagnon, M. LaVigne, M. P. Field, et al. (2011). "Seawater nutrient and carbonate ion concentrations recorded as P/Ca, Ba/Ca, and U/Ca in the deep-sea coral *Desmophyllum dianthus*." Geochimica et Cosmochimica Acta **75**(9): 2529-2543.

Angerer, L. M., D. W. Oleksyn, C. Y. Logan, D. R. McClay, L. Dale, et al. (2000). "A BMP pathway regulates cell fate allocation along the sea urchin animal-vegetal embryonic axis." Development **127**(5): 1105-1114.

Anthony, K. R. N., D. I. Kline, G. Diaz-Pulido, S. Dove and O. Hoegh-Guldberg (2008). "Ocean acidification causes bleaching and productivity loss in coral reef builders." Proceedings of the National Academy of Sciences **105**(45): 17442-17446.

Armbrust, E. V., J. A. Berges, C. Bowler, B. R. Green, D. Martinez, et al. (2004). "The genome of the diatom T*halassiosira pseudonana*: ecology, evolution, and metabolism." Science **306**(5693): 79-86.

Asara, J. M., M. H. Schweitzer, L. M. Freimark, M. Phillips and L. C. Cantley (2007). "Protein sequences from mastodon and *Tyrannosaurus rex* revealed by mass spectrometry." Science **316**(5822): 280-285.

Asenath-Smith, E., H. Li, E. C. Keene, Z. W. Seh and L. A. Estroff (2012). "Crystal growth of calcium carbonate in hydrogels as a model of biomineralization." Advanced Functional Materials **22**(14): 2891-2914.

Ashkenazy, H., E. Erez, E. Martz, T. Pupko and N. Ben-Tal (2010). "ConSurf 2010: calculating evolutionary conservation in sequence and structure of proteins and nucleic acids." Nucleic Acids Research **38**(suppl 2): W529-W533.
Aytuna, A. S., A. Gursoy and O. Keskin (2005). "Prediction of protein–protein interactions by combining structure and sequence conservation in protein interfaces." Bioinformatics **21**(12): 2850-2855.
Baas Becking, L. G. M. and D. Moore (1961). "Biogenic sulfides." Economic Geology **56**(2): 259-272.
Barnes, D. and C. Crossland (1976). "Urease activity in the staghorn coral, *Acropora acuminata*." Comparative Biochemistry and Physiology Part B: Comparative Biochemistry **55**(3): 371-376.
Baron, M. (2003). "An overview of the Notch signalling pathway." Seminars in Cell & Developmental Biology **14**(2): 113-119.
Barron, M. J., S. J. Brookes, C. E. Draper, D. Garrod, J. Kirkham, et al. (2008). "The cell adhesion molecule nectin-1 is critical for normal enamel formation in mice." Human Molecular Genetics **17**(22): 3509-3520.
Beerling, D. J. and D. L. Royer (2011). "Convergent Cenozoic CO_2 history." Nature Geosci **4**(7): 418-420.
Beniash, E. (2011). "Biominerals—hierarchical nanocomposites: the example of bone." Wiley Interdisciplinary Reviews: Nanomedicine and Nanobiotechnology **3**(1): 47-69.
Beniash, E., L. Addadi and S. Weiner (1999). "Cellular control over spicule formation in sea urchin embryos: a structural approach." Journal of Structural Biology **125**(1): 50-62.
Benson, S. C., N. C. Benson and F. Wilt (1986). "The organic matrix of the skeletal spicule of sea urchin embryos." The Journal of Cell Biology **102**(5): 1878-1886.
Berntson, E. A., S. C. France and L. S. Mullineaux (1999). "Phylogenetic relationships within the class Anthozoa (phylum Cnidaria) based on nuclear 18S rDNA sequences." Molecular Phylogenetics and Evolution **13**(2): 417-433.
Bertucci, A., A. Moya, S. Tambutté, D. Allemand, C. T. Supuran, et al. (2013). "Carbonic anhydrases in anthozoan corals—A review." Bioorganic & Medicinal Chemistry **21**(6): 1437-1450.
Bertucci, A., S. Tambutté, C. Supuran, D. Allemand and D. Zoccola (2011). "A new coral carbonic anhydrase in *Stylophora pistillata*." Marine Biotechnology **13**(5): 992-1002.
Bhattacharya, D., S. Agrawal, M. Aranda, S. Baumgarten, M. Belcaid, et al. (in review). "Basis for ecological success of reef-forming corals elucidated using comparative genomics." Science.
Birkedal-Hansen, H., W. G. I. Moore, M. K. Bodden, L. J. Windsor, B. Birkedal-Hansen, et al. (1993). "Matrix metalloproteinases: A review." Critical Reviews in Oral Biology & Medicine **4**(2): 197-250.
Blank, S., M. Arnoldi, S. Khoshnavaz, L. Treccani, M. Kuntz, et al. (2003). "The nacre protein perlucin nucleates growth of calcium carbonate crystals." Journal of Microscopy **212**(3): 280-291.

Boorungsiman, S., E. Gentleman, R. Carzaniga, N. D. Evans, D. W. McComb, et al. (2012). "The role of intracellular calcium phosphate in osteoblast-mediated bone apatite formation." Proceedings of the National Academy of Sciences **109**(35): 14170-14175.
Borell, E. M., A. R. Yuliantri, K. Bischof and C. Richter (2008). "The effect of heterotrophy on photosynthesis and tissue composition of two scleractinian corals under elevated temperature." Journal of Experimental Marine Biology and Ecology **364**(2): 116-123.
Budd, A. F., S. L. Romano, N. D. Smith and M. S. Barbeitos (2010). "Rethinking the phylogeny of Scleractinian corals: a review of morphological and molecular data." Integrative and Comparative Biology **50**(3): 411-427.
Burki, F., S. I. Nikolaev, I. Bolivar, J. Guiard and J. Pawlowski (2006). "Analysis of expressed sequence tags from a naked foramineran *Reticulomyxa filosa*." Genome **49**(8): 882-887.
Burriesci, M. S., T. K. Raab and J. R. Pringle (2012). "Evidence that glucose is the major transferred metabolite in dinoflagellate–cnidarian symbiosis." Journal of Experimental Biology **215**(19): 3467-3477.
Byrne, M. E., D. A. Ball, J.-L. Guerquin-Kern, I. Rouiller, T.-D. Wu, et al. (2010). "*Desulfovibrio magneticus* RS-1 contains an iron- and phosphorus-rich organelle distinct from its bullet-shaped magnetosomes." Proceedings of the National Academy of Sciences **107**(27): 12263-12268.
Canalis, E., A. N. Economides and E. Gazzerro (2003). "Bone morphogenetic proteins, their antagonists, and the skeleton." Endocrine Reviews **24**(2): 218-235.
Carreiro-Silva, M., T. Cerqueira, A. Godinho, M. Caetano, R. S. Santos, et al. (2014). "Molecular mechanisms underlying the physiological responses of the cold-water coral *Desmophyllum dianthus* to ocean acidification." Coral Reefs: 1-12.
Cazin, J., T. R. Kozel, D. M. Lupan and W. R. Burt (1969). "Extracellular deoxyribonuclease production by yeasts." Journal of Bacteriology **100**(2): 760-762.
Cesar, H., L. Burke and L. Pet-Soede (2003). The economics of worldwide coral reef degredation.
Checa, A. (2000). "A new model for periostracum and shell formation in Unionidae (Bivalvia, Mollusca)." Tissue and Cell **32**(5): 405-416.
Clendenon, S. G., B. Shah, C. A. Miller, G. Schmeisser, A. Walter, et al. (2009). "Cadherin-11 controls otolith assembly: Evidence for extracellular cadherin activity." Developmental Dynamics **238**(8): 1909-1922.
Clode, P. L. and A. T. Marshall (2002). "Low temperature FESEM of the calcifying interface of a scleractinian coral." Tissue and Cell **34**(3): 187-198.
Clode, P. L. and A. T. Marshall (2003). "Calcium associated with a fibrillar organic matrix in the scleractinian coral *Galaxea fascicularis*." Protoplasma **220**(3): 153-161.
Clode, P. L., R. A. Stern and A. T. Marshall (2007). "Subcellular imaging of isotopically labeled carbon compounds in a biological sample by ion microprobe (NanoSIMS)." Microscopy Research and Technique **70**(3): 220-229.

Cohen, A. L., D. C. McCorkle, S. d. Putron, G. A. Gaetani and K. A. Rose (2009). "Morphological and compositional changes in the skeletons of new coral recruits reared in acidified seawater : Insights into the biomineralization response to ocean acidification." Geochemistry Geophysics Geosystems **10**: 1-12.
Comeau, S., P. J. Edmunds, N. B. Spindel and R. C. Carpenter (2013). "The responses of eight coral reef calcifiers to increasing partial pressure of CO_2 do not exhibit a tipping point." Limnology and Oceanography **58**(1): 388-398.
Conesa, A., S. Götz, J. M. García-Gómez, J. Terol, M. Talón, et al. (2005). "Blast2GO: a universal tool for annotation, visualization and analysis in functional genomics research." Bioinformatics **21**(18): 3674-3676.
Corstjens, P. L. A. M., Y. Araki and E. L. González (2001). "A coccolithophorid calcifying vesicle with a vacuolar-type ATPase proton pump: cloning and immunolocalization of the V0 subunit c." Journal of Phycology **37**(1): 71-78.
Craig, R. and R. C.Beavis (2004). "TANDEM: matching proteins with tandem mass spectra." Bioinformatics **20**: 1466-1467.
Crook, E., D. Potts, M. Rebolledo-Vieyra, L. Hernandez and A. Paytan (2012). "Calcifying coral abundance near low-pH springs: Implications for future ocean acidification." Coral Reefs **31**(1): 239-245.
Cserzo, M., F. Eisenhaber, B. Eisenhaber and I. Simon (2002). "On filtering false positive transmembrane protein predictions." Protein Engineering **15**: 745-752.
Cuif, J.-P. and Y. Dauphin (1998). "Microstructural and physico-chemical characterization of 'centers of calcification' in septa of some recent scleractinian corals." Paläontologische Zeitschrift **72**(3-4): 257-269.
Cuif, J.-P., Y. Dauphin, P. Berthet and J. Jegoudez (2004). "Associated water and organic compounds in coral skeletons: Quantitative thermogravimetry coupled to infrared absorption spectrometry." Geochemistry Geophysics Geosystems **5**(11): Q11011.
Cuif, J. P., Y. Dauphin, B. Farre, G. Nehrke, J. Nouet, et al. (2008). "Distribution of sulphated polysaccharides within calcareous biominerals suggests a widely shared two-step crystallization process for the microstructural growth units." Mineralogical Magazine **72**(1): 233-237.
de Jong, D. S., W. T. Steegenga, J. M. A. Hendriks, E. J. J. van Zoelen, W. Olijve, et al. (2004). "Regulation of Notch signaling genes during BMP2-induced differentiation of osteoblast precursor cells." Biochemical and Biophysical Research Communications **320**(1): 100-107.
Derycke, L., L. Morbidelli, M. Ziche, O. De Wever, M. Bracke, et al. (2006). "Soluble N-cadherin fragment promotes angiogenesis." Clinical and Experimental Metastasis **23**(3): 187-201.
Desai, N. A. and V. Shankar (2000). "Purification and characterization of the single-strand-specific and guanylic-acid-preferential deoxyribonuclease activity of the extracellular nuclease from *Basidiobolus haptosporus*." European Journal of Biochemistry **267**(16): 5123-5135.
Dobbs, F. C., R. C. Zimmerman and L. A. Drake (2004). "Occurrence of intracellular crystals in leaves of *Thalassia testudinum*." Aquatic Botany **80**(1): 23-28.

Domart-Coulon, I., J. Stolarski, C. Brahmi, E. Gutner-Hoch, K. Janiszewska, et al. (2014). "Simultaneous extension of both basic microstructural components in scleractinian coral skeleton during night and daytime, visualized by *in situ* ^{86}Sr pulse labeling." Journal of Structural Biology **185**(1): 79-88.
Domart-Coulon, I. J., D. C. Elbert, E. P. Scully, P. S. Calimlim and G. K. Ostrander (2001). "Aragonite crystallization in primary cell cultures of multicellular isolates from a hard coral, *Pocillopora damicornis*." Proceedings of the National Academy of Sciences **98**(21): 11885-11890.
Doney, S. C., V. J. Fabry, R. A. Feely and J. A. Kleypas (2009). "Ocean acidification: The other CO_2 problem." Annual Review of Marine Science **1**(1): 169-192.
Dove, P. M., J. J. D. Yoreo and S. Weiner, Eds. (2003). Reviews in Mineralogy and Geochemistry: Biomineralizaiton. Washington, D.C., Mineralogical Society of America.
Drake, J. L., T. Mass and P. G. Falkowski (2014). "The evolution and future of carbonate precipitation in marine invertebrates: Witnessing extinction or documenting resilience in the Anthropocene?" Elementa Science of the Anthropocene **2**(1): 000026.
Drake, J. L., T. Mass, L. Haramaty, E. Zelzion, D. Bhattacharya, et al. (2013). "Proteomic analysis of skeletal organic matrix from the stony coral *Stylophora pistillata*." Proceedings of the National Academy of Sciences **110**(10): 3788-3793.
Drake, J. L., T. Mass, L. Haramaty, E. Zelzion, D. Bhattacharya, et al. (2013). "Reply to Ramos-Silva et al.: Regarding coral skeletal proteome." Proceedings of the National Academy of Sciences **110**(24): E2147-E2148.
Drenkard, E. J., A. L. Cohen, D. C. McCorkle, S. J. Putron, V. R. Starczak, et al. (2013). "Calcification by juvenile corals under heterotrophy and elevated CO_2." Coral Reefs: 1-9.
Drescher, B., R. M. Dillaman and A. R. Taylor (2012). "Coccolithogenesis In *Scyphosphaera apsteinii* (Prymnesiophyceae)." Journal of Phycology **48**(6): 1343-1361.
Ducklow, H. W. and R. Mitchell (1979). "Composition of mucus released by coral reef coelenterates." Limnology and Oceanography **24**(4): 706-714.
Edmunds, P. J. (2011). "Zooplanktivory ameliorates the effects of ocean acidification on the reef coral *Porites* spp." Limnology and Oceanography **56**(6): 2402-2410.
Edmunds, P. J. and C. B. Wall (2014). "Evidence that high pCO_2 affects protein metabolism in tropical reef corals." The Biological Bulletin **227**(1): 68-77.
Ehrlich, H. (2010). "Chitin and collagen as universal and alternative templates in biomineralization." International Geology Review **52**(7-8): 661+699.
Erwin, D. H., M. Laflamme, S. M. Tweedt, E. A. Sperling, D. Pisani, et al. (2011). "The Cambrian conundrum: Early divergence and later ecological success in the early history of animals." Science **334**(6059): 1091-1097.
Fabricius, K. E., C. Langdon, S. Uthicke, C. Humphrey, S. Noonan, et al. (2011). "Losers and winners in coral reefs acclimatized to elevated carbon dioxide concentrations." Nature Climate Change **1**: 165-169.

Falini, G., S. Albeck, S. Weiner and L. Addadi (1996). "Control of aragonite or calcite precipitation by mollusk shell macromolecules." Science **271**: 67-69.
Falini, G. and S. Fermani (2004). "Chitin mineralization." Tissue engineering **10**(1-2): 1-6.
Falini, G., M. Reggi, S. Fermani, F. Sparla, S. Goffredo, et al. (2013). "Control of aragonite deposition in colonial corals by intra-skeletal macromolecules." Journal of Structural Biology **183**(2): 226-238.
Falkowski, P. G., Z. Dubinsky, L. Muscatine and J. W. Porter (1984). "Light and the bioenergetics of a symbiotic coral." Bioscience **34**(11): 705-709.
Fang, D., C. Pan, H. Lin, Y. Lin, G. Xu, et al. (2012). "Ubiquitylation functions in the calcium carbonate biomineralization in the extracellular matrix." PLoS ONE **7**(4): e35715.
Feely, R. A., S. C. Doney and S. R. Cooley (2009). "Ocean acidification: Present conditions and future changes in a high-CO_2 world." Oceanography **22**(4): 36-47.
Feely, R. A., C. L. Sabine, K. Lee, W. Berelson, J. Kleypas, et al. (2004). "Impact of anthropogenic CO_2 on the $CaCO_3$ system in the oceans." Science **305**(5682): 362-366.
Feng, Q., Z. Fang, Z. Yan, R. Xing, L. Xie, et al. (2009). "The structure–function relationship of MSI7, a matrix protein from pearl oyster *Pinctada fucata*." Acta Biochimica et Biophysica Sinica **41**(11): 955-962.
Ferrier-Pages, C., F. Boisson, D. Allemand and E. Tambutte (2002). "Kinetics of strontium uptake in the scleractinian coral *Stylophora pistillata*." Marine Ecology Progress Series **245**: 8.
Fine, M. and D. Tchernov (2007). "Scleractinian coral species survive and recover from decalcification." Science **315**(5820): 1811.
Fortin, D., B. Davis and T. Beveridge (1996). "Role of *Thiobacillus* and sulfate-reducing bacteria in iron biocycling in oxic and acidic mine tailings." FEMS Microbiology Ecology **21**(1): 11-24.
Fraser, H. B., A. E. Hirsh, L. M. Steinmetz, C. Scharfe and M. W. Feldman (2002). "Evolutionary rate in the protein interaction network." Science **296**(5568): 750-752.
Fukuda, I., S. Ooki, T. Fujita, E. Murayama, H. Nagasawa, et al. (2003). "Molecular cloning of a cDNA encoding a soluble protein in the coral exoskeleton." Biochemical and Biophysical Research Communications **304**(1): 11-17.
Furla, P., I. Galgani, E. Durand and D. Allemand (2000). "Sources and mechanisms of inorganic carbon transport for coral calcification and photosynthesis." Journal of Experimental Biology **203**: 3445-3457.
Gagnon, A. C., J. F. Adkins and J. Erez (2012). "Seawater transport during coral biomineralization." Earth and Planetary Science Letters **329–330**(0): 150-161.
Gal, A., K. Kahil, N. Vidavsky, R. T. DeVol, P. U. P. A. Gilbert, et al. (2014). "Particle accretion mechanism underlies biological crystal growth from an amorphous precursor phase." Advanced Functional Materials **24**(34): 5420-5426.
Gal, A., S. Weiner and L. Addadi (2015). "A perspective on underlying crystal growth mechanisms in biomineralization: solution mediated growth versus nanosphere particle accretion." CrystEngComm.

Gazeau, F., C. Quiblier, J. M. Jansen, J.-P. Gattuso, J. J. Middelburg, et al. (2007). "Impact of elevated CO_2 on shellfish calcification." Geophysical Research letters **34**(7): L07603.
George, N. C., C. E. Killian and F. H. Wilt (1991). "Characterization and expression of a gene encoding a 30.6-kDa *Strongylocentrotus purpuratus* spicule matrix protein." Developmental Biology **147**(2): 334-342.
Gerbaud, V., D. Pignol, E. Loret, J. A. Bertrand, Y. Berland, et al. (2000). "Mechanism of calcite crystal growth inhibition by the N-terminal undecapeptide of lithostathine." Journal of Biological Chemistry **275**(2): 1057-1064.
Gilbert, M., W. J. Shaw, J. R. Long, K. Nelson, G. P. Drobny, et al. (2000). "Chimeric peptides of statherin and osteopontin that bind hydroxyapatite and mediate cell adhesion." Journal of Biological Chemistry **275**(21): 16213-16218.
Gilbert, P. U. P. A. and F. Wilt (2011). Molecular aspects of biomineralization of the echinoderm endoskeleton. Molecular Biomineralization. W. E. G. Müller, Springer Berlin Heidelberg**:** 199-223.
Girard, J.-P. and T. A. Springer (1996). "Modulation of endothelial cell adhesion by hevin, an acidic protein associated with high endothelial venules." Journal of Biological Chemistry **271**(8): 4511-4517.
Goffredo, S., P. Vergni, M. Reggi, E. Caroselli, F. Sparla, et al. (2011). "The skeletal organic matrix from mediterranean coral *Balanophyllia europaea* influences calcium carbonate precipitation." PLoS ONE **6**(7).
Goldberg, H. A., K. J. Warner, M. C. Li and G. K. Hunter (2001). "Binding of bone sialoprotein, osteopontin and synthetic polypeptides to hydroxyapatite." Connective Tissue Research **42**(1): 25-37.
Goldberg, W. M. (1974). "Evidence of a sclerotized collagen from the skeleton of a gorgonian coral." Comparative Biochemistry and Physiology Part B: Comparative Biochemistry **49**(3): 525-526.
Gorbunov, M. and P. Falkowski (2004). Fluorescence Induction and Relaxation (FIRe) technique and instrumentation for monitoring photosynthetic processes and primary production in aquatic ecosystems. Photosynthesis: Fundamental Aspects to Global Perspectives. A. v. d. Est and D. Bruce**:** 1029-1031.
Goreau, T. F. (1959). "The physiology of skeleton formation in corals. I. A method for measuring the rate of calcium deposition by corals under different conditions." Biological Bulletin **116**: 59-75.
Gothmann, A. M., J. Stolarski, J. F. Adkins, B. Schoene, K. J. Dennis, et al. (2015). "Fossil corals as an archive of secular variations in seawater chemistry since the Mesozoic." Geochimica et Cosmochimica Acta **160**(0): 188-208.
Gotliv, B.-A., L. Addadi and S. Weiner (2003). "Mollusk shell acidic proteins: in search of individual functions." ChemBioChem **4**(6): 522-529.
Gotliv, B.-A., N. Kessler, J. L. Sumerel, D. E. Morse, N. Tuross, et al. (2005). "Asprich: A novel aspartic acid-rich protein family from the prismatic shell matrix of the bivalve *Atrina rigida*." ChemBioChem **6**(2): 304-314.
Hayes, R. L. and N. I. Goreau (1977). "Intracellular crystal-bearing vesicles in the epidermis of Scleractinian corals, *Astrangia danae* (Agassiz) and *Porites porites* (Pallas)." The Biological Bulletin **152**(1): 26-40.

Hayward, D. C., S. Hetherington, C. A. Behm, L. C. Grasso, S. Foret, et al. (2011). "Differential gene expression at coral settlement and metamorphosis - a subtractive hybridization study." PLoS ONE **6**(10): e26411.
Hazelaar, S., H. J. van der Strate, W. W. C. Gieskes and E. G. Vrieling (2003). "Possible role of ubiquitin in silica biomineralization in diatoms: Identification of a homologue with high silica affinity." Biomolecular Engineering **20**(4–6): 163-169.
He, G., T. Dahl, A. Veis and A. George (2003). "Nucleation of apatite crystals in vitro by self-assembled dentin matrix protein 1." Nature Materials **2**(8): 552-558.
Heathfield, B. M. (1970). "Calcification in echinoderms: effects of temperature and diamox on incorporation of calcium-45 in vitro by regenerating spines of *Strongylocentrotus purpuratus*." The Biological Bulletin **139**(1): 151-163.
Helman, Y., F. Natale, R. M. Sherrell, M. LaVigne, V. Starovoytov, et al. (2008). "Extracellular matrix production and calcium carbonate precipitation by coral cells *in vitro*." Proceedings of the National Academy of Sciences **105**(1): 54-58.
Hildebrand, M., M. J. Doktycz and D. P. Allison (2008). "Application of AFM in understanding biomineral formation in diatoms." Pflügers Archiv - European Journal of Physiology **456**: 127-137.
Hoegh-Guldberg, O. and J. F. Bruno (2010). "The impact of climate change on the world's marine ecosystems." Science **328**(5985): 1523-1528.
Hoegh-Guldberg, O., P. J. Mumby, A. J. Hooten, R. S. Steneck, P. Greenfield, et al. (2007). "Coral reefs under rapid climate change and ocean acidification." Science **318**(5857): 1737-1742.
Hofmann, G. E., J. P. Barry, P. J. Edmunds, R. D. Gates, D. A. Hutchins, et al. (2010). "The effect of ocean acidification on calcifying organisms in marine ecosystems: an organism-to-ecosystem perspective." Annual Review of Ecology, Evolution, and Systematics **41**(1): 127-147.
Hofmann, K. and W. Stoffel (1993). "TMbase - A database of membrane spanning proteins segments." Biological Chemistry Hoppe-Seyler **374**: 166.
Holcomb, M., A. L. Cohen, R. I. Gabitov and J. L. Hutter (2009). "Compositional and morphological features of aragonite precipitated experimentally from seawater and biogenically by corals." Geochimica et Cosmochimica Acta **73**(14): 4166-4179.
Holcomb, M., D. C. McCorkle and A. L. Cohen (2010). "Long-term effects of nutrient and CO_2 enrichment on the temperate coral *Astrangia poculata* (Ellis and Solander, 1786)." Journal of Experimental Marine Biology and Ecology **386**(1–2): 27-33.
Holcomb, M., E. Tambutté, D. Allemand and S. Tambutté (2014). "Light enhanced calcification in *Stylophora pistillata*: effects of glucose, glycerol and oxygen." PeerJ **2**: e375.
Holcomb, M., A. A. Venn, E. Tambutte, S. Tambutte, D. Allemand, et al. (2014). "Coral calcifying fluid pH dictates response to ocean acidification." Nature Scientific Reports **4**.
Honisch, B., N. G. Hemming, A. G. Grottoli, A. .Amat, G. N. Hanson, et al. (2004). "Assessing scleractinian corals as recorders for paleo-pH: Empirical

calibration and vital effects." Geochimica et Cosmochimica Acta **68**(18): 3675-3685.
Houlbrèque, F. and C. Ferrier-Pagès (2009). "Heterotrophy in tropical scleractinian corals." Biological Reviews **84**(1): 1-17.
Houlbrèque, F., S. Reynaud, C. Godinot, F. Oberhänsli, R. Rodolfo-Metalpa, et al. (2015). "Ocean acidification reduces feeding rates in the scleractinian coral *Stylophora pistillata*." Limnology and Oceanography **60**(1): 89-99.
Houlbrèque, F., R. Rodolfo-Metalpa, R. Jeffree, F. Oberhänsli, J. L. Teyssié, et al. (2012). "Effects of increased pCO_2 on zinc uptake and calcification in the tropical coral *Stylophora pistillata*." Coral Reefs **31**(1): 101-109.
http://people.oregonstate.edu/~meyere/data.html.
Huang, Y., B. Niu, Y. Gao, L. Fu and W. Li (2010). "CD-HIT Suite: A web server for clustering and comparing biological sequences." Bioinformatics.
Hüning, A., F. Melzner, J. Thomsen, M. Gutowska, L. Krämer, et al. (2013). "Impacts of seawater acidification on mantle gene expression patterns of the Baltic Sea blue mussel: implications for shell formation and energy metabolism." Marine Biology **160**(8): 1845-1861.
Hunter, G. K. and H. A. Goldberg (1993). "Nucleation of hydroxyapatite by bone sialoprotein." Proceedings of the National Academy of Sciences **90**(18): 8562-8565.
Hyman, L. H. (1955). The Invertebrates. New York, McGraw-Hill.
Illies, M., M. Peeler, A. Dechtiaruk and C. Ettensohn (2002). "Identification and developmental expression of new biomineralization proteins in the sea urchin *Strongylocentrotus purpuratus*." Development Genes and Evolution **212**(9): 419-431.
Ingersoll, E. P. and F. H. Wilt (1998). "Matrix metalloproteinase inhibitors disrupt spicule formation by primary mesenchyme cells in the sea urchin embryo." Developmental Biology **196**(1): 95-106.
IPCC (2007). Contribution of Working Group I to the Fourth Assessment Report of the Intergovernmental Panel on Climate Change. S. Solomon, D. Qin, M. Manning et al. New York, NY, Cambridge University Press.
Jackson, D., C. McDougall, K. Green, F. Simpson, G. Worheide, et al. (2006). "A rapidly evolving secretome builds and patterns a sea shell." BMC Biology **4**(1): 40.
Jackson, D. J., L. Macis, J. Reitner, B. M. Degnan and G. Wörheide (2007). "Sponge paleogenomics reveals an ancient role for carbonic anhydrase in skeletogenesis." Science **316**(5833): 1893-1895.
Jackson, D. J., K. Mann, V. Häussermann, M. B. Schilhabel, C. Lüter, et al. (2015). "The *Magellania venosa* biomineralizing proteome: A window into brachiopod shell evolution." Genome Biology and Evolution **7**(5): 1349-1362.
Jackson, D. J., C. McDougall, B. Woodcroft, P. Moase, R. A. Rose, et al. (2010). "Parallel evolution of nacre building gene sets in molluscs." Mol Biol Evol **27**(3): 591-608.
Jian-Ping, D., C. Jun, B. Yi-Fei, H. Bang-Xing, G. Shang-Bin, et al. (2010). "Effects of pearl powder extract and its fractions on fibroblast function relevant to wound repair." Pharmaceutical Biology **48**(2): 122-127.

Jiang, L., L. He and M. Fountoulakis (2004). "Comparison of protein precipitation methods for sample preparation prior to proteomic analysis." Journal of Chromatography A **1023**: 317-320.
Joubert, C., D. Piquemal, B. Marie, L. Manchon, F. Pierrat, et al. (2010). "Transcriptome and proteome analysis of *Pinctada margaritifera* calcifying mantle and shell: Focus on biomineralization." BMC Genomics **11**(1): 613.
Jury, C., F. Thomas, M. Atkinson and R. Toonen (2013). "Buffer capacity, ecosystem feedbacks, and seawater chemistry under global change." Water **5**(3): 1303-1325.
Kaniewska, P., P. R. Campbell, D. I. Kline, M. Rodriguez-Lanetty, D. J. Miller, et al. (2012). "Major cellular and physiological impacts of ocean acidification on a reef building coral." PLoS ONE **7**(4): e34659.
Karlsson, J. and P. Artursson (1991). "A method for the determination of cellular permeability coefficients and aqueous boundary layer thickness in monolayers of intestinal epithelial (Caco-2) cells grown in permeable filter chambers." International Journal of Pharmaceutics **71**(1): 55-64.
Kawaguchi, J., Y. Azuma, K. Hoshi, I. Kii, S. Takeshita, et al. (2001). "Targeted disruption of cadherin-11 leads to a reduction in bone density in calvaria and long bone metaphyses." Journal of Bone and Mineral Research **16**(7): 1265-1271.
Kawaguti, S. and D. Sakumoto (1948). "The effect of light on the calcium deposition of corals." Bulletin of the Oceanograpaical Institute of Taiwan **4**: 65-70.
Kawasaki, K., A. V. Buchanan and K. M. Weiss (2009). "Biomineralization in humans: making the hard choices in life." Annual Review of Genetics **43**(1): 119-142.
Kelley, L. A. and M. J. Sternberg (2009). "Protein structure prediction on the Web: a case study using the Phyre server." Nature Protocols **4**(3): 363-371.
Kelly, M. W., J. L. Padilla-Gamiño and G. E. Hofmann (2013). "Natural variation and the capacity to adapt to ocean acidification in the keystone sea urchin *Strongylocentrotus purpuratus*." Global Change Biology **19**(8): 2536-2546.
Keshavmurthy, S., S.-Y. Yang, A. Alamaru, Y.-Y. Chuang, M. Pichon, et al. (2013). "DNA barcoding reveals the coral “laboratory-rat”, *Stylophora pistillata* encompasses multiple identities." Sci. Rep. **3**.
Killian, C. E., R. A. Metzler, Y. U. T. Gong, I. C. Olson, J. Aizenberg, et al. (2009). "Mechanism of calcite co-orientation in the sea urchin tooth." Journal of the American Chemical Society **131**(51): 18404-18409.
Killian, C. E. and F. H. Wilt (2008). "Molecular aspects of biomineralization of the echinoderm endoskeleton." Chemical reviews **108**(11): 4463-4474.
Klumpp, D. W., B. L. Bayne and A. J. S. Hawkins (1992). "Nutrition of the giant clam *Tridacna gigas* (L.) I. Contribution of filter feeding and photosynthates to respiration and growth." Journal of Experimental Marine Biology and Ecology **155**(1): 105-122.
Knoll, A. H. (2003). "Biomineralization and evolutionary history." Reviews in Mineralogy and Geochemistry **54**(1): 329-356.

Kono, M., N. Hayashi and T. Samata (2000). "Molecular mechanism of the nacreous layer formation in *Pinctada maxima*." Biochemical and Biophysical Research Communications **269**(1): 213-218.
Kopp, C., M. Pernice, I. Domart-Coulon, C. Djediat, J. E. Spangenberg, et al. (2013). "Highly dynamic cellular-level response of symbiotic coral to a sudden increase in environmental nitrogen." mBio **4**(3).
Kroeker, K. J., R. L. Kordas, R. N. Crim and G. G. Singh (2010). "Meta-analysis reveals negative yet variable effects of ocean acidification on marine organisms." Ecology Letters **13**(11): 1419-1434.
Krogh, A., B. Larsson, G. v. Heijne and E. L. Sonnhammer (2001). "Predicting transmembrane protein topology with a hidden Markov model: application to complete genomes." Journal of Molecular Biology **305**(3): 567-580.
Kuzminov, F. I., C. M. Brown, V. V. Fadeev and M. Y. Gorbunov (2013). "Effects of metal toxicity on photosynthetic processes in coral symbionts, *Symbiodinium* spp." Journal of Experimental Marine Biology and Ecology **446**(0): 216-227.
Kvitt, H., E. Kramarsky-Winter, K. Maor-Landaw, K. Zandbank, A. Kushmaro, et al. (2015). "Breakdown of coral colonial form under reduced pH conditions is initiated in polyps and mediated through apoptosis." Proceedings of the National Academy of Sciences **112**(7): 2082-2086.
Kvitt, H., H. Rosenfeld, K. Zandbank and D. Tchernov (2011). "Regulation of apoptotic pathways by *Stylophora pistillata* (Anthozoa, Pocilloporidae) to survive thermal stress and bleaching." PLoS ONE **6**(12): e28665.
Labrenz, M., G. K. Druschel, T. Thomsen-Ebert, B. Gilbert, S. A. Welch, et al. (2000). "Formation of sphalerite (ZnS) deposits in natural biofilms of sulfate-reducing bacteria." Science **290**(5497): 1744-1747.
Lannig, G., S. Eilers, H. O. Pörtner, I. M. Sokolova and C. Bock (2010). "Impact of ocean acidification on energy metabolism of oyster, *Crassostrea gigas*—changes in metabolic pathways and thermal response." Marine drugs **8**(8): 2318-2339.
Laurent, J., A. Venn, É. Tambutté, P. Ganot, D. Allemand, et al. (2013). "Regulation of intracellular pH in cnidarians: response to acidosis in Anemonia viridis." FEBS Journal **281**(3): 683-695.
LaVigne, M., K. A. Matthews, A. G. Grottoli, K. M. Cobb, E. Anagnostou, et al. (2010). "Coral skeleton P/Ca proxy for seawater phosphate: Multi-colony calibration with a contemporaneous seawater phosphate record." Geochimica et Cosmochimica Acta **74**(4): 1282-1293.
Leaf, D. S., J. A. Anstrom, J. E. Chin, M. A. Harkey, R. M. Showman, et al. (1987). "Antibodies to a fusion protein identify a cDNA clone encoding MSP130, a primary mesenchyme-specific cell surface protein of the sea urchin embryo." Developmental Biology **121**(1): 29-40.
Leclercq, N., J.-P. Gattuso and J. Jaubert (2002). "Primary production, respiration, and calcification of a coral reef mesocosm under increased CO_2 partial pressure." Limnology and Oceanography **47**(2): 558-564.
Lee, P. N., S. Kumburegama, H. Q. Marlow, M. Q. Martindale and A. H. Wikramanayake (2007). "Asymmetric developmental potential along the animal–

vegetal axis in the anthozoan cnidarian, *Nematostella vectensis*, is mediated by Dishevelled." Developmental Biology **310**(1): 169-186.
Lee, P. N., K. Pang, D. Q. Matus and M. Q. Martindale (2006). "A WNT of things to come: evolution of Wnt signaling and polarity in cnidarians." Seminars in Cell & Developmental Biology **17**(2): 157-167.
Levy, S., G. Sutton, P. C. Ng, L. Feuk, A. L. Halpern, et al. (2007). "The diploid genome sequence of an individual human." PLoS Biol **5**(10): e254.
Li, W. and A. Godzik (2006). "CD-Hit: a fast program for clustering and comparing large sets of protein or nucleotide sequences." Bioinformatics **22**(13): 1658-1659.
Liaw, L., M. Almeida, C. E. Hart, S. M. Schwartz and C. M. Giachelli (1994). "Osteopontin promotes vascular cell adhesion and spreading and is chemotactic for smooth muscle cells in vitro." Circulation Research **74**(2): 214-224.
Liew, Y. J., M. Aranda, A. Carr, S. Baumgarten, D. Zoccola, et al. (2014). "Identification of microRNAs in the coral *Stylophora pistillata*." PLoS ONE **9**(3): e91101.
Liu, W., X. Huang, J. Lin and M. He (2012). "Seawater acidification and elevated temperature affect gene expression patterns of the pearl oyster *Pinctada fucata*." PLoS ONE **7**(3): e33679.
Lowenstam, H. A. and S. Weiner (1989). On Biomineralization. New York, New York, Oxford University Press.
Ma, J.-J., B. Feng, Y. Zhang, J.-W. Li, A.-G. Lu, et al. (2009). "Higher CO_2-insufflation pressure inhibits the expression of adhesion molecules and the invasion potential of colon cancer cells." World Journal of Gastroenterology : WJG **15**(22): 2714-2722.
Ma, Y., S. R. Cohen, L. Addadi and S. Weiner (2008). "Sea urchin tooth design: An “all-calcite” polycrystalline reinforced fiber composite for grinding rocks." Advanced Materials **20**(8): 1555-1559.
Ma, Z., J. Huang, J. Sun, G. Wang, C. Li, et al. (2007). "A novel extrapallial fluid protein controls the morphology of nacre lamellae in the pearl oyster, *Pinctada fucata*." Journal of Biological Chemistry **282**(32): 23253-23263.
Mann, K., E. Edsinger-Gonzales and M. Mann (2012). "In-depth proteomic analysis of a mollusc shell: acid-soluble and acid-insoluble matrix of the limpet *Lottia gigantea*." Proteome science **10**(1): 1-18.
Mann, K., A. Poustka and M. Mann (2008). "In-depth, high-accuracy proteomics of sea urchin tooth organic matrix." Proteome science **6**(1): 33.
Mann, K., A. Poustka and M. Mann (2008). "The sea urchin (*Strongylocentrotus purpuratus*) test and spine proteomes." Proteome science **6**(1): 22.
Mann, K., A. J. Poustka and M. Mann (2010). "Phosphoproteomes of *Strongylocentrotus purpuratus* shell and tooth matrix: identification of a major acidic sea urchin tooth phosphoprotein, phosphodontin." Proteome Sci **8**(6).
Mann, K., F. H. Wilt and A. J. Poustka (2010). "Proteomic analysis of sea urchin (*Strongylocentrotus purpuratus*) spicule matrix." Proteome Science **8**: 33.
Mann, S. (2001). Biomineralization: Principles and Concepts in Bioinorganic Materials Chemistry. New York, Oxford University Press.

Mannello, F., L. Canesi, G. Gazzanelli and G. Gallo (2001). "Biochemical properties of metalloproteinases from the hemolymph of the mussel *Mytilus galloprovincialis* Lam." Comparative Biochemistry and Physiology Part B: Biochemistry and Molecular Biology **128**(3): 507-515.
Manzello, D. P., I. C. Enochs, N. Melo, D. K. Gledhill and E. M. Johns (2012). "Ocean acidification refugia of the Florida Reef Tract." PLoS ONE **7**(7): e41715.
Maor-Landaw, K., S. Karako-Lampert, H. W. Ben-Asher, S. Goffredo, G. Falini, et al. (2014). "Gene expression profiles during short-term heat stress in the red sea coral *Stylophora pistillata*." Global Change Biology **20**(10): 3026-3035.
Marie, B., C. Joubert, A. Tayalé, I. Zanella-Cléon, C. Belliard, et al. (2012). "Different secretory repertoires control the biomineralization processes of prism and nacre deposition of the pearl oyster shell." Proceedings of the National Academy of Sciences **109**(51): 20986-20991.
Marie, B., A. Marie, D. Jackson, L. Dubost, B. Degnan, et al. (2010). "Proteomic analysis of the organic matrix of the abalone *Haliotis asinina* calcified shell." Proteome science **8**(1): 54.
Marie, B., N. Roy, I. Zanella-Cléon, M. Becchi and F. Marin (2011). "Molecular evolution of mollusc shell proteins: Insights from proteomic analysis of the edible mussel *Mytilus*." Journal of Molecular Evolution **72**(5-6): 531-546.
Marie, B., N. Trinkler, I. Zanella-Cleon, N. Guichard, M. Becchi, et al. (2011). "Proteomic identification of novel proteins from the calcifying shell matrix of the Manila clam *Venerupis philippinarum*." Marine Biotechnology **13**(5): 955-962.
Marin, F. (2007). Unusually Acidic Proteins in Biomineralization. Handbook of Biomineralization. E. Baurlein and J. Picket-Heaps. Max Planck Institute for Biochemistry, Max Planck Institute for Biochemistry.
Marin, F., P. Corstjens, B. de Gaulejac, E. de Vrind-De Jong and P. Westbroek (2000). "Mucins and molluscan calcification: molecular characterization of mucoperlin, a novel mucin-like protein from the nacreous shell layer of the fan mussel *Pinna nobilis* (Bivalvia, Pteriomorphia)." Journal of Biological Chemistry **275**(27): 20667-20675.
Marin, F., N. Le Roy and B. Marie (2012). "The formation and mineralization of mollusc shell." Frontiers in Bioscience **4**: 1099-1125.
Marin, F. and G. Luquet (2004). "Molluscan shell proteins." Comptes Rendus Palevol **3**(6–7): 469-492.
Marin, F., B. Marie, S. B. Hamada, P. Ramos-Silva, N. Le Roy, et al. (2013). "'Shellome': Proteins involved in mollusk shell biomineralization-diversity, functions." Recent Advances in Pearl Research: 149-166.
Marks, M. H., R. S. Bear and C. H. Blake (1949). "X-ray diffraction evidence of collagen-type protein fibers in the Echinodermata, Coelenterata and Porifera." Journal of Experimental Zoology **111**: 55-78.
Marshall, A. T., P. L. Clode, R. Russell, K. Prince and R. Stern (2007). "Electron and ion microprobe analysis of calcium distribution and transport in coral tissues." Journal of Experimental Biology **210**(14): 2453-2463.
Marubini, F., C. Ferrier-Pagès, P. Furla and D. Allemand (2008). "Coral calcification responds to seawater acidification: a working hypothesis towards a physiological mechanism." Coral Reefs **27**(3): 491-499.

Mass, T., Jeana L. Drake, L. Haramaty, J. D. Kim, E. Zelzion, et al. (2013). "Cloning and characterization of four novel coral acid-rich proteins that precipitate carbonates in vitro." Current Biology **23**(12): 1126-1131.
Mass, T., J. L. Drake, L. Haramaty, Y. Rosenthal, O. M. E. Schofield, et al. (2012). "Aragonite precipitation by “proto-polyps” in coral cell cultures." PLoS ONE **7**(4): e35049.
Mass, T., J. L. Drake, E. C. Peters, W. Jiang and P. G. Falkowski (2014). "Immunolocalization of skeletal matrix proteins in tissue and mineral of the coral *Stylophora pistillata*." Proceedings of the National Academy of Sciences **111**(35): 12728-12733.
Mass, T., J. L. Drake, H. M. Putnam, E. Zelzion, R. D. Gates, et al. (in review). "Temporal expression of biomineralization proteins during early development in the stony coral *Pocillopora damicornis*."
McClay, D. R., R. E. Peterson, R. C. Range, A. M. Winter-Vann and M. J. Ferkowicz (2000). "A micromere induction signal is activated by beta-catenin and acts through Notch to initiate specification of secondary mesenchyme cells in the sea urchin embryo." Development **127**(23): 5113-5122.
McCulloch, M., J. Falter, J. Trotter and P. Montagna (2012). "Coral resilience to ocean acidification and global warming through pH up-regulation." Nature Clim. Change **2**: 623-627.
Medakovic, D. (2000). "Carbonic anhydrase activity and biomineralization process in embryos, larvae, and adult blue mussels *Mytilus edulis* L." Helgoland Marine Research **54**: 1-6.
Mehr, S. F., R. DeSalle, H.-T. Kao, A. Narechania, Z. Han, et al. (2013). "Transcriptome deep-sequencing and clustering of expressed isoforms from Favia corals." BMC Genomics **14**: 546.
Meibom, A., J.-P. Cuif, F. Houlbreque, S. Mostefaoui, Y. Dauphin, et al. (2008). "Compositional variations at ultra-structure length scales in coral skeleton." Geochimica et Cosmochimica Acta **72**(6): 1555-1569.
Melzner, F., J. Thomsen, W. Koeve, A. Oschlies, M. Gutowska, et al. (2013). "Future ocean acidification will be amplified by hypoxia in coastal habitats." Marine Biology **160**(8): 1875-1888.
Michenfelder, M., G. Fu, C. Lawrence, J. C. Weaver, B. A. Wustman, et al. (2003). "Characterization of two molluscan crystal-modulating biomineralization proteins and identification of putative mineral binding domains." Biopolymers **70**(4): 522-533.
Milliman, J. D. (1993). "Production and accumulation of calcium carbonate in the ocean: Budget of a nonsteady state." Global Biogeochemical Cycles **7**(4): 927-957.
Miyamoto, H., T. Miyashita, M. Okushima, S. Nakano, T. Morita, et al. (1996). "A carbonic anhydrase from the nacreous layer in oyster pearls." Proceedings of the National Academy of Sciences **93**(18): 9657-9660.
Miyashita, T., R. Takagi, M. Okushima, S. Nakano, H. Miyamoto, et al. (2000). "Complementary DNA cloning and characterization of pearlin, a new class of matrix protein in the nacreous layer of oyster pearls." Marine Biotechnology **2**(5): 409-418.

Moya, A., L. Huisman, E. E. Ball, D. C. Hayward, L. C. Grasso, et al. (2012). "Whole transcriptome analysis of the coral *Acropora millepora* reveals complex responses to CO_2-driven acidification during the initiation of calcification." Molecular Ecology **21**(10): 2440-2454.
Moya, A., S. Tambutté, A. Bertucci, E. Tambutté, S. Lotto, et al. (2008). "Carbonic anhydrase in the scleractinian coral *Stylophora pistillata*." Journal of Biological Chemistry **283**(37): 25475-25484.
Moya, A., S. Tambutté, E. Tambutté, D. Zoccola, N. Caminiti, et al. (2006). "Study of calcification during a daily cycle of the coral *Stylophora pistillata*: implications for `light-enhanced calcification'." Journal of Experimental Biology **209**(17): 3413-3419.
Mueller, C. W., P. K. Weber, M. R. Kilburn, C. Hoeschen, M. Kleber, et al. (2013). "Advances in the analysis of biogeochemical interfaces: NanoSIMS to investigate soil microenvironments." Adv. Agron **121**: 1-46.
Müller, W. E. G. (2011). Molecular Biomineralization: Aquatic Organisms Forming Extraordinary Materials. New York, NY, Springer.
Munday, P. L., R. R. Warner, K. Monro, J. M. Pandolfi and D. J. Marshall (2013). "Predicting evolutionary responses to climate change in the sea." Ecology Letters **16**(12): 1488-1500.
Murdock, D. J. E. and P. C. J. Donoghue (2011). "Evolutionary origins of animal skeletal biomineralization." Cells Tissues Organs **194**(2-4): 98-102.
Muscatine, L., E. Tambutte and D. Allemand (1997). "Morphology of coral desmocytes, cells that anchor the calicoblastic epithelium to the skeleton." Coral Reefs **16**(4): 205-213.
Norris, R. D., S. K. Turner, P. M. Hull and A. Ridgwell (2013). "Marine ecosystem responses to Cenozoic global change." Science **341**(6145): 492-498.
Nose, A., A. Nagafuchi and M. Takeichi (1988). "Expressed recombinant cadherins mediate cell sorting in model systems." Cell **54**(7): 993-1001.
Nudelman, F., B. A. Gotliv, L. Addadi and S. Weiner (2006). "Mollusk shell formation: Mapping the distribution of organic matrix components underlying a single aragonitic tablet in nacre." Journal of Structural Biology **153**(2): 176-187.
Ogawa, D., T. Bobeszko, T. Ainsworth and W. Leggat (2013). "The combined effects of temperature and CO_2 lead to altered gene expression in *Acropora aspera*." Coral Reefs: 1-13.
Olszta, M. J., D. J. Odom, E. P. Douglas and L. B. Gower (2003). "A new paradigm for biomineral formation: mineralization via an amorphous liquid-phase precursor." Connective Tissue Research **44 Suppl 1**: 326-334.
Orr, J. C., V. J. Fabry, O. Aumont, L. Bopp, S. C. Doney, et al. (2005). "Anthropogenic ocean acidification over the twenty-first century and its impact on calcifying organisms." Nature **437**(7059): 681-686.
Pandolfi, J. M., S. R. Connolly, D. J. Marshall and A. L. Cohen (2011). "Projecting coral reef futures under global warming and ocean acidification." Science **333**(6041): 418-422.
Paradies, N. E. and G. B. Grunwald (1993). "Purification and characterization of NCAD90, a soluble endogenous form of N-cadherin, which is generated by

proteolysis during retinal development and retains adhesive and neurite-promoting function." Journal of Neuroscience Research **36**(1): 33-45.
Paris, G., J. S. Fehrenbacher, A. L. Sessions, H. J. Spero and J. F. Adkins (2014). "Experimental determination of carbonate-associated sulfate $\delta^{34}S$ in planktonic foraminifera shells." Geochemistry, Geophysics, Geosystems **15**(4): 1452-1461.
Paulsson, M., Y. Sommarin and D. Heinegard (1983). "Metabolism of cartilage proteins in cultured tissue sections." Biochemistry Journal **212**: 659-667.
Péterfi, Z., Á. Donkó, A. Orient, A. Sum, Á. Prókai, et al. (2009). "Peroxidasin is secreted and incorporated into the extracellular matrix of myofibroblasts and fibrotic kidney." The American Journal of Pathology **175**(2): 725-735.
Pierrot, D. E., E. Lewis and D. W. R. Wallas (2006). "MS Excel program developed for CO2 system calculations." ORNL/CDIAC-105a. Carbon dioxide information analysis center, Oak Ridge National Laboratory, U.S. Department of Energy, OakRidge, Tennessee.
Politi, Y., T. Arad, E. Klein, S. Weiner and L. Addadi (2004). "Sea urchin spine calcite forms via a transient amorphous calcium carbonate phase." Science **306**(5699): 1161-1164.
Politi, Y., J. Mahamid, H. Goldberg, S. Weiner and L. Addadi (2007). "Asprich mollusk shell protein: in vitro experiments aimed at elucidating function in $CaCO_3$ crystallization." CrystEngComm **9**(12): 1171-1177.
Politi, Y., R. A. Metzler, M. Abrecht, B. Gilbert, F. H. Wilt, et al. (2008). "Transformation mechanism of amorphous calcium carbonate into calcite in the sea urchin larval spicule." Proceedings of the National Academy of Sciences **105**(45): 17362-17366.
Pors Nielsen, S. (2004). "The biological role of strontium." Bone **35**(3): 583-588.
Porter, S. M. (2010). "Calcite and aragonite seas and the de novo acquisition of carbonate skeletons." Geobiology **8**(4): 256-277.
Puverel, S., E. Tambutte, L. Pereira-Mouries, D. Zoccola, D. Allemand, et al. (2005). "Soluble organic matrix of two Scleractinian corals: partial and comparative analysis." Comparative Biochemistry and Physiology Part B **141**: 480-487.
Puverel, S., E. Tambutte, D. Zocoola, I. Dumart-Coulon, A. Bouchot, et al. (2005). "Antibodies against the organic matrix in scleractinians: a new tool to study coral biomineralization." Coral Reefs **24**: 149-156.
Rahman, A., T. Oomori and G. Woerheide (2011). "Calcite formation in soft coral sclerites is determined by a single reactive extracellular protein." Journal of Biological Chemistry.
Rahman, M. A., T. Oomori and G. Wörheide (2011). "Calcite formation in soft coral sclerites is determined by a single reactive extracellular protein." Journal of Biological Chemistry **286**(36): 31638-31649.
Ramos-Silva, P., J. Kaandorp, L. Huisman, B. Marie, I. Zanella-Cleon, et al. (2013). "The skeletal proteome of the coral *Acropora millepora*: The evolution of calcification by cooption and domain shuffling." Molecular Biology and Evolution.
Ramos-Silva, P., F. Marin, J. Kaandorp and B. Marie (2013). LETTER: Biomineralization toolkit: the importance of sample cleaning prior to the

characterization of biomineral proteomes. Proceedings of the National Academy of Sciences.
Raven, J. (2005). Acidification due to increasing carbon dioxide. Policy Document 12/05. London, The Royal Society.
Rho, H. K. and D. R. McClay (2011). "The control of foxN2/3 expression in sea urchin embryos and its function in the skeletogenic gene regulatory network." Development **138**(5): 937-945.
Ries, J. B., A. L. Cohen and D. C. McCorkle (2009). "Marine calcifiers exhibit mixed responses to CO_2-induced ocean acidification." Geology **37**(12): 1131-1134.
Rinkevich, B. and Y. Loya (1984). "Does light enhance calcification in hermatypic corals?" Marine Biology **80**(1): 1-6.
Roberts, J. M., P. S. Davies, L. M. Fixter and T. Preston (1999). "Primary site and initial products of ammonium assimilation in the symbiotic sea anemone *Anemonia viridis*." Marine Biology **135**(2): 223-236.
Rodolfo-Metalpa, R., P. Montagna, S. Aliani, M. Borghini, S. Canese, et al. (2015). "Calcification is not the Achilles' heel of cold-water corals in an acidifying ocean." Global Change Biology **21**(6): 2238-2248.
Rollion-Bard, C. and D. Blamart (2015). "Possible controls on Li, Na, and Mg incorporation into aragonite coral skeletons." Chemical Geology **396**(0): 98-111.
Rosati, R., G. S. B. Horan, G. J. Pinero, S. Garofalo, D. R. Keene, et al. (1994). "Normal long-bone growth and development in type-X collagen null mice." Nature Genetics **8**(2): 129-135.
Rosic, N., P. Kaniewska, C.-K. Chan, E. Ling, D. Edwards, et al. (2014). "Early transcriptional changes in the reef-building coral *Acropora aspera* in response to thermal and nutrient stress." BMC Genomics **15**(1): 1052.
Roy, A., A. Kucukural and Y. Zhang (2010). "I-TASSER: a unified platform for automated protein structure and function prediction." Nat. Protocols **5**(4): 725-738.
Samata, T., N. Hayashi, M. Kono, K. Hasegawa, C. Horita, et al. (1999). "A new matrix protein family related to the nacreous layer formation of *Pinctada fucata*." FEBS Letters **462**(1–2): 225-229.
Sarashina, I. and K. Endo (2001). "The complete primary structure of molluscan shell protein 1 (MSP-1), an acidic glycoprotein in the shell matrix of the scallop *Patinopecten yessoensis*." Marine Biotechnology **3**(4): 362-369.
Sarashina, I. and K. Endo (2006). "Skeletal matrix proteins of invertebrate animals: comparative analysis of their amino acid sequences." Paleontological Research **10**(4): 311-336.
Sea Urchin Genome Sequencing Consortium, E. Sodergren, G. M. Weinstock, E. H. Davidson, R. A. Cameron, et al. (2006). "The genome of the sea urchin *Strongylocentrotus purpuratus*." Science **314**(5801): 941-952.
Shamberger, K. E. F., A. L. Cohen, Y. Golbuu, D. C. McCorkle, S. J. Lentz, et al. (2014). "Diverse coral communities in naturally acidified waters of a Western Pacific reef." Geophysical Research letters **41**(2): 499-504.

Sheppard Brennand, H., N. Soars, S. A. Dworjanyn, A. R. Davis and M. Byrne (2010). "Impact of ocean warming and ocean acidification on larval development and calcification in the sea rchin *Tripneustes gratilla*." PLoS ONE **5**(6): e11372.
Shinzato, C., E. Shoguchi, T. Kawashima, M. Hamada, K. Hisata, et al. (2011). "Using the *Acropora digitifera* genome to understand coral responses to environmental change." Nature **476**(7360): 320-323.
Shiraga, H., W. Min, W. J. VanDusen, M. D. Clayman, D. Miner, et al. (1992). "Inhibition of calcium oxalate crystal growth in vitro by uropontin: another member of the aspartic acid-rich protein superfamily." Proceedings of the National Academy of Sciences **89**(1): 426-430.
Silliman, B. (1846). "On the chemical composition of the calcareous corals." Am J Sci **1**: 189-199.
Silver, F. H. and W. J. Landis (2011). "Deposition of apatite in mineralizing vertebrate extracellular matrices: A model of possible nucleation sites on type I collagen." Connective Tissue Research **52**(3): 242-254.
Smith, L. L., H.-K. Cheung, L. E. Ling, J. Chen, D. Sheppard, et al. (1996). "Osteopontin N-terminal domain contains a cryptic adhesive sequence recognized by α9β1 integrin." Journal of Biological Chemistry **271**(45): 28485-28491.
Smith, S. V. and R. W. Buddemeier (1992). "Global Change and Coral Reef Ecosystems." Annual Review of Ecology and Systematics **23**: 89-118.
Stanley, G. D. (2003). "The evolution of modern corals and their early history." Earth-Science Reviews **60**(3–4): 195-225.
Stanley, G. D., Jr. and B. Schootbrugge (2009). The evolution of the coral–algal symbiosis. Coral Bleaching. M. H. Oppen and J. Lough, Springer Berlin Heidelberg. **205:** 7-19.
Strahl, J., I. Stolz, S. Uthicke, N. Vogel, S. H. C. Noonan, et al. (2015). "Physiological and ecological performance differs in four coral taxa at a volcanic carbon dioxide seep." Comparative Biochemistry and Physiology Part A: Molecular & Integrative Physiology **184**(0): 179-186.
Stumpp, M., S. Dupont, M. C. Thorndyke and F. Melzner (2011). "CO_2 induced seawater acidification impacts sea urchin larval development II: Gene expression patterns in pluteus larvae." Comparative Biochemistry and Physiology Part A: Molecular & Integrative Physiology **160**(3): 320-330.
Sudo, S., T. Fujikawa, T. Nagakura, T. Ohkubo, K. Sakaguchi, et al. (1997). "Structures of mollusc shell framework proteins." Nature **387**(6633): 563-564.
Sullivan, J. C., J. F. Ryan, J. A. Watson, J. Webb, J. C. Mullikin, et al. "StellaBase: The *Nematostella vectensis* genomics database." Nucleic Acids Research **34**(suppl 1): D495-D499.
Sunagawa, S., M. K. DeSalvo, C. R. Voolstra, A. Reyes-Bermudez and M. Medina (2009). "Identification and gene expression analysis of a taxonomically restricted cysteine-rich protein family in reef-building corals." PLoS ONE **4**(3): e4865.
Suyemitsu, T., Y. Tonegawa and K. Ishihara (1990). "Similarities between the primary structures of exogastrula-inducing peptides and peptide B purified from embryos of the Sea Urchin, *Anthocidaris crassipina*." **7**(5).

Suzuki, M., E. Murayama, H. Inoue, N. Ozaki, H. Tohse, et al. (2004). "Characterization of Prismalin-14, a novel matrix protein from the prismatic layer of the Japanese pearl oyster (*Pinctada fucata*)." Biochem. J. **382**(1): 205-213.
Suzuki, M., K. Saruwatari, T. Kogure, Y. Yamamoto, T. Nishimura, et al. (2009). "An acidic matrix protein, Pif, Is a key macromolecule for nacre formation." Science **325**(5946): 1388-1390.
Swanson, R. and O. Hoegh-Guldberg (1998). "Amino acid synthesis in the symbiotic sea anemone *Aiptasia pulchella*." Marine Biology **131**(1): 83-93.
Takami, A., H. Kato, R. Takagi and T. Miyashita (2013). "Studies on the *Pinctada fucata* BMP-2 gene: Structural similarity and functional conservation of its osteogenic potential within the animal kingdom." International Journal of Zoology **2013**: 9.
Takeuchi, T., T. Kawashima, R. Koyanagi, F. Gyoja, M. Tanaka, et al. (2012). "Draft genome of the pearl oyster *Pinctada fucata*: A platform for understanding bivalve biology." DNA Research **19**(2): 117-130.
Takeuchi, T., I. Sarashina, M. Iijima and K. Endo (2008). "In vitro regulation of $CaCO_3$ crystal polymorphism by the highly acidic molluscan shell protein Aspein." FEBS Letters **582**(5): 591-596.
Tambutte, D. Allemand, E. Mueller and J. Jaubert (1996). "A compartmental approach to the mechanism of calcification in hermatypic corals." Journal of Experimental Biology **199**(5): 1029-1041.
Tambutté, E., S. Tambutté, N. Segonds, D. Zoccola, A. Venn, et al. (2012). "Calcein labelling and electrophysiology: Insights on coral tissue permeability and calcification." Proceedings of the Royal Society B: Biological Sciences **279**(1726): 19-27.
Tambutte, E., A. A. Venn, M. Holcomb, N. Segonds, N. Techer, et al. (2015). "Morphological plasticity of the coral skeleton under CO_2-driven seawater acidification." Nat Commun **6**.
Tambutté, S., M. Holcomb, C. Ferrier-Pagès, S. Reynaud, É. Tambutté, et al. (2011). "Coral biomineralization: From the gene to the environment." Journal of Experimental Marine Biology and Ecology **408**(1–2): 58-78.
Tchernov, D., T. Mass and D. F. Gruber (2012). "Symbiotic transition of algae–coral triggered by paleoclimatic events?" Trends in ecology & evolution **27**(4): 194-195.
Tittensor, D. P., A. R. Baco, J. M. Hall-Spencer, J. C. Orr and A. D. Rogers (2010). "Seamounts as refugia from ocean acidification for cold-water stony corals." Marine Ecology **31**: 212-225.
Todgham, A. E. and G. E. Hofmann (2009). "Transcriptomic response of sea urchin larvae *Strongylocentrotus purpuratus* to CO_2-driven seawater acidification." Journal of Experimental Biology **212**(16): 2579-2594.
Traylor-Knowles, N., B. Granger, T. Lubinski, J. Parikh, S. Garamszegi, et al. (2011). "Production of a reference transcriptome and a transcriptomic database (PocilloporaBase) for the cauliflower coral, *Pocillopora damicornis*." BMC Genomics **12**(1): 585.
Treccani, L., K. Mann, F. Heinemann and M. Fritz (2006). "Perlwapin, an abalone nacre protein with three four-Ddsulfide core (whey acidic protein) domains,

inhibits the growth of calcium carbonate crystals." Biophysical journal **91**(7): 2601-2608.
Tsukamoto, D., I. Sarashina and K. Endo (2004). "Structure and expression of an unusually acidic matrix protein of pearl oyster shells." Biochemical and Biophysical Research Communications **320**(4): 1175-1180.
Urry, L. A., P. C. Hamilton, C. E. Killian and F. H. Wilt (2000). "Expression of spicule matrix proteins in the sea urchin embryo during normal and experimentally altered spiculogenesis." Developmental Biology **225**(1): 201-213.
Valle, N., J. Drillet, A. Pic and H. N. Migeon (2011). "Nano-SIMS investigation of boron distribution in steels." Surface and Interface Analysis **43**(1-2): 573-575.
Venn, A. A., E. Tambutte, M. Holcomb, J. Laurent, D. Allemand, et al. (2012). "Impact of seawater acidification on pH at the tissue–skeleton interface and calcification in reef corals." Proceedings of the National Academy of Sciences **early edition**: 1-6.
Venn, A. A., E. Tambutté, M. Holcomb, J. Laurent, D. Allemand, et al. (2013). "Impact of seawater acidification on pH at the tissue–skeleton interface and calcification in reef corals." Proceedings of the National Academy of Sciences **110**(5): 1634-1639.
Veron, J. (1986). Corals of Australia and the Indo-Pacific. Honolulu, HI, University of Hawaii Press.
Veron, J. E. N. (2000). Corals of the World. Monterey, CA, Sea Challengers.
Vidal-Dupiol, J., D. Zoccola, E. Tambutté, C. Grunau, C. Cosseau, et al. (2013). "Genes related to ion-transport and energy production are upregulated in response to CO_2-driven pH decrease in corals: New insights from transcriptome analysis." PLoS ONE **8**(3): e58652.
Vitt, U. A., S. Y. Hsu and A. J. W. Hsueh (2001). "Evolution and classification of cystine knot-containing hormones and related extracellular signaling molecules." Molecular Endocrinology **15**(5): 681-694.
Wainwright, S. A. (1963). "Skeletal organization in the coral, *Pocillopora damicornis*." Quarterly Journal of Microscopical Science **s3-104**(66): 169-183.
Wall, C. B., T. Y. Fan and P. J. Edmunds (2014). "Ocean acidification has no effect on thermal bleaching in the coral *Seriatopora caliendrum*." Coral Reefs **33**(1): 119-130.
Wang, X., W. Fan, L. Xie and R. Zhang (2008). "Molecular cloning and distribution of a plasma membrane calcium ATPase homolog from the pearl oyster *Pinctada fucata*." Tsinghua Science & Technology **13**(4): 439-446.
Watanabe, T., I. Fukuda, K. China and Y. Isa (2003). "Molecular analyses of protein components of the organic matrix in the exoskeleton of two scleractinian coral species." Comparative Biochemistry and Physiology Part B: Biochemistry and Molecular Biology **136**(4): 767-774.
Weiner, S. and L. Addadi (2011). "Crystallization pathways in biomineralization." Annual Review of Materials Research **41**: 21-40.
Weiner, S. and L. Hood (1975). "Soluble protein of the organic matrix of mollusk shells: a potential template for shell formation." Science **190**(4218): 987-989.

Weiss, I. M., N. Tuross, L. Addadi and S. Weiner (2002). "Mollusc larval shell formation: amorphous calcium carbonate is a precursor phase for aragonite." Journal of Experimental Zoology **293**(5): 478-491.
White, A. T., H. P. Vogt and T. Arin (2000). "Philippine coral reefs under threat: the economic losses caused by reef destruction." Marine Pollution Bulletin **40**(7): 598-605.
Wikramanayake, A. H., R. Peterson, J. Chen, L. Huang, J. M. Bince, et al. (2004). "Nuclear β-catenin-dependent Wnt8 signaling in vegetal cells of the early sea urchin embryo regulates gastrulation and differentiation of endoderm and mesodermal cell lineages." genesis **39**(3): 194-205.
Wilt, F., C. E. Killian, L. Croker and P. Hamilton (2013). "SM30 protein function during sea urchin larval spicule formation." Journal of Structural Biology **183**(2): 199-204.
Winters, G., Y. Loya and S. Beer (2006). "In situ measured seasonal variations in F_v/F_m of two common Red Sea corals." Coral Reefs **25**(4): 593-598.
Woessner, J. F. (1991). "Matrix metalloproteinases and their inhibitors in connective tissue remodeling." The FASEB Journal **5**(8): 2145-2154.
Wu, S.-Y., M. Ferkowicz and D. R. McClay (2007). "Ingression of primary mesenchyme cells of the sea urchin embryo: A precisely timed epithelial mesenchymal transition." Birth Defects Research Part C: Embryo Today: Reviews **81**(4): 241-252.
Xuan Ri, S., K. Hideyuki and T. Koretaro (2007). "Characterization of molecular species of collagen in scallop mantle." Food Chemistry **102**(4): 1187-1191.
Yano, M., K. Nagai, K. Morimoto and H. Miyamoto (2006). "Shematrin: A family of glycine-rich structural proteins in the shell of the pearl oyster *Pinctada fucata*." Comparative Biochemistry and Physiology Part B: Biochemistry and Molecular Biology **144**(2): 254-262.
Young, S. D. (1971). "Organic material from scleractinian coral skeletons - I. Variation in composition between several species." Comparitive Biochemistry and Physiology **40B**: 113-120.
Young, S. D., J. D. O'Connor and L. Muscatine (1971). "Organic material from scleractinian coral skeletons--II. Incorporation of ^{14}C into protein, chitin and lipid." Comparative Biochemistry and Physiology Part B: Comparative Biochemistry **40**(4): 945-958.
Yuen, K. I., Ai M. Loong, Kum C. Hiong, Wai P. Wong, Shit F. Chew, et al. (2006). "Light induces an increase in the pH of and a decrease in the ammonia concentration in the extrapallial luid of the giant clam *Tridacna squamosa*." Physiological and Biochemical Zoology **79**(3): 656-664.
Zachos, J. C., U. Röhl, S. A. Schellenberg, A. Sluijs, D. A. Hodell, et al. (2005). "Rapid acidification of the ocean during the Paleocene-Eocene Thermal Maximum." Science **308**(5728): 1611-1615.
Zachos, J. C., M. W. Wara, S. Bohaty, M. L. Delaney, M. R. Petrizzo, et al. (2003). "A transient rise in tropical sea surface temperature during the Paleocene-Eocene Thermal Maximum." Science **302**(5650): 1551-1554.
Zeebe, R. E. and D. Wolf-Gladrow (2001). CO2 in Seawater: Equilibrium, Kinetics, Isotopes. New York, New York, Elsevier.

Zhang, C., L. Xie, J. Huang, X. Liu and R. Zhang (2006). "A novel matrix protein family participating in the prismatic layer framework formation of pearl oyster, *Pinctada fucata*." Biochemical and Biophysical Research Communications **344**(3): 735-740.
Zhang, C. and R. Zhang (2006). "Matrix proteins in the outer shells of molluscs." Marine Biotechnology **8**(6): 572-586.
Zhang, G., X. Fang, X. Guo, L. Li, R. Luo, et al. (2012). "The oyster genome reveals stress adaptation and complexity of shell formation." Nature **490**(7418): 49-54.
Zoccola, D., A. Moya, G. Béranger, E. Tambutté, D. Allemand, et al. (2009). "Specific expression of BMP2/4 ortholog in biomineralizing tissues of corals and action on mouse BMP receptor." Marine Biotechnology **11**(2): 260-269.
Zoccola, D., E. Tambutté, E. Kulhanek, S. Puverel, J.-C. Scimeca, et al. (2004). "Molecular cloning and localization of a PMCA P-type calcium ATPase from the coral *Stylophora pistillata*." Biochimica et Biophysica Acta (BBA) - Biomembranes **1663**(1–2): 117-126.